

Stratigraphy and Vertical Hydraulic Conductivity of the St. Francois Confining Unit in the Viburnum Trend and Evaluation of the Unit in the Viburnum Trend and Exploration Areas, Southeastern Missouri

Water-Resources Investigations Report 03-4329



Stratigraphy and Vertical Hydraulic Conductivity of the St. Francois Confining Unit in the Viburnum Trend and Evaluation of the Unit in the Viburnum Trend and Exploration Areas, Southeastern Missouri

By Michael J. Kleeschulte¹ and Cheryl M. Seeger²

Water-Resources Investigations Report 03-4329

Rolla, Missouri
2003

¹U.S. Geological Survey

²Missouri Department of Natural Resources, Geological Survey and Resource Assessment Division

U.S. Department of the Interior

Gale A. Norton, Secretary

U.S. Geological Survey

Charles G. Groat, Director

The use of firm, trade, and brand names in this report is for identification purposes only and does not constitute endorsement by the U.S. Geological Survey.

For additional information write to:

District Chief
U.S. Geological Survey, WRD
1400 Independence Road
Mail Stop 100
Rolla, Missouri 65401

Copies of this report can be purchased from:

U.S. Geological Survey
Branch of Information Services
Box 25286
Denver, CO 80225-0286

CONTENTS

Abstract.....	1
Introduction	2
Purpose and Scope.....	8
Exploration Borehole Data.....	8
Geohydrologic Units.....	9
Acknowledgments	10
Stratigraphy	10
Davis Formation	11
Derby-Doerun Dolomite.....	15
Thickness and Net Shale Thickness of the St. Francois Confining Unit.....	15
Vertical Hydraulic Conductivity	18
Methodology.....	18
Evaluation of the St. Francois Confining Unit along the Viburnum Trend	20
Evaluation of the St. Francois Confining Unit along the Viburnum Trend and Exploration Areas	25
Summary and Conclusions	27
References	29

FIGURES

1. Map showing location of the Viburnum Trend, exploration areas, and study area	3
2. Stratigraphic column for an exploration hole in Reynolds County, Missouri, and a general lithologic description of formations in the Viburnum Trend	5
3. Geohydrologic section from southeastern Crawford County along the Viburnum Trend to west-central Reynolds County.....	6
4. Borehole-numbering system used for this report.....	9
5.–10. Maps showing:	
5. Location of exploration boreholes	12
6. Structure of the top of the Bonneterre Formation.....	13
7. Structure of the top of the Davis Formation	14
8. Structure of the top of the Derby-Doerun Dolomite.....	16
9. Thickness of the St. Francois confining unit	17
10. Net shale thickness of the combined St. Francois confining unit and the upper Bonneterre Formation.....	19
11.–12. Boxplots showing:	
11. The vertical hydraulic conductivity and porosity of the St. Francois confining unit and upper Bonneterre Formation plotted by formations and rock types along the Viburnum Trend.....	23
12. The vertical hydraulic conductivity of the St. Francois confining unit and rock types along the Viburnum Trend and in the exploration areas.....	26

TABLES

1. Viburnum Trend core log analysis data.....	32
2. Adjacent property core log analysis data.....	44
3. Porosity, vertical permeability, and vertical hydraulic conductivity data.....	54
4. Summary of Kruskal-Wallis statistical test p-values	22
5. Summary of vertical hydraulic conductivity values for the St. Francois confining unit along the Viburnum Trend.....	24

VERTICAL DATUM

Vertical coordinate information is referenced to the National Geodetic Vertical Datum of 1929 (NGVD 29). Altitude, as used in the report, refers to distance above or below NGVD 29. NGVD 29 can be converted to the North American Vertical Datum of 1988 (NAVD 88) by using the National Geodetic Survey conversion utility available at URL

<http://www.ngs.noaa.gov/TOOLS/Vertcon/vertcon.html>.

Stratigraphy and Vertical Hydraulic Conductivity of the St. Francois Confining Unit in the Viburnum Trend and Evaluation of the Unit in the Viburnum Trend and Exploration Areas, Southeastern Missouri

By Michael J. Kleeschulte¹ and Cheryl M. Seeger²

Abstract

The confining ability of the St. Francois confining unit (Derby-Doerun Dolomite and Davis Formation) was evaluated in ten townships (T. 31–35 N. and R. 01–02 W.) along the Viburnum Trend of southeastern Missouri. Vertical hydraulic conductivity data were compared to similar data collected during two previous studies 20 miles south of the Viburnum Trend, in two lead-zinc exploration areas that may be a southern extension of the Viburnum Trend. The surficial Ozark aquifer is the primary source of water for domestic and public-water supplies and major springs in southern Missouri. The St. Francois confining unit lies beneath the Ozark aquifer and impedes the movement of water between the Ozark aquifer and the underlying St. Francois aquifer (composed of the Bonneterre Formation and Lamotte Sandstone). The Bonneterre Formation is the primary host formation for lead-zinc ore deposits of the Viburnum Trend and potential host formation in the exploration areas.

For most of the more than 40 years the mines have been in operation along the Viburnum Trend, about 27 million gallons per day were being pumped from the St. Francois aquifer for mine dewatering. Previous studies conducted along the Viburnum Trend have concluded that no large cones of depression have developed in the potenti-

ometric surface of the Ozark aquifer as a result of mining activity. Because of similar geology, stratigraphy, and depositional environment between the Viburnum Trend and the exploration areas, the Viburnum Trend may be used as a pertinent, full-scale model to study and assess how mining may affect the exploration areas.

Along the Viburnum Trend, the St. Francois confining unit is a complex series of dolostones, limestones, and shales that generally is 230 to 280 feet thick with a net shale thickness ranging from less than 25 to greater than 100 feet with the thickness increasing toward the west. Vertical hydraulic conductivity values determined from laboratory permeability tests were used to represent the St. Francois confining unit along the Viburnum Trend. The Derby-Doerun Dolomite and Davis Formation are statistically similar, but the Davis Formation would be the more hydraulically restrictive medium. The shale and carbonate values were statistically different. The median vertical hydraulic conductivity value for the shale samples was 62 times less than the carbonate samples. Consequently, the net shale thickness of the confining unit along the Viburnum Trend significantly affects the effective vertical hydraulic conductivity. As the percent of shale increases in a given horizon, the vertical hydraulic conductivity decreases.

The range of effective vertical hydraulic conductivity for the confining unit in the Viburnum Trend was estimated to be a minimum of 2×10^{-13} ft/s (foot per second) and a maximum of 3×10^{-12} ft/s. These vertical hydraulic conductivity

¹U.S. Geological Survey

²Missouri Department of Natural Resources,
Geological Survey and Resource Assessment Division

values are considered small and verify conclusions of previous studies that the confining unit effectively impedes the flow of ground water between the Ozark aquifer and the St. Francois aquifer along the Viburnum Trend.

Previously-collected vertical hydraulic conductivity data for the two exploration areas from two earlier studies were combined with the data collected along the Viburnum Trend. The nonparametric Kruskal-Wallis statistical test shows the vertical hydraulic conductivity of the St. Francois confining unit along the Viburnum Trend, and west and east exploration areas are statistically different. The vertical hydraulic conductivity values generally are the largest in the Viburnum Trend and are smallest in the west exploration area. The statistical differences in these values do not appear to be attributed strictly to either the Derby-Doerun Dolomite or Davis Formation, but instead they are caused by the differences in the carbonate vertical hydraulic conductivity values at the three locations.

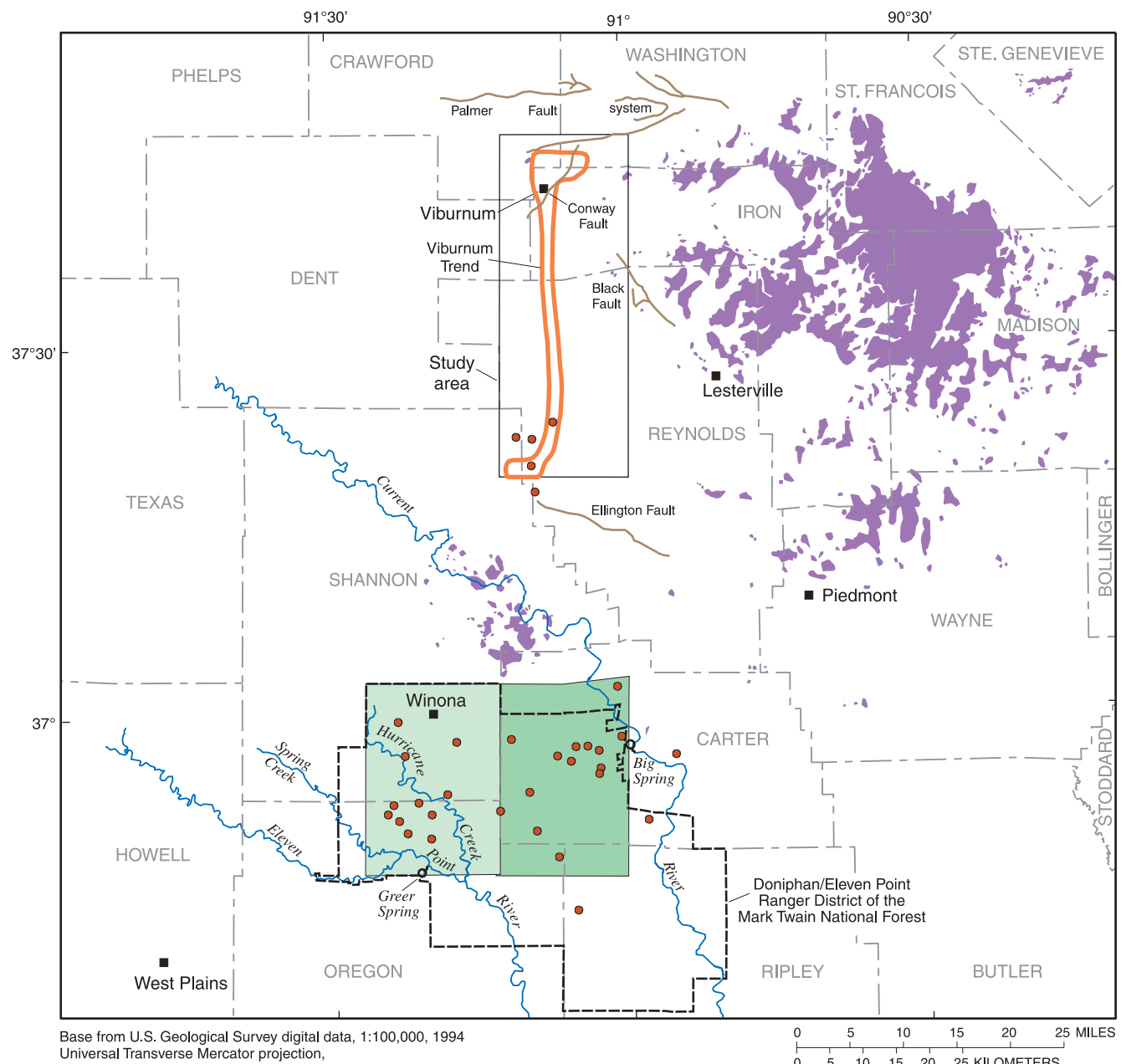
The calculated effective vertical hydraulic conductivity range for the St. Francois confining unit at each location is: 2×10^{-13} to 3×10^{-12} ft/s for the Viburnum Trend; 3×10^{-14} (minimum reporting level) to 1×10^{-12} ft/s for the west exploration area; and 3×10^{-13} to 2×10^{-12} ft/s for the east exploration area. Based on the calculated vertical hydraulic conductivity ranges, the St. Francois confining unit is considered ‘tight’ at all locations. However, in relation to each other, the west exploration area is the tightest, and the most conductive area is the Viburnum Trend. No apparent large cones of depression have developed in the potentiometric surface of the Ozark aquifer as a result of mining activity in the Viburnum Trend. Therefore, using similar mining practices as those along the Viburnum Trend, no large cones of depression in the Ozark aquifer would be expected in the exploration areas, unless preferred-path secondary permeability has developed along faults or fractures or resulted from exploration activities.

INTRODUCTION

Initial ore production from the first Viburnum area mine began in the 1960’s. Lead is the primary element extracted, but substantial amounts of zinc, copper, and silver also are mined. Other major ore bodies were discovered by 1964 along a 30-mi (mile) linear zone that is now referred to as the Viburnum Trend (Wharton, 1979; fig. 1). By 1970, two new smelters and five new mine-mill complexes were in operation. From the early 1970’s into the early 1990’s, lead and zinc production from the Viburnum Trend reached then record highs. Throughout the late 1970’s, the area was the largest lead producing area in the world, accounting for more than 15 percent of the total recorded world output.

The Bonneterre Formation of Upper Cambrian age is the primary host formation for the lead-zinc ore deposits of the Viburnum Trend, and together with the underlying Lamotte Sandstone forms the carbonate rock (dolostone and limestone) and sandstone St. Francois aquifer (figs. 2 and 3). The formation ranges from about 400 ft (feet) below land surface in the northern part of the Viburnum Trend to about 1,000 ft below land surface in the southern part (fig. 3). The St. Francois confining unit overlies the St. Francois aquifer and consists of dense carbonate and shale of the Derby-Doerun Dolomite and Davis Formation. The confining unit is considered the barrier that confined ascending ore-forming hydrothermal solutions to the Bonneterre Formation. Formations of Upper Cambrian and Lower Ordovician age consisting of the Potosi Dolomite to the Roubidoux Formation are exposed at land surface along the Viburnum Trend and overlie the St. Francois confining unit. These rocks form the Ozark aquifer, the primary source of water for private and public-water supplies and major springs in southern Missouri. The geologic names used in this report follow the nomenclature used by the Missouri Department of Natural Resources, Geological Survey and Resource Assessment Division (GSRAD), formerly known as the Division of Geology and Land Survey.

Mine dewatering before ore extraction is part of normal mine operation. Twenty-six million gallons of water per day were pumped from the St. Francois aquifer in 1971 (Warner and others, 1974) and in 1999 the total pumpage was slightly larger at 27 million gallons per day (Denis Murphy, The Doe Run Company, written commun., 2000). These withdrawal rates from the St. Francois aquifer are typical for the Viburnum Trend and have been occurring for most of the more than 40



Base from U.S. Geological Survey digital data, 1:100,000, 1994
Universal Transverse Mercator projection,
Zone 15

EXPLANATION

- [Green Box] WEST EXPLORATION AREA
- [Green Box] EAST EXPLORATION AREA
- [Purple Box] ST. FRANCOIS MOUNTAINS PRECAMBRIAN ROCK OUTCROP
- BOREHOLE WITH ROCK CORE SAMPLE (KLEESCHULTE AND SEEGER, 2000, 2001)

Figure 1. Location of the Viburnum Trend, exploration areas, and study area.



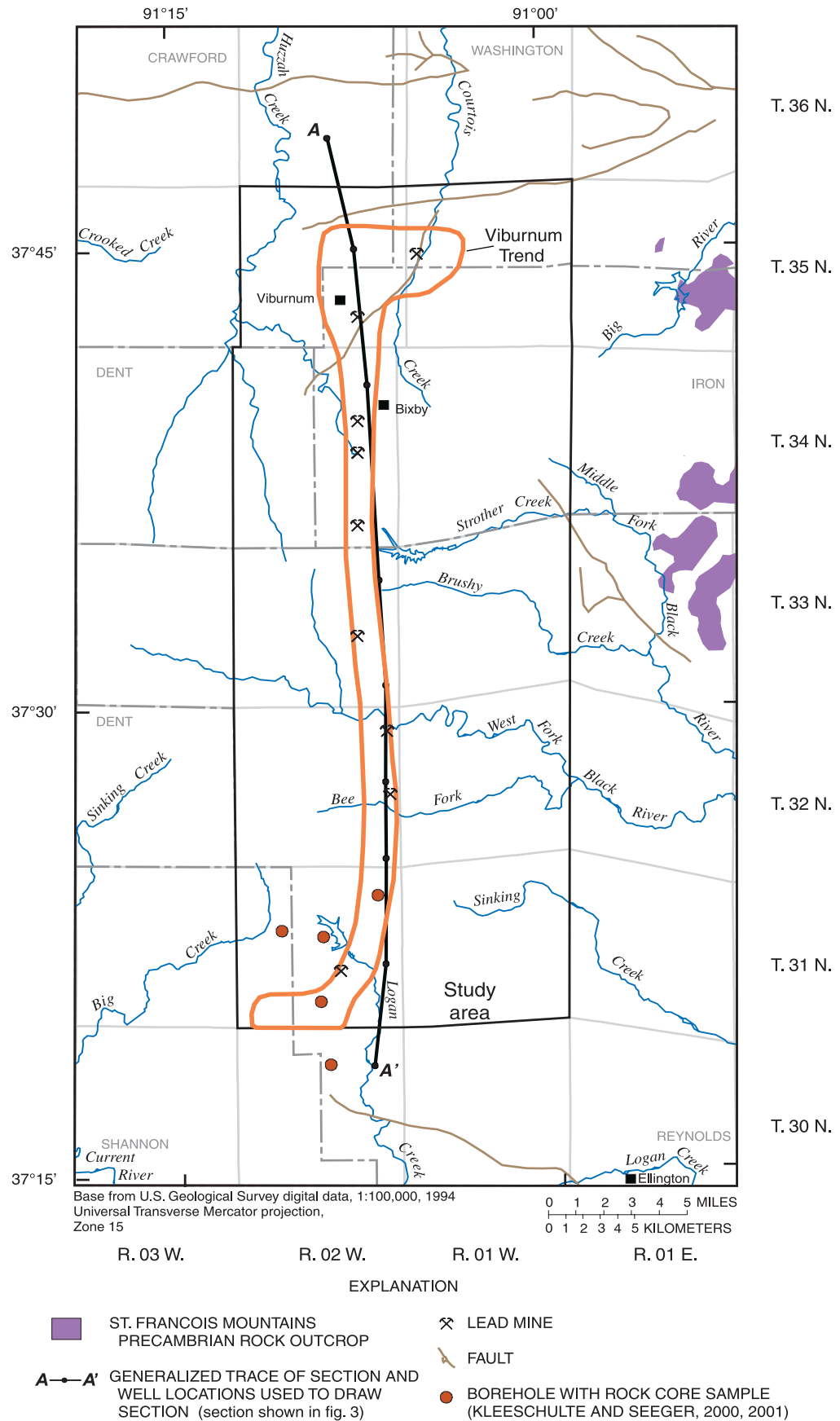


Figure 1. Location of the Viburnum Trend, exploration areas, and study area—Continued.

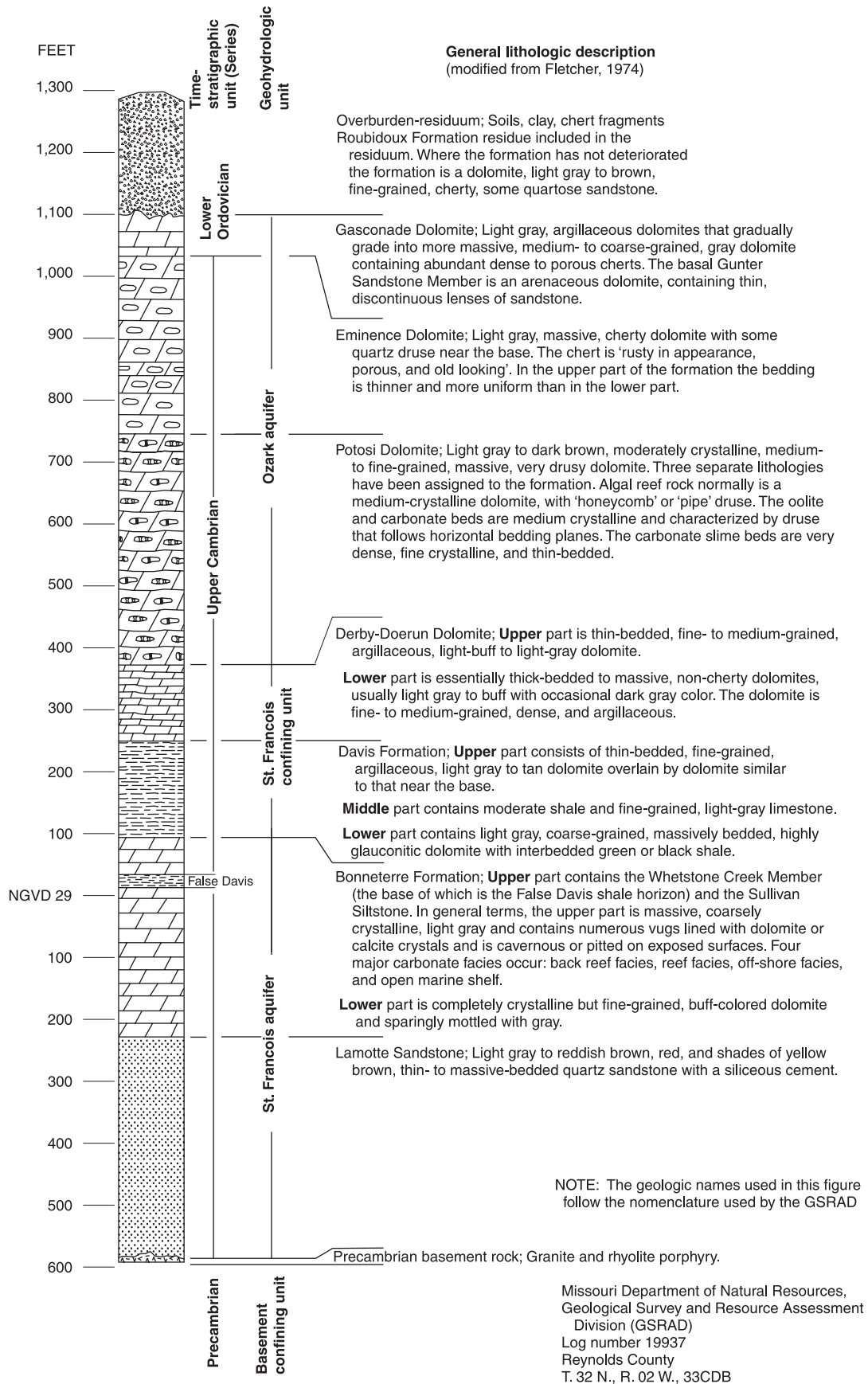


Figure 2. Stratigraphic column for an exploration hole in Reynolds County, Missouri, and a general lithologic description of formations in the Viburnum Trend.

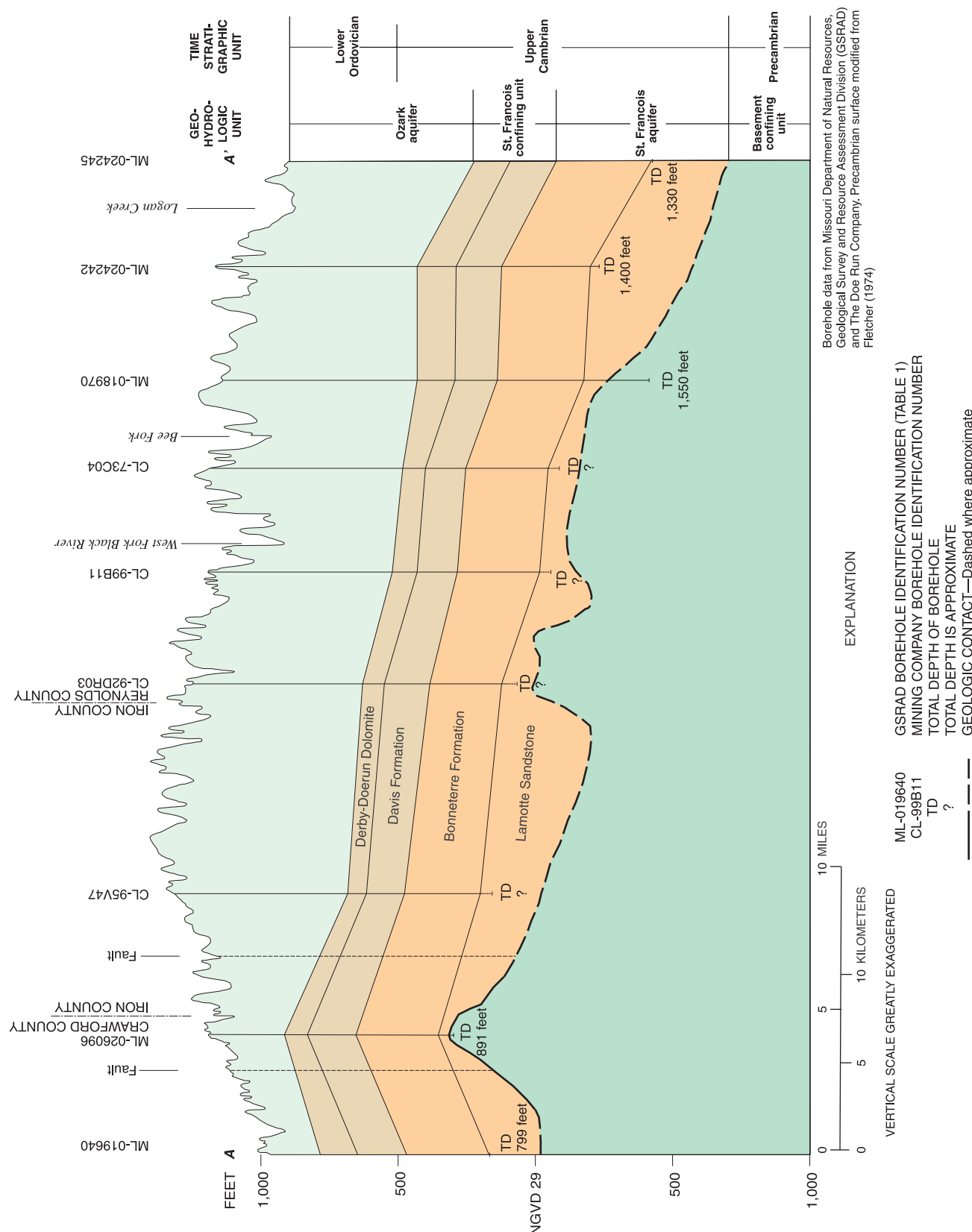


Figure 3. Geohydrologic section from southeastern Crawford County along the Viburnum Trend to west-central Reynolds County (trace shown on fig. 1).

years the mines have been in operation. Previous studies conducted along the Viburnum Trend to assess the effects of mine dewatering in the St. Francois aquifer on water levels in the surficial Ozark aquifer have concluded that no large cones of depression have developed in the potentiometric surface of the Ozark aquifer as a result of mining activity. However, some localized leakage of water from the Ozark aquifer into the St. Francois aquifer probably is occurring at mine shafts, ventholes, and inadequately plugged exploration drill holes. Therefore, small areas of drawdown may exist (Warner and others, 1974; Miller and Vandike, 1997; Kleeschulte, 2001).

Fletcher (1974) states that faults along the Viburnum Trend can be grouped into three systems: the Palmer Fault system to the north, which includes the Conway Fault; the Black Fault in the east central part; and the Ellington Fault to the south (fig. 1). The Palmer Fault system forms the northern boundary of the Viburnum Trend and is a group of normal faults. McCracken (1971) describes the fault system as being 45 mi long consisting of one or more parallel faults cutting rocks from the Roubidoux Formation to the Precambrian basement rock. McCracken states the faults are all normal and high-angle with a maximum offset of 1,200 ft on the east side of the fault in Washington County, and offsets decreasing westward to 200 ft in Crawford County. Fletcher interpreted the stratigraphy so offsets did not exceed 150 ft. The Conway Fault was interpreted by Fletcher (1974) to be a left lateral wrench fault with a minor offset. The Black Fault has a displacement of 300 ft and brings the Potosi Dolomite (Ozark aquifer) in contact with the Bonneterre Formation (McCracken, 1971). The fault may extend northwest to connect with (or be cut off by) the Palmer Fault system. The Ellington Fault was interpreted by Fletcher (1974) as a normal fault, with the southern side being downthrown with a maximum offset that does not exceed 50 ft. Pratt (1982) shows a more detailed map than Fletcher (1974) of the faults along the Viburnum Trend; however, for the purposes of this report, a generalized overview of the major faults is sufficient without the multiplicity of minor displacement faults. Based on conversations with several mine geologists who have worked in the Viburnum Trend, they state that based on their experiences, permeability does not increase around the faults. Instead, the confining unit (Davis Formation in particular) is a vertical barrier to ground-water flow and the faults serve as lateral barriers.

From the 1960's to the end of the 1990's, lead and zinc exploration occurred in two exploration areas in the Doniphan/Eleven Point Ranger District of the Mark Twain National Forest (fig. 1). These exploration areas are 20 mi south of the Viburnum Trend, and a possible southern extension of the Trend. The exploration peaked in the late 1970's and early 1980's, resulting in several hundred exploration holes being drilled in the National Forest. The exploration areas lie within a larger region of well-developed karst terrain with an extensive network of solution-enlarged fractures ranging from small channels to large conduits. The two largest springs in Missouri (Big Spring and Greer Spring, fig. 1) are in this area, and discharge from these springs helps sustain flow in two nationally designated streams; the Current River (Ozark National Scenic Riverway) and the Eleven Point River (Eleven Point Wild and Scenic River). The potential for lead-zinc mining in this environmentally sensitive and federally designated scenic area has concerned the Forest Service and the Bureau of Land Management (BLM) in regard to possible effects that mining may have on the water resources of the area. The concerns include but are not limited to the effects that mine dewatering in the St. Francois aquifer may have upon water resources of the surficial Ozark aquifer.

As a result of these concerns, two previous studies (Kleeschulte and Seeger, 2000, 2001) assessed the confining ability of the St. Francois confining unit in the west exploration area and the adjacent property toward Big Spring, referred to in this report as the east exploration area (fig. 1). These studies described the depositional environment and stratigraphy, and quantified the vertical hydraulic conductivity of 94 rock core samples collected from 28 boreholes in the confining unit. Both studies conclude that the vertical hydraulic conductivity of the confining unit is small. The confining unit effectively impedes ground-water flow between the Ozark and St. Francois aquifers, unless preferred-path secondary permeability has developed along faults and fractures that extend through the confining unit.

Mining has been occurring in the Viburnum Trend for more than 40 years with no appreciable drawdown being observed in the Ozark aquifer. Because of the similarity in geology, stratigraphy, and depositional environment between the Viburnum Trend and the exploration areas in the Doniphan/Eleven Point Ranger District of the Mark Twain National Forest, the Viburnum Trend may be used as a pertinent, full-scale model

to study and assess how mining may affect aquifers in the exploration areas. To address these needs, the confining ability of the St. Francois confining unit along the Viburnum Trend was quantified and compared with the results from the exploration areas to evaluate potential mine dewatering effects in the exploration areas.

Purpose and Scope

This report describes the stratigraphy and vertical hydraulic conductivity of the St. Francois confining unit in a 400 mi² (square mile) study area of 10 townships (T. 31–35 N. and R. 01–02 W.; fig. 1) along the Viburnum Trend in Crawford, Iron, Washington, Dent, Reynolds, and Shannon Counties of southeastern Missouri. The vertical hydraulic conductivity data for the study area also was evaluated by comparing it to the vertical hydraulic conductivity data collected in the west and east exploration areas by Kleeschulte and Seeger (2000, 2001). This was accomplished by evaluating borehole core log data and examining available rock core samples. These stratigraphic data were used to prepare maps that depict the altitude of the top of the Derby-Doerun Dolomite and Davis Formation of the St. Francois confining unit, and the Bonneterre Formation (base of the Davis Formation) of the St. Francois aquifer. Maps showing the total thickness and net shale thickness (cumulative shale thicknesses) of the confining unit also were drawn. Forty rock core samples from the St. Francois confining unit and the St. Francois aquifer were collected and sent for laboratory permeability and porosity determination as part of this study. The vertical hydraulic conductivity of the rock core samples was calculated from the laboratory permeability values. These data were added to an existing vertical hydraulic conductivity and porosity data base for the St. Francois confining unit and St. Francois aquifer created from rock core samples analyzed from the exploration areas and the Viburnum Trend.

Exploration Borehole Data

Several thousand exploration holes have been drilled along the Viburnum Trend to delineate ore bodies. The BLM, GSRAD, and The Doe Run Company have copies of many of the core logs from the various mining companies that have explored or mined in the area. The BLM receives copies of core logs from exploration holes drilled on Federal lands, the GSRAD acquired donated copies of logs from several mining

companies, and The Doe Run Company owns and operates the active mines in the Viburnum Trend and received core logs from predecessor mining companies. Much of the core log data used in this report came from the public-access core log files at the GSRAD. However, even with these log data, no core log data were available for several areas. Because the Viburnum Trend is an active mining area, the core logs on file at the BLM are classified as confidential and unavailable for viewing. A request was made and granted by The Doe Run Company for permission to examine the core log information for holes located in selected areas where no data were publicly available. Consequently, additional core logs were available for restricted use during the study described in this report.

The core logs provided general site information such as location and land-surface altitude of the borehole, total depth of the borehole, and depths to the top of formations. In some cases, the logs provided detailed lithologic descriptions for the interval from the base of the Potosi Dolomite into the Lamotte Sandstone or Precambrian basement, typically an interval from 500 to 600 ft. The core logs and available core samples that were examined as part of this study were the primary source of the stratigraphic data contained in this report. The analyzed rock core samples were obtained from The Doe Run Company and the GSRAD.

Borehole locations reported on the core logs were defined to the nearest quarter-quarter-quarter section or as distance from the north/south and east/west section line. Land-surface altitudes were typically determined at the time of drilling using altimeters or topographic maps; however, occasionally the site was surveyed and altitudes were reported to the nearest foot. The reported altitudes were verified during this study using U.S. Geological Survey 7.5-minute topographic maps that generally had contour intervals of 20 ft; therefore, the land-surface altitudes are accurate to about 10 ft (one-half the contour interval). In a few instances, the reported land-surface altitudes on the core logs did not agree with the land surface shown on the topographic maps for the given location. When this situation occurred, the altitude shown on the topographic map at the borehole location was used.

In this report, the locations of exploration boreholes (tables 1 and 2, at the back of this report) are shown by latitude and longitude coordinates and by the local well number, which follows the General Land Office coordinate system (fig. 4). According to this system, the first three sets of numbers representing a bore-

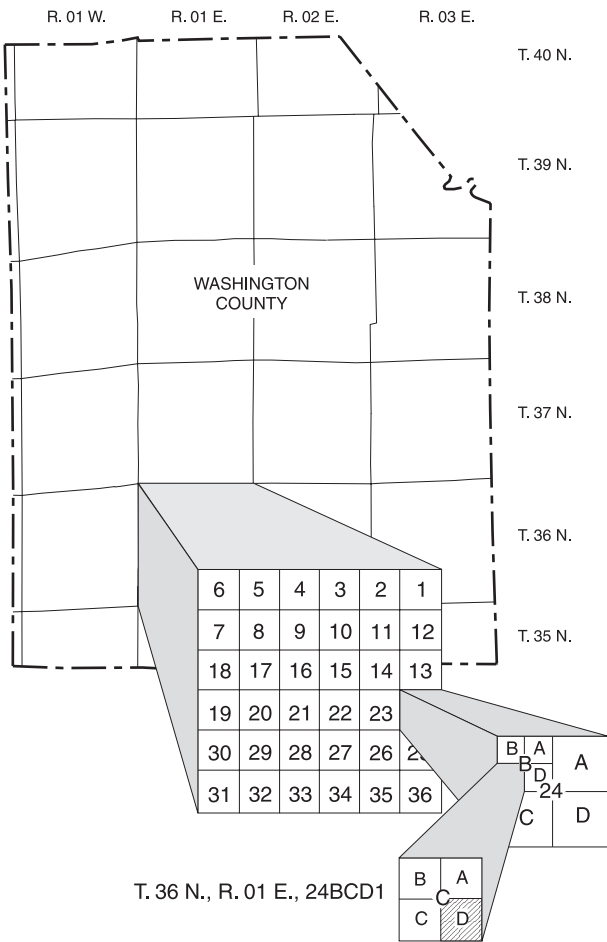


Figure 4. Borehole-numbering system used for this report.

hole location designate township, range, and section. The letters that follow indicate quarter section, quarter-quarter section, and quarter-quarter-quarter section. The quarter sections are represented by letters A, B, C, and D in counterclockwise order, starting in the northeastern quadrant. Occasionally, the borehole location was described as being in the center of a particular quarter section or in the northern, southern, eastern, or western one-half of a quarter section. In these cases, abbreviations (Cr for center; N2, S2, E2, or W2 for northern, southern, eastern, or western one-half of a quarter section) were used to convey this meaning.

Considerable interpretation was necessary to identify stratigraphic boundaries in some of the core logs and core samples because of variable stratigraphic nomenclature applied by the different mining companies and the different criteria for assigning the contacts between these formations. The conformable and transitional contacts that exist between all the formations

from the Potosi Dolomite to the Bonneterre Formations also make it difficult to distinguish the contacts between formations. This may account for some of the irregularity shown on structure maps in this report.

Geohydrologic Units

Delineation of geohydrologic units is based on hydraulic properties and the hydrologic relation of each unit to adjacent geohydrologic units at a regional scale. The terms aquifer and confining unit, as defined regionally, may not adequately describe the hydraulic properties of a sequence of rocks locally because of the variation in water-yielding capability of the same rock sequence from one area to another. Although this report is concerned with the St. Francois confining unit, the geohydrologic units from the Precambrian basement through the surficial aquifer will be briefly discussed so that the entire geologic framework of the area can be described and the relation of one unit to another shown.

The lowermost geohydrologic unit in the study area is the Basement confining unit of Precambrian age (figs. 2 and 3), which is predominantly granite and rhyolite. Imes (1989) states that this confining unit is virtually impermeable. In areas where extensive faulting and fracturing has occurred, Imes reports the Basement confining unit can yield small quantities of water. In areas where the unit crops out, well yields are less than 10 gallons per minute. The surface of the Basement confining unit can be highly irregular. Isolated Precambrian basement knobs mapped in the subsurface of the study area and adjacent property by Fletcher (1974) indicate these knobs may extend 600 to 1,000 ft above the surrounding basement rock.

The St. Francois aquifer (Imes, 1990a) overlies the Basement confining unit and consists of the Lamotte Sandstone and the Bonneterre Formation (figs. 2 and 3). In areas of southeastern Missouri near the St. Francois Mountains (about 10 mi east of the study area; fig. 1) where the St. Francois aquifer is close to land

surface, the aquifer yields adequate supplies of water for domestic and small capacity public-supply wells. The thickness of the St. Francois aquifer can vary considerably because of the irregular surface of the underlying basement rocks.

The Davis Formation and the Derby-Doerun Dolomite form the St. Francois confining unit (Imes, 1990b) that overlies the St. Francois aquifer (figs. 2 and 3). Imes and Emmett (1994) state in their regional study of the Ozark Plateaus aquifer system that substantial secondary porosity and permeability have not developed regionally in the St. Francois confining unit. The fine-grained nature of the formations indicates they have minimal permeability, even in areas containing little or no shale. Regionally, the physical and hydraulic characteristics of the unit generally impede the movement of ground water between the overlying Ozark aquifer and the underlying St. Francois aquifer (Imes and Emmett, 1994). This report will attempt to verify and quantify the general statement made by Imes and Emmett that the confining unit impedes the movement of ground water between aquifers locally along the Viburnum Trend.

The Ozark aquifer (Imes, 1990c) is the uppermost geohydrologic unit in the study area and consists of rocks from the base of the Potosi Dolomite to the top of the Roubidoux Formation (figs. 2 and 3). This predominantly carbonate aquifer is dolostone with some sandstone, and is the most widely used aquifer in southern Missouri. In the study area, ground water in the aquifer normally occurs under water-table conditions.

Acknowledgments

Gratitude is extended to The Doe Run Company for assistance and cooperation in obtaining rock core samples and for access to specific, classified core logs. Special recognition is extended to Tom Schott and Bob Dunn of The Doe Run Company for the time they spent in helping the authors collect this information. Much of the data in this report could not have been obtained without their support.

STRATIGRAPHY

The entire Upper Cambrian Series, of which the St. Francois confining unit is a part, represents a series of transgressions and regressions by ancient seas. The repeated advancing and subsequent retreat of the sea

over land areas created a complex series of dolostones, limestones, shales, sandstones, and siltstones. The stratigraphic sequence is controlled, in large part, by pre-Upper Cambrian faulting and erosion of the igneous Precambrian basement, and by faulting during the deposition of Upper Cambrian sediments. Rift-related faulting created a series of mountains and basins; erosion of Precambrian basement knobs provided detrital material for alluvial fan deposits and fluvial braided streams (lowermost Upper Cambrian). A transgression with continued deposition of clastic material led to the accumulation of the marine Lamotte Sandstone. Inundation and development of an intrashelf basin (lowermost Bonneterre Formation) followed; deposition of fan deltas was still active during the earliest stages (Lamotte Sandstone-Bonneterre Formation transition). Intrashelf basin development was followed by a cycle of regression and transgression. The shelf eventually filled with detrital material to form a ramp (Sullivan Siltstone member) from the land areas to the depositional basins, but was again inundated during Whetstone Creek member deposition (fig. 2). The Davis Formation-Whetstone Creek member contact indicates abrupt intrashelf basin development, followed by repeated shallowing and flooding, leading to the deposition of the rest of the Upper Cambrian section (Derby-Doerun Dolomite, Potosi Dolomite, and Eminence Dolomite; Palmer, 1989, 1991). Periods of epigenetic dolomitization of paleokarsted limestones developed whiterock horizons. “Whiterock” is a term that originated in the southeast Missouri lead district to describe coarse-crystalline white, light gray, or light brown dolostones that are the product of epigenetic dolomitization of reddened-paleokarsted limestones. Whiterock generally does not have apparent preserved primary depositional fabrics; however, occasional ghost textures are suggestive of deposition in an extremely shallow platform interior (Howe, 1968). Carbonate rocks are described in this section using the Dunham classification system (Dunham, 1962).

The St. Francois confining unit is a complex series of dolostones, limestones, and shales. Usually, the shale content of a geohydrologic unit is the primary indicator of the confining unit effectiveness as a flow barrier. As the shale content of a unit increases, the hydraulic conductivity of the unit decreases, inhibiting the flow of water through the unit. Because of this, the net shale thickness of the Derby-Doerun Dolomite and the Davis Formation was determined for this report at boreholes where either detailed lithologic descriptions

were provided or where core samples were available for inspection. The detailed descriptions typically divided the cored section into small intervals in which the lithology had similar characteristics. The rock was described as to color, texture, grain size, physical features (stromatolites, staining, and vugs), and percent of each rock type (shale, dolostone, and limestone). The net shale thickness was calculated by multiplying the reported percent shale in an interval by the thickness of the described interval. The net shale thicknesses of all the intervals were summed to determine the total net shale thickness for the rock core. If borehole core samples from the St. Francois confining unit were available for inspection, these samples were relogged for net shale thickness determination.

There were 315 borehole logs (fig. 5, tables 1 and 2) used to describe the stratigraphy for this study. Of this total, 175 boreholes are in the study area (table 1); the remainder are on adjacent property and are considered supplemental stratigraphic data (table 2) used to refine contours near the study area boundaries. Faults shown on the structure maps were modified from Fletcher (1974). Of the available core logs in the study area, 173 logs contained stratigraphic information for the St. Francois confining unit. The altitudes used in defining the geologic formation tops were determined by subtracting the depth of the formation top reported on the core log from the recorded land-surface altitude. The lithologic summaries that are presented in this section are necessarily brief and focused on lithologic properties that potentially affect vertical hydraulic conductivity.

Davis Formation

The Davis Formation is the basal part of large-scale shallowing-upward sequences. Horizontal burrows are indicative of slow periodic deposition in a marine subtidal setting during early stages of shelf flooding. Intraclast conglomerate beds can be interpreted as storm-generated mass-flow deposits that presumably moved down slopes of a few degrees or less. The intrashelf basin facies tends to thin towards the geographic center of the deeper depositional basins where shale is more abundant. An increase in the volume of carbonate beds indicates proximity to the intrashelf basin edge. Oolites in some carbonate layers are likely grain flows (Palmer, 1989, 1991).

The Davis Formation is an intrashelf basin facies consisting of shales interbedded with shaly limestones,

clean limestones, and local dolostones, with both shale- and carbonate-dominant sequences. In the basal to lower parts of some Davis Formation sections, shales are interbedded with thin glauconitic fine-grained quartzose sandstones. Shales generally are light to dark green, with some gray to dark gray beds. The entire formation contains as much as 47 percent or greater shale content. Carbonate-filled burrows comprise the only carbonate in some shale layers. Davis Formation carbonates primarily are tan to gray dolomitic mudstone and packstone, or grainstone. They are fine to medium grained and fine to medium crystalline. The carbonates contain pellets, fossil fragments, oolites, glauconite, and few stromatolites. Occasional intraclast conglomerates are noted and scattered arkosic or porphyry conglomeratic layers are present.

The core log data (tables 1 and 2) were used to draw the structural contour maps developed for the base (top of Bonneterre Formation; fig. 6) and top (fig. 7) of the Davis Formation. The Davis Formation base is coincident with the base of the St. Francois confining unit and the top of the Bonneterre Formation. The Davis Formation (and St. Francois confining unit) locally is absent in the St. Francois Mountains region, and no attempt was made to delineate where the confining unit is absent. The formation regionally tends to dip radially outward from the mountain area. Faults were considered when contouring the structural surface; however, because of few data in the area of the Conway Fault, the effect of the fault (fig. 1) is not noticeable on the altitude of the Davis Formation base. However, the Palmer Fault system shows an appreciable offset in several boreholes located in T. 35 N., R. 01 W. and T. 36 N., R. 01 E. (figs. 6 and 7), but the data did not indicate vertical offsets in T. 35 N., R. 02 W. A considerable offset to the base of the Davis Formation also is observed to the east of the Black Fault (fig. 6).

The altitude of the base of the Davis Formation (top of Bonneterre Formation; fig. 6) ranges from more than 900 ft above National Geodetic Vertical Datum of 1929 (NGVD 29) in the northeastern part of the study area to nearly 100 ft below NGVD 29 in the southwestern part. This map is based on 147 boreholes with Bonneterre Formation data (table 1). In the extreme northern part of the study area, the structure contours show the dip of the base of the Davis Formation is predominately to the west. The dip gradually changes to

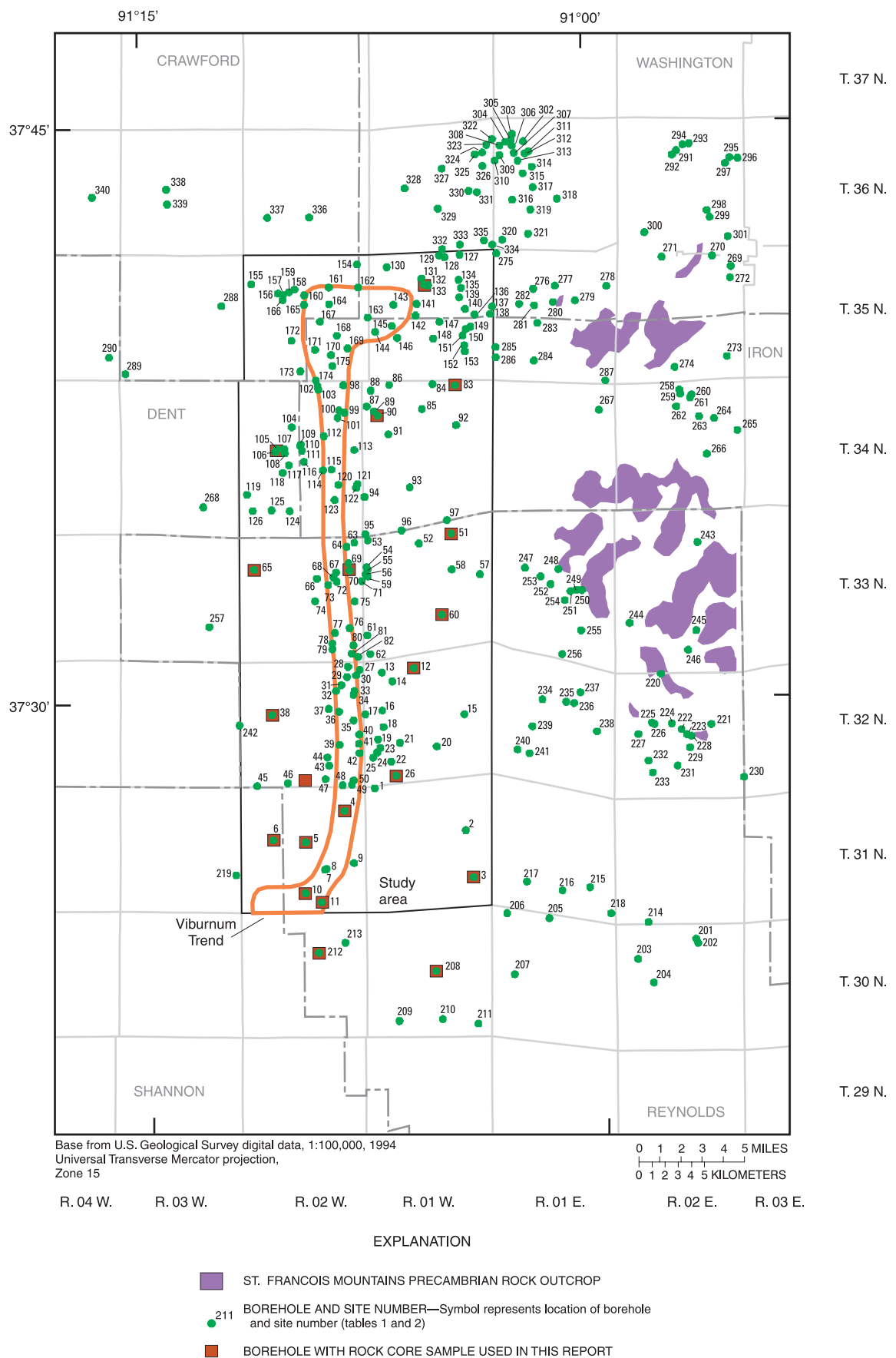


Figure 5. Location of exploration boreholes.

12 Vertical Hydraulic Conductivity of the St. Francois Confining Unit in the Viburnum Trend and Exploration Areas, Missouri

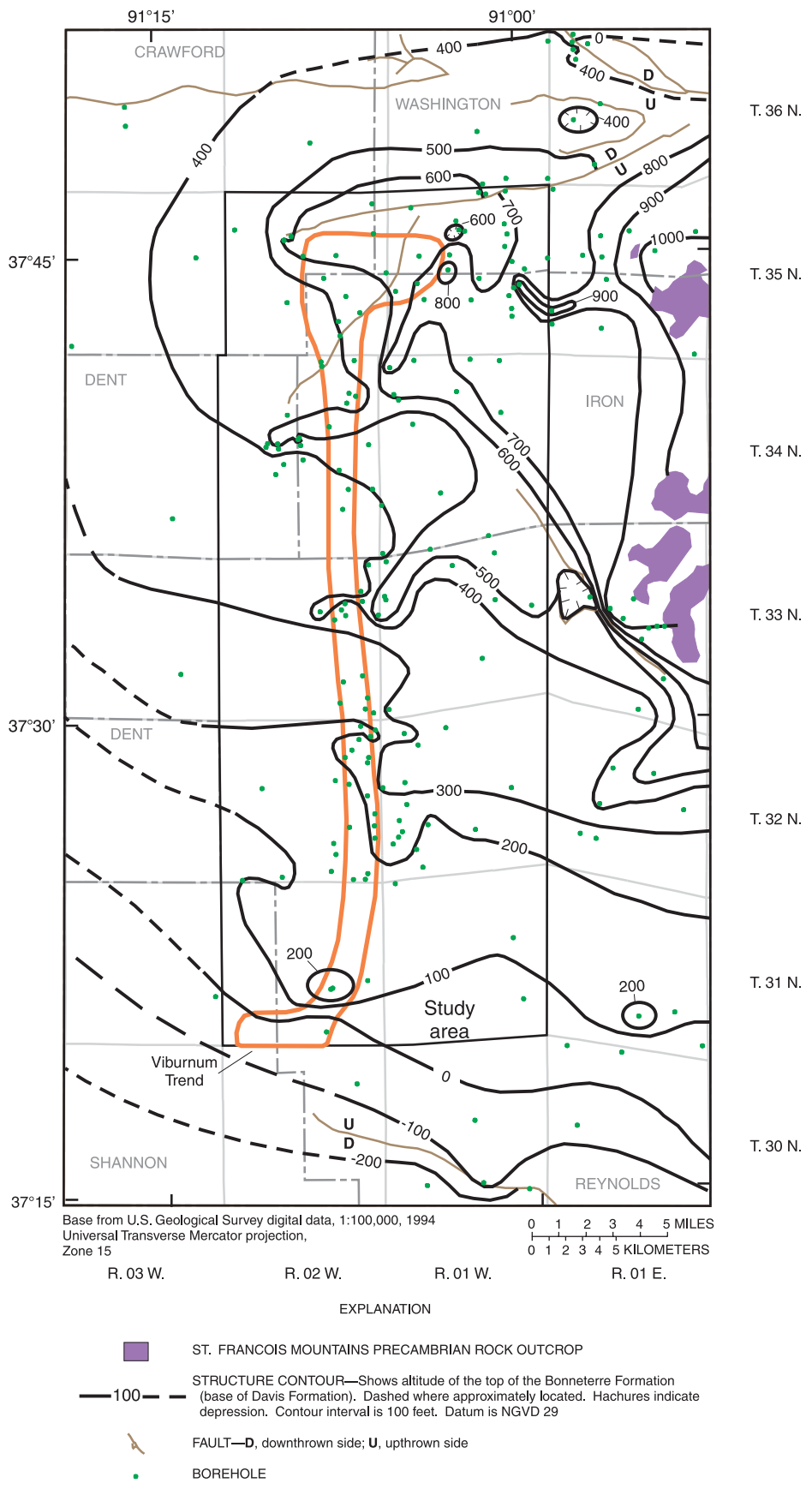


Figure 6. Structure of the top of the Bonneterre Formation (base of Davis Formation).

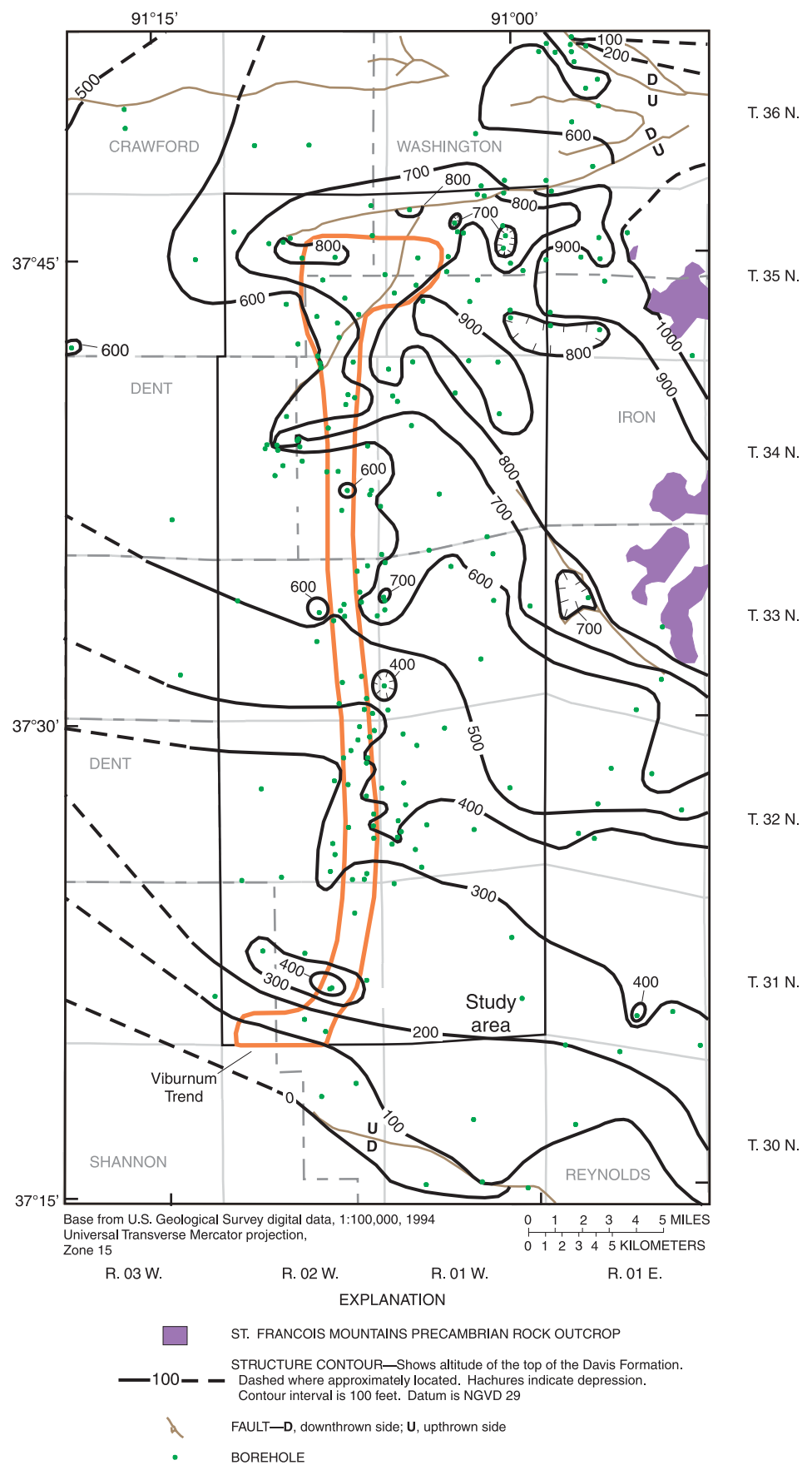


Figure 7. Structure of the top of the Davis Formation.

the south in the central part of the area, and this trend continues through the southern extent of the area. Ninety-three data points located outside of the study area (table 2) were used to contour near the study area boundary.

Large knobs that occur on the Precambrian basement surface in the study area can also express themselves in the overlying strata. Mappable structural features that appear as subsurface ridges or highs can be seen at the base of the Davis Formation in T. 32 N. to T. 34 N. along the border between R. 01 W. and R. 02 W. and in T. 35 N., R. 01 W. (fig. 6). These features may be formed by differential subsidence between the thinner sediments on top of Precambrian knobs and ridges and the thicker sediments on the adjacent flanks (R.W. Harrison, U.S. Geological Survey, oral commun., 1996).

The altitude of the top of the Davis Formation (fig. 7) in the study area ranges from more than 900 ft above NGVD 29 in the northeastern part to less than 100 ft above NGVD 29 in the southern part. The altitudes are based on 159 borehole logs, which identified the depth of the top of the Davis Formation within the study area (table 1) and 83 supplemental logs on adjacent property (table 2). The dip of the formation top is similar to that for the base. In the northern part of the study area (T. 34–35 N.), the generally westward dip is masked by several structural highs that take the form of either isolated highs or ridges that correspond well with Precambrian knobs mapped deeper in the subsurface by Fletcher (1974). The dip gradually trends to the south in the central part of the study area. The effects of the Black Fault (fig. 1) on the structural contours are not as apparent at the top of the formation as at the base, except in the structural low adjacent to the fault shown in T. 33 N., R. 01 E. The offset of the formation top is apparent at localized areas along the Palmer Fault system and the Ellington Fault.

More localized features appear to be present on the structural map showing the top of the Davis Formation than on the formation base. These features are small, isolated highs or larger features such as ridges. Structural lows also appear at several locations with the deepest adjacent to the Black Fault.

Derby-Doerun Dolomite

The Derby-Doerun Dolomite represents a pair of carbonate ramp cycles that include ribbon rock carbonates (succession of thin layers of rocks with different

composition) that grade up-section to sequences of thinner mudstone and thicker grainstone or packstone beds. Mudstone-grainstone sequences and local conglomerates support this depositional hypothesis. Stromatolite zones indicate isolated buildups within the section. Intraclast conglomerate beds (storm-generated mass-flow deposits) moved down slopes of only a few degrees. The basal shaly sequence represents a transition with the Davis Formation (Palmer, 1989, 1991).

The Derby-Doerun Dolomite in the study area is composed of light gray to gray or light tan to brown mudstones, grainstones, and mudstone-matrix stromatolite boundstones, with minor wackestones. Dolostones are fine to medium grained and fine to coarse crystalline. Whiterock and mottled beds are present. The dolostones contain fossil fragments and minor glauconite. Scattered thin black to dark gray and green shales are present. Shale content and thickness increase near the contact with the Davis Formation.

The altitude of the top of the Derby-Doerun Dolomite (fig. 8), which also is the top of the St. Francois confining unit, ranges from more than 1,000 ft above NGVD 29 in the northeastern part of the study area to about 200 ft above NGVD 29 in the southwestern part. These altitudes are based on 151 borehole logs in the study area with Derby-Doerun Dolomite data (table 1) and 90 supplemental borehole logs on adjacent property (table 2). The structure contours show a similar pattern as the contours for the top of the Davis Formation. Several large highs or ridges in the northern part of the study area (T. 34–35 N.) mask the general westward dip of the formation. The dip gradually trends to the south in the central part of the study area. One prominent difference between the top of the Derby-Doerun Dolomite and top of the Davis Formation is the absence of the structural low feature in T. 33 N., R. 01 E. (fig. 8), which appears to be filled by the Derby-Doerun Dolomite.

Thickness and Net Shale Thickness of the St. Francois Confining Unit

Based on logs from 123 boreholes that completely penetrate the St. Francois confining unit in the study area (table 1) and 49 supplemental logs in adjacent property (table 2), the thickness of the confining unit ranges from less than 200 to more than 350 ft in the study area (fig. 9). Local areas of thickening or thinning occur, but in general the unit is from 230 to 280 ft thick. The confining unit thickens in the western part of the

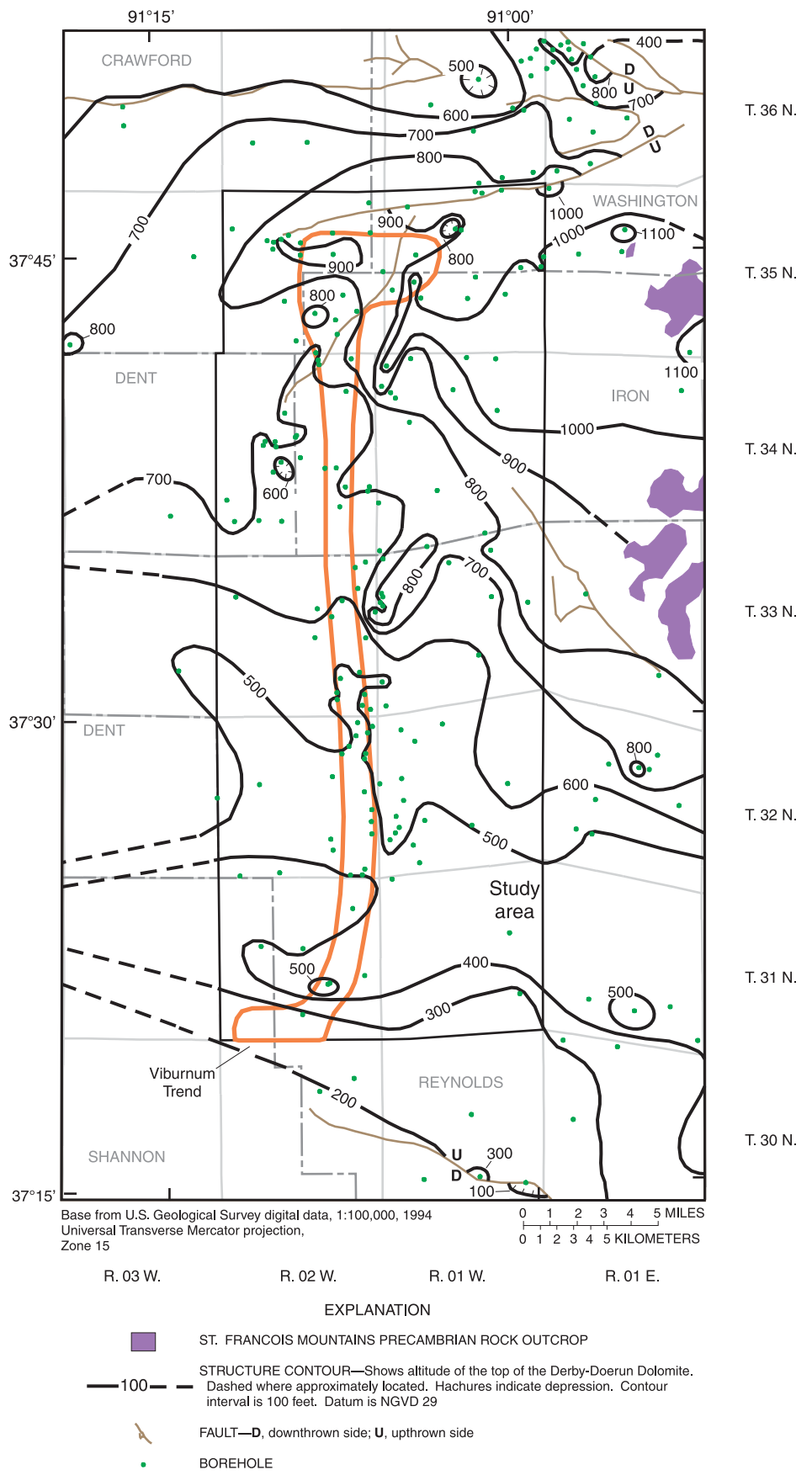


Figure 8. Structure of the top of the Derby-Doerun Dolomite.

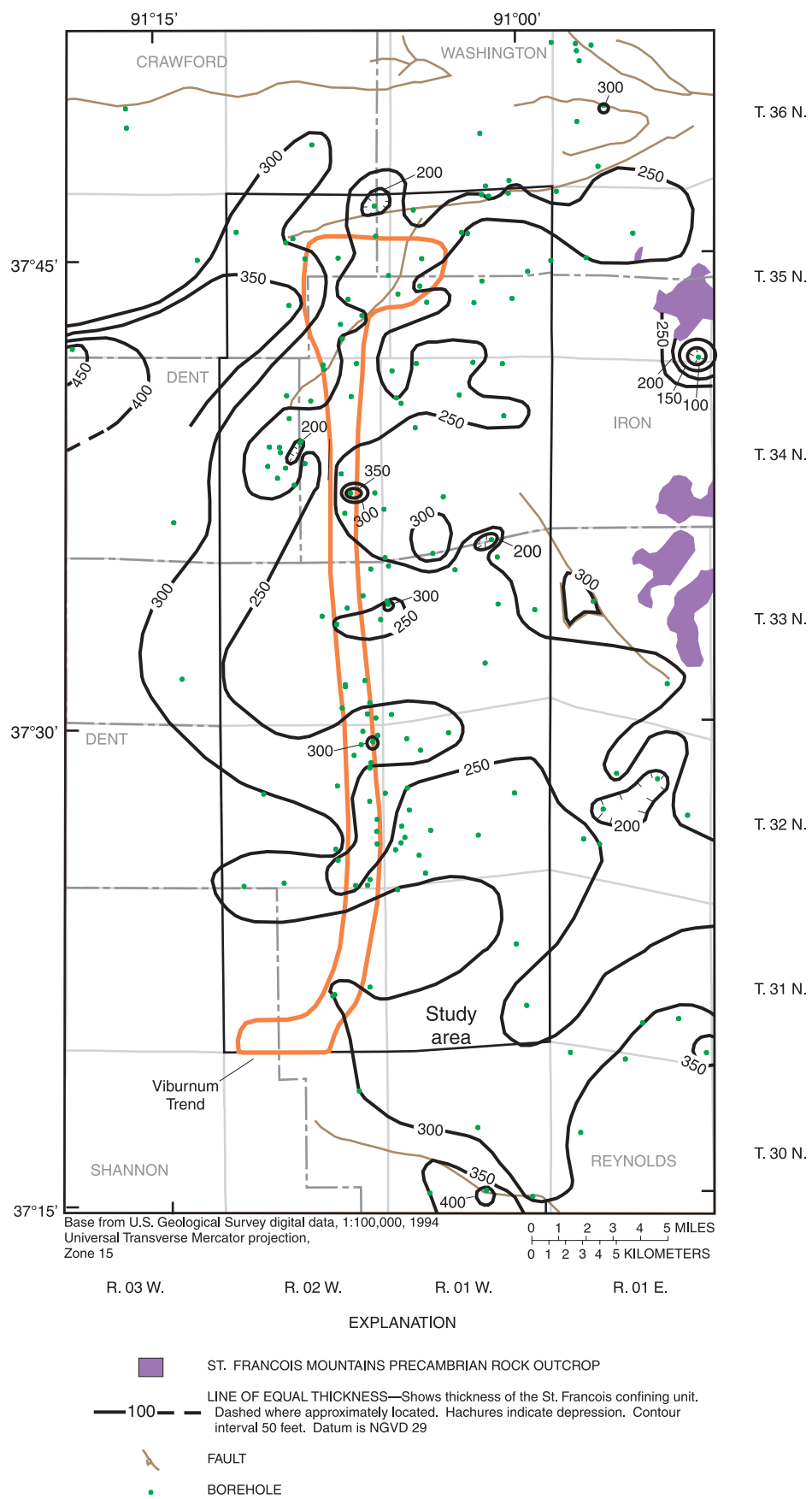


Figure 9. Thickness of the St. Francois confining unit.

study area, especially in the area west of the Conway Fault.

The net shale thickness map (fig. 10) is for the rock sequence from the top of the Derby-Doerun Dolomite to the base of a persistent shale unit located at the base of the Whetstone Creek Member in the upper Bonneterre Formation. This shale unit is referred to locally as the False Davis (fig. 2). This method to determine the net shale thickness is consistent with that used to determine the net shale thickness reported by Kleeschulte and Seeger (2000, 2001). Fourteen net shale thickness values were calculated solely from detailed borehole core log descriptions (table 1) and 22 values were determined by relogging available core samples at the GSRAD McCracken Core Library. Based on the 36 data values, the net shale thickness ranges from less than 25 to greater than 100 ft, with the thickness increasing to the west. This increase is consistent with the current understanding of the geologic environment at the time these formations were deposited. The deeper part of the basin, west of the Viburnum Trend, would have been a low-energy setting that would have allowed the deposition of silts and clays and the formation of shale deposits.

VERTICAL HYDRAULIC CONDUCTIVITY

Shale typically has a smaller vertical hydraulic conductivity than carbonate rocks (Freeze and Cherry, 1979). By determining the thickness of the confining unit, estimating the net shale thickness of the confining unit, and measuring the vertical hydraulic conductivity of the various rock types present in the unit, the effective vertical hydraulic conductivity of the confining unit can be estimated. The permeability of rock core samples from the study area was measured in a laboratory and used to calculate the confining unit vertical hydraulic conductivity. Permeability measures the ease with which a porous medium (rock core) can transmit a liquid under a pressure gradient. It is a function of the medium alone and is not dependent on the fluid used or the force field causing the movement of the liquid (Lohman and others, 1972). Hydraulic conductivity is a measure of the ease with which a specific fluid can be transmitted through a porous medium, and is a function of the medium and of the density and viscosity of the fluid being transmitted.

Representing 250 ft of rock core with only 2 or 3 samples from each borehole has inherent deficiencies. Samples chosen for laboratory analysis are representa-

tive of typical formation lithologies in the sampled borehole. While fractures were not common in the available cores, they occasionally were observed. No rock core samples were sent to the laboratory for analysis that had observed fractures or were broken. This decision could skew the vertical hydraulic conductivity data set, but was necessary to ensure the samples would properly seal in the instrument used to measure permeability.

Methodology

Effective vertical permeability and porosity were determined in the laboratory from rock core samples using methods described by the American Petroleum Institute (1998). Vertical hydraulic conductivity and effective vertical hydraulic conductivity were calculated. Statistical techniques were used to compare vertical hydraulic conductivity among formations and rock types at three locations (Viburnum Trend, and the west and east exploration areas).

The laboratory simulated the in-situ conditions at the depth from which the core samples were collected. The permeability of a medium is inversely proportional to the net confining stresses to which the sample is subjected. A net confining stress [calculated using a pressure gradient of 0.758 pounds per square inch (psi) per foot depth] was applied to each core sample during the permeability analysis (Jim Seale, Core Laboratories, Inc., written commun., 1999). The fluid used during the permeability tests was water prepared to chemically imitate water from the city of Viburnum (fig. 1) public-water supply, which pumps water from an abandoned lead mine in the Bonneterre Formation. The vertical hydraulic conductivity of each sample was, in essence, directly measured because the laboratory water had similar density and viscosity properties as water that flows through the confining unit in the study area.

The core samples were prepared for analysis by cutting each sample to a right-angle cylinder (using air as the bit lubricant), extracting any precipitated salt with methanol, then oven drying the sample for 24 hours at a temperature of 240 degrees Fahrenheit. The bulk volumes of the samples were determined by fluid displacement (Archimedes' principle). Dry weights were recorded and the grain densities were calculated. Helium porosity (American Petroleum Institute, 1998) of the rock core at room conditions was obtained by

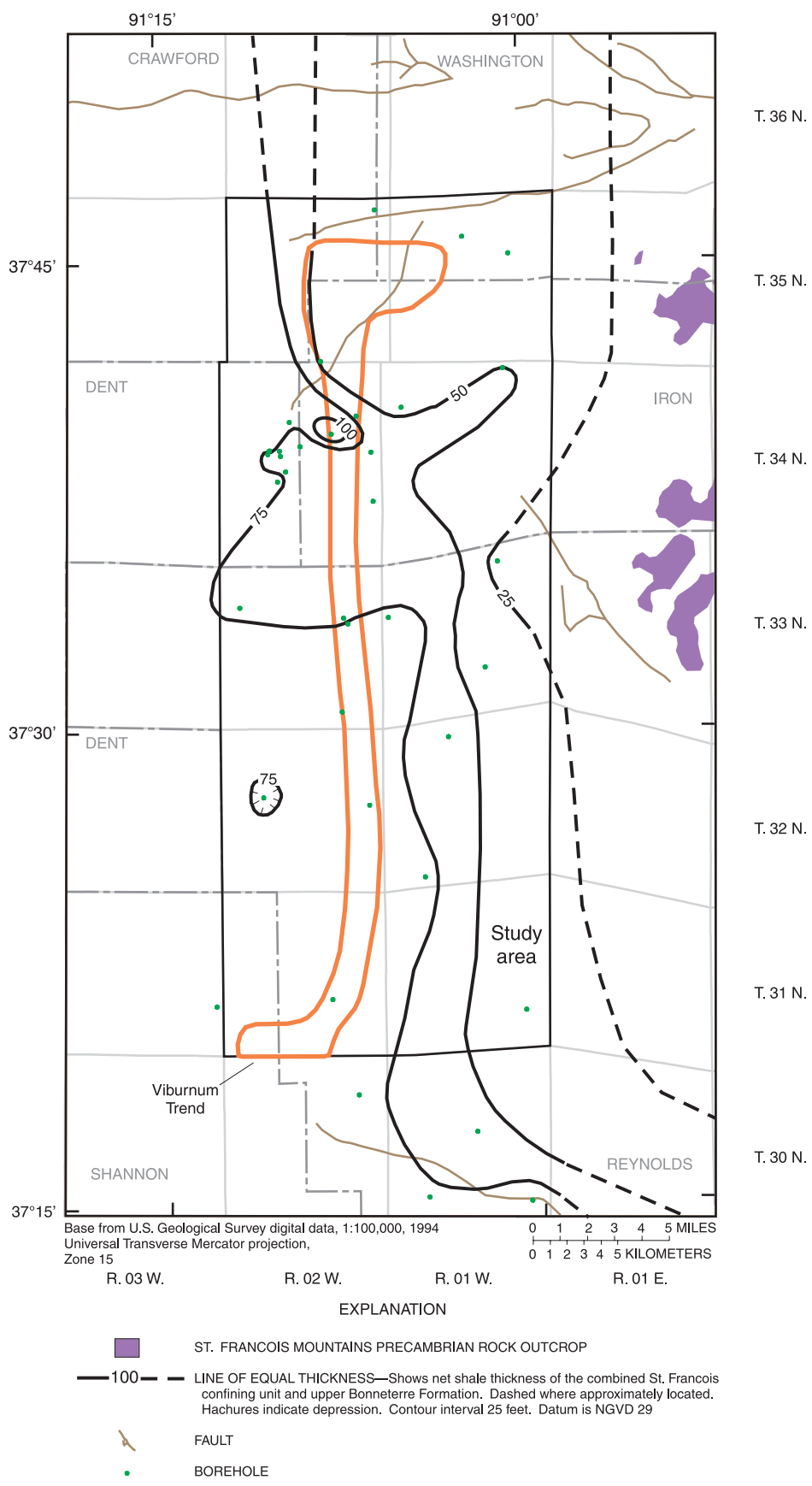


Figure 10. Net shale thickness of the combined St. Francois confining unit and the upper Bonneterre Formation.

measuring grain volume using Boyle's Law (Jim Seale, written commun., 1999).

The core samples were evacuated and pressure saturated at 1,000 psi with the transmitted fluid. Saturation were verified gravimetrically upon removal from the saturation cell. The core samples were then placed in individual core holders, and the calculated net confining stress was applied. The differential flow pressure, time, and water volumes produced at room temperature were recorded. If the permeability was less than the minimum reporting level (1×10^{-9} darcy), the test ended after 48 hours. The effective vertical permeability of the rock core was calculated using the following equation (Jim Seale, written commun., 1999):

$$k = \frac{Q\mu L}{A(Pu - Pd)}, \quad (1)$$

where k = effective permeability, in darcies
(1 darcy = 9.87×10^{-9} centimeter squared);

Q = flow rate, in cubic centimeters per second;

μ = fluid viscosity, in centipoise
(1 centipoise = 0.01 gram per centimeter-second);

L = core length, in centimeters;

A = core area, in square centimeters;

Pu = upgradient pressure, in atmospheres
(1 atmosphere = 14.7 pounds per square inch); and

Pd = downgradient pressure, in atmospheres.

Hydraulic conductivity is related to permeability by (American Petroleum Institute, 1998):

$$K = \frac{k\rho g}{\mu}, \quad (2)$$

where K = hydraulic conductivity, in centimeters per second;

k = effective permeability, in darcies;

ρ = mass density of the fluid, in grams per cubic centimeters;

g = acceleration of gravity, in centimeters per second squared; and

μ = fluid viscosity, in centipoise.

After substitution, the conversion of effective permeability in darcies to hydraulic conductivity in foot per second becomes:

$$K = (3.17) \times 10^{-5} k. \quad (3)$$

The effective vertical hydraulic conductivity of the confining unit was calculated using the expression for two rock types in series having different vertical hydraulic conductivities:

$$\frac{d_t}{K_t} = \frac{d_1}{K_1} + \frac{d_2}{K_2}, \quad (4)$$

where d_t = total thickness of the confining unit, in feet;

d_1, d_2 = thickness of rock type 1 and rock type 2, in feet;

K_t = effective vertical hydraulic conductivity of the confining unit, in foot per second; and

K_1, K_2 = vertical hydraulic conductivity of rock type 1 and rock type 2, in foot per second.

The computer software SYSTAT (SYSTAT Software Inc., 2002) was used for statistical hypothesis tests, summary statistics, and the preparation of boxplots. A level of significance (α -value) below 0.05 caused rejection of the null hypothesis that states the vertical hydraulic conductivity of the data sets being compared are equal. The "attained significance level" (p-value) is a probability value determined from the data (Helsel and Hirsch, 1995). It measures the "believability" of the null hypothesis. The larger the p-value, the more likely is the observed test statistic when the null hypothesis is true and the weaker the evidence to reject the null hypothesis. Boxplots using a logarithmic scale were used to graphically present the vertical hydraulic conductivity data.

Evaluation of the St. Francois Confining Unit along the Viburnum Trend

A total of 40 rock core samples from 18 spatially distributed boreholes were sent to the laboratory for vertical hydraulic conductivity and porosity determination for this report (fig. 5). Thirty-eight rock core samples were from 16 boreholes along the Viburnum Trend and the other two samples were duplicate Derby-Doerun Dolomite samples from the western exploration area analyzed during previous studies (Kleeschulte and Seeger, 2000, 2001). One of the 38 core samples from the Viburnum Trend also was a duplicate Derby-Doerun Dolomite sample that was analyzed by Kleeschulte and Seeger (2000). Data from the 3 duplicate samples were used for quality control and assurance.

Thirty-seven vertical hydraulic conductivity values (one core sample deteriorated in the saturation chamber before the vertical hydraulic conductivity could be determined) and 38 porosity values determined for this report were added to an existing data base for the St. Francois confining unit and St. Francois aquifer. This existing data base already included vertical hydraulic conductivity and porosity values from 94 rock core samples from 28 boreholes in the exploration areas (fig. 1; table 3, at the back of this report) and 24 rock core samples from 5 boreholes along the Viburnum Trend that were analyzed during previous studies (fig. 1; Kleeschulte and Seeger, 2000, 2001).

Combining the previously collected and new vertical hydraulic conductivity data changed the spatial distribution that was trying to be maintained. Nineteen of the 24 previously collected vertical hydraulic conductivity and porosity values from the Viburnum Trend (6 Derby-Doerun Dolomite and 13 Davis Formation values) and one duplicate Derby-Doerun Dolomite sample analyzed for this report were from boreholes in T. 31 N., R. 02 W. (fig. 1). This heavily biased the number of samples from this one township. To make the data set more spatially representative, the data from T. 31 N., R. 02 W. were combined, and only the median vertical hydraulic conductivity value for the Derby-Doerun Dolomite and the median vertical hydraulic conductivity value for the Davis Formation were used to represent the formations in that area. The same approach was used to represent the three lithologies that were present in that township. These samples are denoted by borehole identification in table 3 as “Generic F” (formation) or “Generic L” (lithology).

The modified vertical hydraulic conductivity data set used for the evaluation of the St. Francois confining unit and St. Francois aquifer (used for comparison purposes) along the Viburnum Trend in this report consisted of 46 values [17 Derby-Doerun Dolomite, 21 Davis Formation, 3 Bonneterre Formation, 2 generic formation (1 Derby-Doerun Dolomite and 1 Davis Formation), and 3 generic lithology (1 carbonate, 1 shale, and 1 carbonate and shale)]. The modified porosity data set for the Viburnum Trend consisted of 42 values (17 Derby-Doerun Dolomite, 22 Davis Formation, and 3 Bonneterre Formation). No generic formation or lithology values were included in the porosity data set.

Four censored values for the Davis Formation were in the modified Viburnum Trend data set. These data were collected by Kleeschulte and Seeger (2000) and had vertical hydraulic conductivity values less than

the minimum reporting level of 3.17×10^{-14} ft/s (foot per second). None of the new vertical hydraulic conductivity values determined for this report and added to the existing St. Francois confining unit data set were less than the minimum reporting level.

A Lilliefors (two-tailed) test for normality (Iman and Conover, 1983) indicated the 40 vertical hydraulic conductivity values for the St. Francois confining unit formations along the Viburnum Trend in the modified data set (17 Derby-Doerun Dolomite, 21 Davis Formation, and 2 generic formation) were not normally distributed ($p = 0.000$). When a logarithmic transformation was applied, the data are considered normally distributed ($p = 0.070$); however, the strength of the evidence was marginal. Because the sample size was small (40 values) and the p-value of the transformed data was slightly greater than the preassigned α -value of 0.05, the nonparametric Kruskal-Wallis test (Helsel and Hirsch, 1995), was chosen to analyze the ranked data. When only two groups are used, the procedure reduces to the Mann-Whitney test (SYSTAT Software Inc., 2002).

Statistical comparisons of vertical hydraulic conductivity values of rock cores from the St. Francois confining unit grouped by formation (Derby-Doerun Dolomite and Davis Formation) show the data from the two formations are statistically similar (p -value = 0.073; table 4). The boxplot of the data (fig. 11A) shows that with the outliers, the data from the two formations span more than 5 orders of magnitude from 8.66×10^{-9} to 3.17×10^{-14} ft/s (tables 3 and 5). The interquartile range (see fig. 11 explanation) for the Derby-Doerun Dolomite (1.64×10^{-11} to 1.04×10^{-12} ft/s) spans slightly more than 1 order of magnitude, and the Davis Formation spans nearly 2 orders of magnitude (6.57×10^{-12} to 8.73×10^{-14} ft/s). The median vertical hydraulic conductivity value for Derby-Doerun Dolomite samples (3.27×10^{-12} ft/s) is similar to the median value for the Davis Formation samples (2.38×10^{-12} ft/s). Although statistics show the vertical hydraulic conductivity of the Derby-Doerun Dolomite and Davis Formation are considered similar, visually on the boxplots, the Davis Formation appears to be the more hydraulically restrictive medium (fig. 11A).

Three samples from the upper Bonneterre Formation (above the False Davis) also were plotted for comparison purposes (fig. 11A). The vertical hydraulic conductivity of these three samples are statistically similar to those of the Derby-Doerun Dolomite (p -value = 0.615) and the Davis Formation (p -value =

Table 4. Summary of Kruskal-Wallis statistical test p-values

[DDR, Derby-Doerun Dolomite; DVS, Davis Formation; Carb, Carbonate sample; Both, Carbonate and shale sample; VT, Viburnum Trend; West, West exploration area; East, East exploration area]

Formation or Rock Type Comparisons	p-value
Viburnum Trend	
Formation	
DDR-DVS	0.073
Rock Type (all three rock types)	0.016
Carb-Shale	.012
Shale-Both	.032
Both-Carb	.118
Viburnum Trend, West and East Exploration Areas	
St. Francois confining unit (all three locations)	0.000
VT-West	.000
VT-East	.074
West-East	.012
Formation	
DDR (all three locations)	0.096
VT-West	.066
VT-East	.128
West-East	.212
DVS (all three locations)	0.034
VT-West	.018
VT-East	.420
West-East	.077
Rock Type	
Carbonate (all three locations)	0.001
VT-West	.001
VT-East	.019
West-East	.020
Shale (all three locations)	0.657
VT-West	.629
VT-East	.165
West-East	.668
Both (all three locations)	0.281
VT-West	.111
VT-East	.279
West-East	.766

0.094). This indicates that the confining ability of the upper Bonneterre Formation (above the False Davis) at the locations tested along the Viburnum Trend is comparable to the Derby-Doerun Dolomite and Davis Formation, even though regionally, the entire Bonneterre Formation is considered an aquifer. However, visually on the boxplots, the Davis Formation appears to have the lowest vertical hydraulic conductivity values compared to the Derby-Doerun Dolomite and upper Bonneterre Formation.

The ranked vertical hydraulic conductivity data from the St. Francois confining unit along the Viburnum Trend also was grouped by rock type (carbonate, shale, and samples containing both carbonate and shale). This data set contains 41 values; the two generic formation values were removed, and the three generic lithology values were added. Multiple comparisons were made to determine if the shale component of the confining unit was indeed more restrictive to flow than the carbonate component. The small shale sample size was caused in part by the age of the core samples. Older core samples become drier causing the shale to separate on small bedding planes (poker chipped) and become fragile. When removing samples from the core box, the shale tends to fall apart and is no longer coherent. A statistical comparison of the vertical hydraulic conductivity values using rock type as the grouping variable shows the three groups are different (p-value = 0.016; table 4). However, when the different rock types are paired and then compared, carbonate samples and samples containing both carbonate and shale shows a statistical similarity (p-value = 0.118). The other groupings, carbonate samples and shale samples (p-value = 0.012) and shale samples and samples containing both carbonate and shale (p-value = 0.032) are statistically different. The small shale sample set may have affected this relation.

The shale samples generally have the smallest vertical hydraulic conductivity and the carbonate samples have the largest (fig. 11B). Samples containing both shale and carbonate appear to have an intermediate value of both rock types indicating the affect that each component (carbonate or shale) has on the overall vertical hydraulic conductivity of the core sample. The variability of the interquartile range of samples containing both carbonate and shale is larger than either the carbonate or shale samples. This could be a result of the varying percentages of carbonate and shale in the samples with mixed lithology. The median vertical hydraulic conductivity of the shale samples (1.00×10^{-13} ft/s;

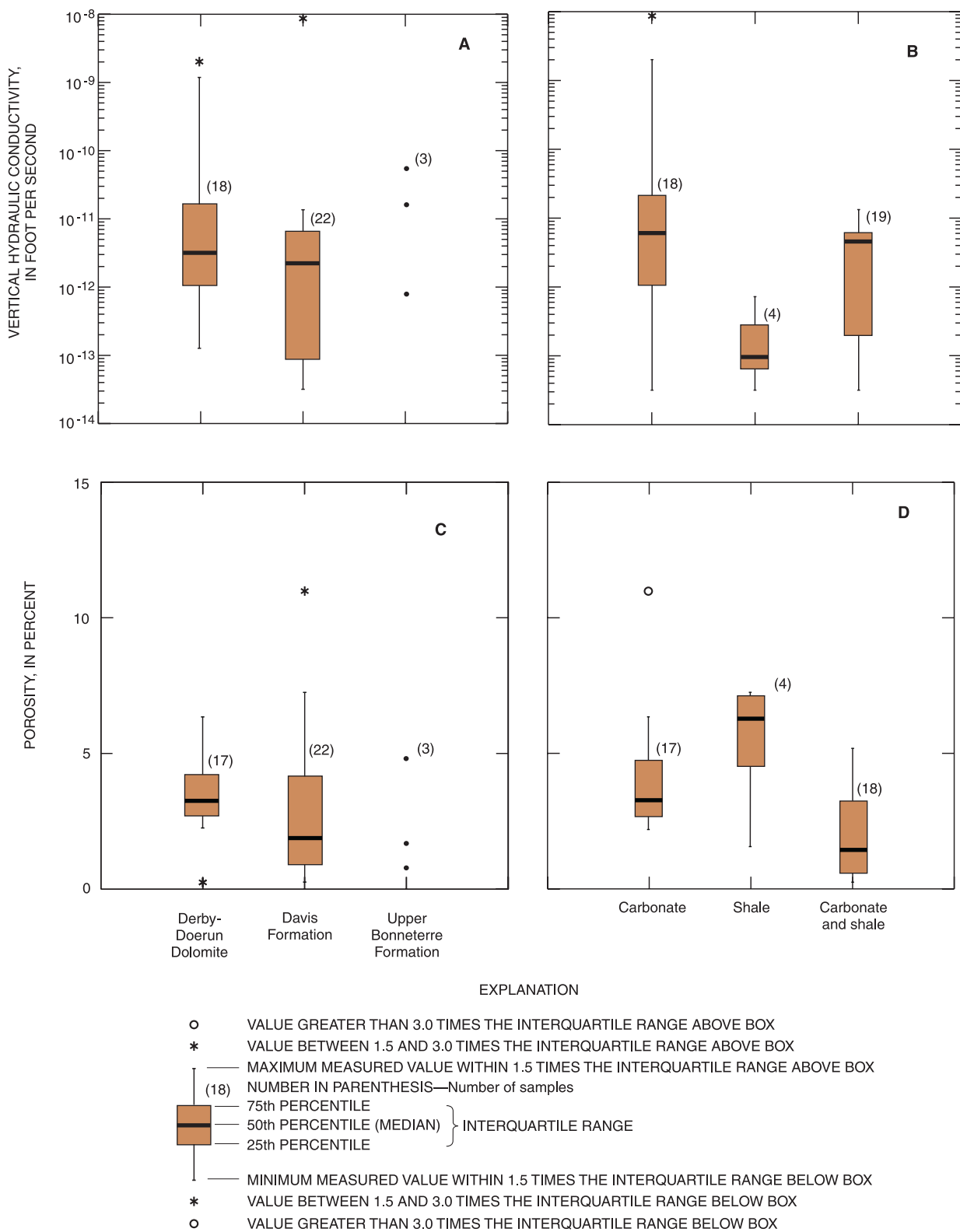


Figure 11. The vertical hydraulic conductivity and porosity of the St. Francois confining unit and upper Bonneterre Formation plotted by formations and rock types along the Viburnum Trend.

Table 5. Summary of vertical hydraulic conductivity values for the St. Francois confining unit along the Viburnum Trend

[ft/s, foot per second]

	Number of samples	Vertical hydraulic conductivity			
		Minimum (ft/s)	Maximum (ft/s)	Median (ft/s)	Interquartile range (ft/s)
Formation					
Derby-Doerun Dolomite	18	1.27×10^{-13}	2.02×10^{-9}	3.27×10^{-12}	1.64×10^{-11} to 1.04×10^{-12}
Davis Formation	22	3.17×10^{-14}	8.66×10^{-9}	2.38×10^{-12}	6.57×10^{-12} to 8.73×10^{-14}
Rock type					
Carbonate	18	3.17×10^{-14}	8.66×10^{-9}	6.17×10^{-12}	2.06×10^{-11} to 1.04×10^{-12}
Shale	4	3.17×10^{-14}	7.26×10^{-13}	1.00×10^{-13}	2.76×10^{-13} to 6.37×10^{-14}
Carbonate and shale	19	3.17×10^{-14}	1.33×10^{-11}	4.56×10^{-12}	6.21×10^{-12} to 2.01×10^{-13}

table 5) was 62 times less than the carbonate samples (median value 6.17×10^{-12} ft/s) and 45 times less than carbonate and shale samples (4.56×10^{-12} ft/s).

Because shale along the Viburnum Trend has the smallest vertical hydraulic conductivity of the three rock types, it would be the most restrictive medium to the flow of water in the confining unit. Consequently, the net shale thickness along the Viburnum Trend significantly affects the effective vertical hydraulic conductivity of the confining unit. As the percentage of shale increases in a given horizon, the vertical hydraulic conductivity decreases.

Porosity values were available for 39 core samples from the St. Francois confining unit along the Viburnum Trend; no values were used for the generic samples. Porosity values range from a minimum of 0.25 to a maximum of 10.98 percent (fig. 11C; table 3). Lilliefors testing (Iman and Conover, 1983) shows the porosity values have a normal distribution (p-value = 0.238). Because the data were normally distributed and from two independent data groups, the two sample separate variance t-test was used to compare the porosity values of Derby-Doerun Dolomite and Davis Formation samples (Helsel and Hirsch, 1995). The test indicated no significant difference (p-value = 0.341) between the two groups. The porosity values of samples from the Davis Formation are more variable than the porosity values of the Derby-Doerun Dolomite samples, which is shown by the interquartile range of the Davis Formation samples having greater than twice the span of the Derby-Doerun Dolomite samples.

Using the two sample separate variance t-test (Helsel and Hirsch, 1995) for comparison of porosity

values of the different rock types (fig. 11D), a statistical similarity exists between the porosity value of samples containing shale and samples containing both carbonate and shale (p-value = 0.079), but this relation is not as strong as the comparison between only carbonate and only shale samples (p-value = 0.432). Samples containing only carbonate and samples containing both carbonate and shale are statistically different (p-value = 0.003). The Spearman rank-order correlation (Helsel and Hirsch, 1995) shows a weak correlation between vertical hydraulic conductivity and porosity ($r = 0.237$).

The vertical hydraulic conductivity of carbonate and shale was statistically different in the St. Francois confining unit along the Viburnum Trend. The range of effective vertical hydraulic conductivity for the confining unit was estimated using minimum and maximum thickness values of the confining unit, total thickness of the carbonate and shale components in the confining unit, and appropriate minimum and maximum vertical hydraulic conductivity values for the carbonate and shale rock types. The St. Francois confining unit along the Viburnum Trend was estimated to have a minimum thickness of 230 ft (approximately the lower percentile) and a maximum thickness of 280 ft (approximately the upper percentile; table 1). A minimum and maximum net shale thickness of 20 and 100 ft, respectively, was also used (fig. 10; table 1). The upper and lower percentiles for carbonate and shale rock types were used to estimate the vertical hydraulic conductivities. The range of 2.06×10^{-11} to 1.04×10^{-12} ft/s was used for carbonate rocks and 2.76×10^{-13} to 6.37×10^{-14} ft/s was used for shale.

By using appropriate minimum and maximum values of confining unit thickness, net shale thickness, and vertical hydraulic conductivity, the range of effective vertical hydraulic conductivity for the St. Francois confining unit in the Viburnum Trend was estimated to be a minimum of 2×10^{-13} ft/s and a maximum of 3×10^{-12} ft/s (fig. 12A). These effective vertical hydraulic conductivity values are considered small and verify conclusions of previous studies (Warner and others, 1974; Miller and Vandike, 1997; Kleeschulte, 2001); the confining unit effectively impedes the flow of ground water between the Ozark aquifer and the St. Francois aquifer along the Viburnum Trend.

Evaluation of the St. Francois Confining Unit along the Viburnum Trend and Exploration Areas

Another objective of this report is to compare the vertical hydraulic conductivity of rock core samples from the St. Francois confining unit in the active mining area of the Viburnum Trend and in the exploration areas where future mining may occur. The west (T. 25–27 N., R. 03–04 W.) and east (T. 25–27 N., R. 01–02 W.) exploration areas both include six townships (fig. 1). For this analysis, previously collected vertical hydraulic conductivity data from two earlier studies (Kleeschulte and Seeger, 2000, 2001) were combined with the data collected along the Viburnum Trend for this report. The data sets are considered comparable because all the analyzed samples were chosen by the same people, using the same selection criteria, and were analyzed by the same laboratory using the same methods. Before combining the data sets, 27 vertical hydraulic conductivity data values from the west exploration area and 2 values from the east exploration area were censored to the minimum reporting level of 3.17×10^{-14} ft/s. A Lilliefors (two-tailed) test for normality (Iman and Conover, 1983) indicated the combined vertical hydraulic conductivity data were not normally distributed ($p = 0.000$), and attempts to transform the data into a normal distribution failed. This failure was caused in part by the numerous censored values being grouped at the lower end of the data set. Consequently, the nonparametric Kruskal-Wallis statistical test (Helsel and Hirsch, 1995) was chosen to test the null hypothesis that the vertical hydraulic conductivity of the St. Francois confining unit was similar along the Viburnum Trend and in the west and east exploration areas.

When the vertical hydraulic conductivity data were grouped by location, the St. Francois confining unit was statistically different in the three locations (p -value = 0.000; table 4). However, when the data in the three locations were analyzed in pairs, the Viburnum Trend and east exploration area showed a statistical similarity (p -value = 0.074). The other combinations, west and east exploration areas (p -value = 0.012) and the Viburnum Trend and west exploration area (p -value = 0.000), showed a statistical difference (fig. 12A). The vertical hydraulic conductivity values visually appear smaller in the west exploration area than at the other two locations.

Statistical analysis were used to determine if the vertical hydraulic conductivity differences between locations primarily were caused by variations in the geologic formations or rock type. Data from the confining unit were grouped by formation and then sub-grouped by location. Analysis of Derby-Doerun Dolomite vertical hydraulic conductivity values (fig. 12B) show similarity at all three locations (p -value = 0.096; table 4). When comparing the Derby-Doerun Dolomite vertical hydraulic conductivity samples by location pairs, the strongest similarity was among the west and east exploration areas (p -value = 0.212), followed by the Viburnum Trend and east exploration area (p -value = 0.128), and then by the Viburnum Trend and the west exploration area (p -value = 0.066).

Statistical analysis of Davis Formation vertical hydraulic conductivity values (fig. 12B) grouped by location showed a statistical difference (p -value = 0.034; table 4). However, comparing location pairs show a strong similarity between samples from the Viburnum Trend and east exploration area (p -value = 0.420); followed by the west and east exploration areas (p -value = 0.077), but no similarity was shown between the Viburnum Trend and west exploration area (p -value = 0.018). The statistical results could be considered paradoxical because comparing the entire Davis Formation data set by location shows a statistical difference, but two of the three possible location pairs shows statistical similarity. Apparently, the differences between the Viburnum Trend and west exploration area is sufficient to cause the α -value for the data set to be less than 0.05. The median and interquartile range of the boxplots indicate the vertical hydraulic conductivity of the Derby-Doerun Dolomite and Davis Formation generally are largest in the Viburnum Trend area and smallest in the west exploration area.

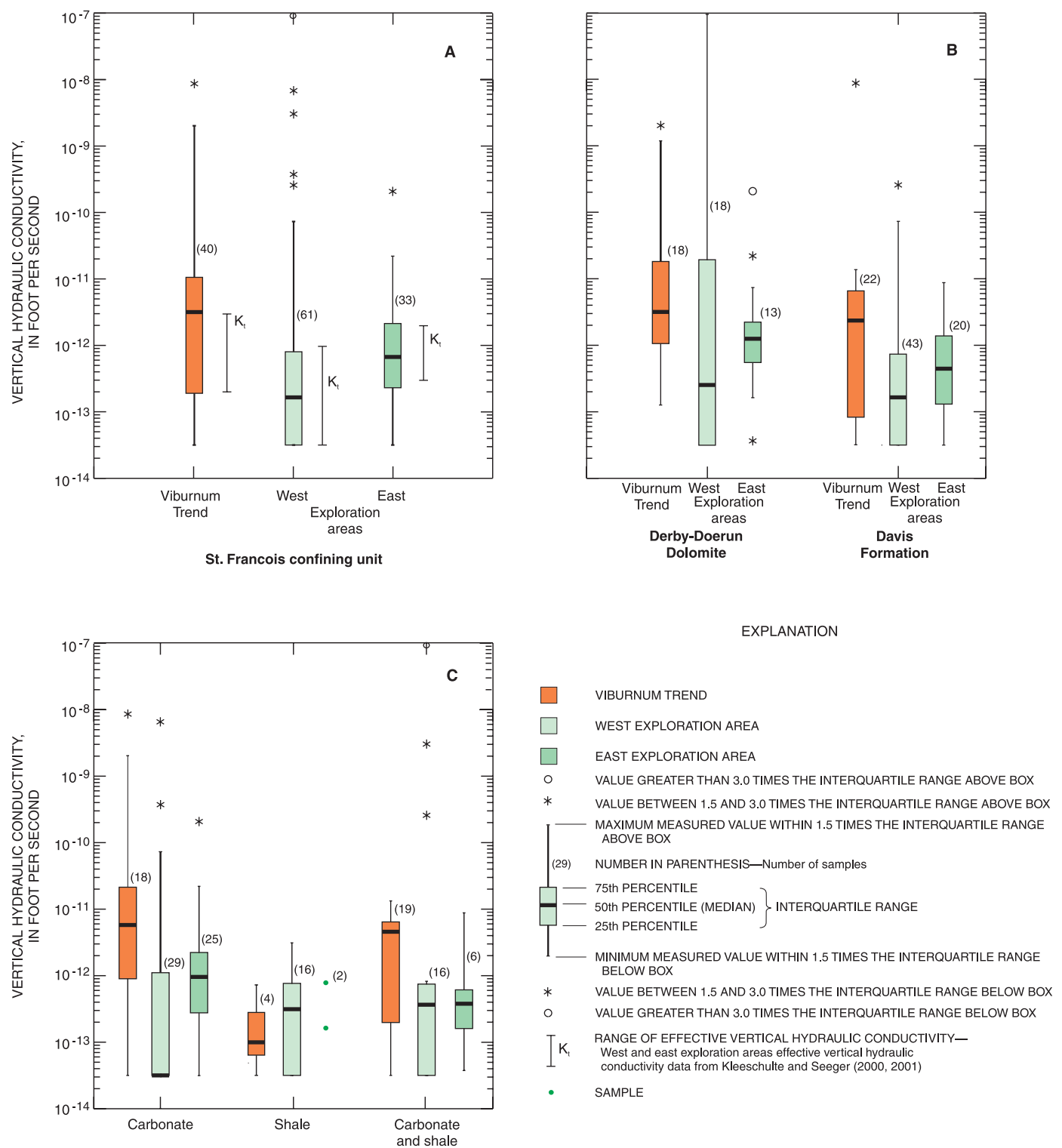


Figure 12. The vertical hydraulic conductivity of the St. Francois confining unit and rock types along the Viburnum Trend and in the exploration areas.

Statistical comparisons of the vertical hydraulic conductivity values of the various rock types (carbonate, shale, and samples containing both carbonate and shale) grouped by location also were performed using the nonparametric Kruskal-Wallis statistical test (Helsel and Hirsch, 1995). When the carbonate values were considered and grouped by location, statistical analysis showed the three locations were statistically different (p -value = 0.001; table 4). The vertical hydraulic conductivity values of carbonate samples analyzed by location pairs showed no statistical similarities between any of the three locations (all the p -values were less than or equal to 0.020). Generally, the carbonate samples from the Viburnum Trend had the largest vertical hydraulic conductivity values and the west exploration area had the smallest (fig. 12C). The shale samples were statistically similar for all locations (p -value = 0.657). The small data sets for the Viburnum Trend and east exploration area plot within the interquartile range of the larger west exploration area data set. The largest statistical similarity for shale samples occurs when comparing the west and east exploration areas (p -value = 0.668), followed by the Viburnum Trend and west exploration area (p -value = 0.629), and the Viburnum Trend and east exploration area (p -value = 0.165). When the mixed lithology samples are considered and grouped by location, the statistical analysis showed a similarity between all locations (p -value = 0.281). The largest p -value occurs when comparing the west and east exploration areas (p -value = 0.766), followed by the Viburnum Trend and east exploration area (p -value = 0.279), and the Viburnum Trend and west exploration area (p -value = 0.111).

In summary, the vertical hydraulic conductivity values by formation and rock type generally are the largest in the Viburnum Trend and smallest in the west exploration area, and no statistical similarity exists between these two areas. The statistical differences in these values do not appear to be attributed strictly to either the Derby-Doerun Dolomite or Davis Formation, but instead they are caused by the differences in the carbonate vertical hydraulic conductivity values at the three locations (fig. 12C).

The calculated effective vertical hydraulic conductivity range for the St. Francois confining unit at each location is: 2×10^{-13} to 3×10^{-12} ft/s for the Viburnum Trend; 3×10^{-14} (minimum reporting level) to 1×10^{-12} ft/s for the west exploration area (Kleeschulte and Seeger, 2000); and 3×10^{-13} to 2×10^{-12} ft/s for the east exploration area (Kleeschulte and Seeger, 2001; fig.

12A). Based on the calculated vertical hydraulic conductivity ranges, the St. Francois confining unit is considered ‘tight’ at all locations, but in relation to each other, the unit in the west exploration area is the tightest, and the unit in the Viburnum Trend is the most conductive. Active mining has been occurring along the Viburnum Trend with no apparent large cones of depression developing in the potentiometric surface of the Ozark aquifer as a result of mining activity. Therefore, using similar mining practices as those along the Viburnum Trend, no large cones of depression in the Ozark aquifer would be expected in the exploration areas, in particular the west exploration area, unless preferred-path secondary permeability has developed along faults or fractures or resulted from exploration activities.

SUMMARY AND CONCLUSIONS

The confining ability of the St. Francois confining unit (Derby-Doerun Dolomite and Davis Formation) was evaluated in 10 townships (T. 31–35 N. and R. 01–02 W.) along the Viburnum Trend of southeastern Missouri by describing the stratigraphy and calculating the vertical hydraulic conductivity of core samples from laboratory measured vertical permeability. These vertical hydraulic conductivity data were compared to the vertical hydraulic conductivity data collected during two previous studies 20 miles south of the Viburnum Trend in two lead-zinc exploration areas which may be a southern extension of the Viburnum Trend. Geologic formations from the base of the Potosi Dolomite to the top of the Rouibidoux Formation form the surficial Ozark aquifer, the primary source of water for domestic and public-water supplies and major springs in southern Missouri. The St. Francois confining unit lies beneath the Ozark aquifer and impedes the movement of water between the overlying Ozark aquifer and the underlying St. Francois aquifer (composed of the Bonneterre Formation and Lamotte Sandstone). The Bonneterre Formation is the primary host formation for lead-zinc ore deposits of the Viburnum Trend and potential host formation in the exploration areas. For most of the more than 40 years the mines have been in operation along the Viburnum Trend, about 27 million gallons per day have been pumped from the St. Francois aquifer for mine dewatering. Previous studies conducted along the Viburnum Trend to assess the effects of mine dewatering in the St. Francois aquifer on water levels in the surficial Ozark aquifer have con-

cluded that no large cones of depression have developed in the potentiometric surface of the Ozark aquifer as a result of mining activity.

Because of the similarity in geology, stratigraphy, and depositional environment between the Viburnum Trend and the exploration areas, the Viburnum Trend may be used as a pertinent, full-scale model to study and assess how mining may affect the exploration areas. The confining ability of the St. Francois confining unit along the Viburnum Trend and in the exploration areas are compared to evaluate potential mine dewatering effects in the exploration areas.

The St. Francois confining unit is a complex series of dolostones, limestones, and shales. Borehole log data describe the unit as generally being 230 to 280 feet thick along the Viburnum Trend. The confining unit thickens in the western part of the study area, especially in the area west of the Conway Fault. The formations of the confining unit regionally tend to dip radially outward from the St. Francois Mountains area. In the northern part of the study area, the dip of the formations may be masked by underlying Precambrian structural highs (knobs), but generally is westward. The dip then gradually trends to the south in the central part of the study area. Based on 36 data values, the net shale thickness ranges from less than 25 to greater than 100 feet in the study area with the thickness increasing toward the west.

Vertical hydraulic conductivity values determined from laboratory permeability tests were used to represent the confining ability of the St. Francois confining unit along the Viburnum Trend. The data were not normally distributed and the nonparametric Kruskal-Wallis test was chosen to test the null hypothesis that the vertical hydraulic conductivity of the data sets being compared are equal. Statistical tests show the values for the Derby-Doerun Dolomite and Davis Formation are similar and boxplots of the data show the Davis Formation would be the more hydraulically restrictive medium. Multiple comparisons on the vertical hydraulic conductivity data from the St. Francois confining unit along the Viburnum Trend grouped by rock type (carbonate, shale, and samples containing both carbonate and shale) showed samples with only shale and only carbonate were statistically different, as were the shale samples and samples containing both carbonate and shale. Shale samples generally have the smallest vertical hydraulic conductivity and the carbonate samples have the largest. Only considering the median values of these data groups, the vertical hydraulic

conductivity of the shale samples [1.00×10^{-13} ft/s (foot per second)] was 62 times less than the carbonate samples (median value 6.17×10^{-12} ft/s) and 45 times less than carbonate and shale samples (4.56×10^{-12} ft/s), making shale a more restrictive medium to the flow of water in the confining unit. Consequently, the net shale thickness of the confining unit along the Viburnum Trend significantly affects the effective vertical hydraulic conductivity. As the percentage of shale increases in a given horizon, the vertical hydraulic conductivity decreases.

By using appropriate minimum and maximum values of confining unit thickness, net shale thickness, and vertical hydraulic conductivity, the range of effective vertical hydraulic conductivity for the confining unit in the Viburnum Trend was estimated to be a minimum of 2×10^{-13} ft/s and a maximum of 3×10^{-12} ft/s. These vertical hydraulic conductivity values are considered small and verify conclusions of previous studies that the confining unit effectively impedes the flow of ground water between the Ozark aquifer and the St. Francois aquifer along the Viburnum Trend.

Another objective of this report is to compare the vertical hydraulic conductivity of rock core samples from the St. Francois confining unit in the active mining area of the Viburnum Trend and the exploration area where future mining may occur. The exploration area was divided into west (T. 25–27 N., R. 03–04 W.) and east (T. 25–27 N., R. 01–02 W.) areas. Previously collected vertical hydraulic conductivity data from two earlier studies were combined with the data collected along the Viburnum Trend for this report. The combined vertical hydraulic conductivity data set was not normally distributed and attempts to transform the data into a normal distribution failed. Consequently, the nonparametric Kruskal-Wallis statistical test was chosen to test the null hypothesis that the vertical hydraulic conductivity of the St. Francois confining unit was similar along the Viburnum Trend and in the west and east exploration areas.

A comparison of the vertical hydraulic conductivities of rock core samples from the St. Francois confining unit shows the Viburnum Trend and west and east exploration areas are statistically different. The vertical hydraulic conductivity values generally are the largest in the Viburnum Trend and are smallest in the west exploration area. The statistical differences in these values do not appear to be attributed strictly to either the Derby-Doerun Dolomite or Davis Formation, but instead they are caused by the differences in the car-

bonate vertical hydraulic conductivity values at the three locations.

The calculated effective vertical hydraulic conductivity range for the St. Francois confining unit at each location is: 2×10^{-13} to 3×10^{-12} ft/s for the Viburnum Trend; 3×10^{-14} (minimum reporting level) to 1×10^{-12} ft/s for the west exploration area; and 3×10^{-13} to 2×10^{-12} ft/s for the east exploration area. Based on the calculated vertical hydraulic conductivity ranges, the St. Francois confining unit is considered ‘tight’ at all locations, but in relation to each other, the unit in the west exploration area is the tightest, and the unit in the Viburnum Trend is most conductive area. No apparent large cones of depression have developed in the potentiometric surface of the Ozark aquifer as a result of mining activity along the Viburnum Trend. Therefore, using similar mining practices as those along the Viburnum Trend, no large cones of depression in the Ozark aquifer would be expected in the exploration areas, unless preferred-path secondary permeability has developed along faults or fractures or resulted from exploration activities.

REFERENCES

- American Petroleum Institute, 1998, Recommended practices for core analysis: Washington, D.C., 195 p.
- Dunham, R.J., 1962, Classification of carbonate rocks according to depositional texture, in Ham, W.E., ed., Classification of Carbonate Rocks—A Symposium: Tulsa, Okla., American Association of Petroleum Geologists Memoir One, p. 108–121.
- Fletcher, C.S., 1974, The geology and hydrogeology of the New Lead Belt, Missouri: Rolla, University of Missouri, unpublished M.S. thesis, 91 p.
- Freeze, R.A., and Cherry, J.A., 1979, Groundwater: Englewood Cliffs, N.J., Prentice-Hall, Inc., 604 p.
- Helsel, D.R., and Hirsch, R.M., 1995, Statistical methods in water resources, in Studies in Environmental Science 49: Amsterdam, The Netherlands, Elsevier Science B.V., 529 p.
- Howe, W.B., 1968, Planar stromatolite and burrowed carbonate mud facies in Cambrian strata of the St. Francois Mountain area: Missouri Geological Survey and Water Resources Report of Investigations No. 41, 113 p.
- Iman, R.L., and Conover, W.J., 1983, A modern approach to statistics: New York, John Wiley and Sons, 497 p.
- Imes, J.L., 1989, Major geohydrologic units in and adjacent to the Ozark Plateaus province, Missouri, Arkansas, Kansas, and Oklahoma—Basement confining unit: U.S. Geological Survey Hydrologic Investigations Atlas HA-711-B, 1 sheet.
- 1990a, Major geohydrologic units in and adjacent to the Ozark Plateaus province, Missouri, Arkansas, Kansas, and Oklahoma—St. Francois aquifer: U.S. Geological Survey Hydrologic Investigations Atlas HA-711-C, 2 sheets.
- 1990b, Major geohydrologic units in and adjacent to the Ozark Plateaus province, Missouri, Arkansas, Kansas, and Oklahoma—St. Francois confining unit: U.S. Geological Survey Hydrologic Investigations Atlas HA-711-D, 3 sheets.
- 1990c, Major geohydrologic units in and adjacent to the Ozark Plateaus province, Missouri, Arkansas, Kansas, and Oklahoma—Ozark aquifer: U.S. Geological Survey Hydrologic Investigations Atlas HA-711-E, 3 sheets.
- Imes, J.L., and Emmett, L.F., 1994, Geohydrology of the Ozark Plateaus aquifer system in parts of Missouri, Arkansas, Oklahoma, and Kansas: U.S. Geological Survey Professional Paper 1414-D, 127 p.
- Kleeschulte, M.J., 2001, Effects of lead-zinc mining on ground-water levels in the Ozark aquifer in the Viburnum Trend, Southeastern Missouri: U.S. Geological Survey Water-Resources Investigations Report 00-4293, 28 p.
- Kleeschulte, M.J., and Seeger, C.M., 2000, Depositional environment, stratigraphy, and vertical hydraulic conductivity of the St. Francois confining unit in the Fristoe Unit of the Mark Twain National Forest, Missouri: U.S. Geological Survey Water-Resources Investigations Report 00-4037, 65 p.
- 2001, Stratigraphy and vertical hydraulic conductivity of the St. Francois confining unit in townships 25–27 N. and ranges 01–02 W., southeastern Missouri: U.S. Geological Survey Water-Resources Investigations Report 01-4270, 63 p.
- Lohman, S.W., and others, 1972, Definitions of selected ground-water terms—Revisions and conceptual refinements: U.S. Geological Survey Water-Supply Paper 1988, 21 p.
- McCracken, M.H., 1971, Structural features of Missouri: Rolla, Missouri Geological Survey and Water Resources, Report of Investigations 49, 99 p.

- Miller, D.E., and Vandike, J.E., 1997, Groundwater resources of Missouri, *in* Missouri State Water Plan Series: Rolla, Missouri, Geological Survey and Resource Assessment, Water Resources Report Number 46, v. II, 210 p.
- Palmer, J.R., 1989, Late Upper Cambrian shelf depositional facies and history, southern Missouri, *in* Gregg, J.M., Palmer, J.R., and Kurtz, V.E., eds., Field guide to the Upper Cambrian of southeastern Missouri: stratigraphy, sedimentology, and economic geology: Rolla, University of Missouri, p. 1–24.
- , 1991, Distribution of lithofacies and inferred depositional environments in the Cambrian System, *in* Martin, J.A., and Pratt, W.P., eds., Geology and mineral-resource assessment of the Springfield 1° x 2° quadrangle, Missouri, as appraised in September 1985: U.S. Geological Survey Bulletin 1942, 115 p.
- Pratt, W.P., 1982, Map showing geologic structures in the Rolla 1° X 2° quadrangle, Missouri 1:250,000: U.S. Geological Survey, Miscellaneous Field Studies 1000A, 1 sheet.
- SYSTAT Software Inc., 2002, SYSTAT user's guide—Statistics I and II: Richmond, Calif., version 10.2, 1,376 p.
- Warner, D.L., Fletcher, C.S., and Cesare, J.A., 1974, Effect of mining operations on ground water levels in the New Lead Belt, Missouri: Rolla, University of Missouri, Project Number A-060-MO, 86 p.
- Wharton, H.M., 1979, Introduction to the southeast Missouri lead district, *in* Vineyard, J.D., ed., The geology and ore deposits of selected mines, Viburnum Trend, Missouri: Rolla, Missouri Division of Geology and Land Survey, Report of Investigations 58, p. 3–14.

TABLES

Table 1. Viburnum Trend core log analysis data

[DDMMSS, degrees, minutes, seconds; all units for depth and thickness are in feet; units for altitude are in feet above NGVD 29; depth and altitude refer to the formation top; --, no data; a, net shale determined by detailed core log]

Site number (fig. 4)	Latitude (DDMMSS)	Longitude (DDMMSS)	Borehole identification	Local well number	Altitude of land surface	Borehole depth	Derby-Doerun Dolomite		Davis Formation			Thickness of St. Francois confining unit		
							Depth	Altitude	Thickness	Depth	Altitude	Thickness	Total	Net shale
1	372446	0910540	ML-019576	T31N R01W 06BACr	1,198	1,741	780	418	140	920	278	160	300	--
2	372257	0910057	ML-019013	T31N R01W 14ACA	980	1,184	575	405	110	685	295	175	285	--
3	372059	0910035	CL-CO-1	T31N R01W 25CB	1,100	--	806	294	--	852	248	--	216	38
4	372351	0910717	CL-AC-37	T31N R02W 11AAA	1,160	--	780	380	--	897	263	--	--	--
5	372235	0910920	CL-AC-84	T31N R02W 15CBB	1,100	--	728	372	--	844	256	--	--	--
6	372241	0911102	CL-AC-45	T31N R02W 17DBB	1,270	--	800	470	--	900	370	--	--	--
7	372125	0910821	CL-LC-12	T31N R02W 23CC	1,170	--	589	581	--	690	480	--	300	82
8	372127	0910816	ML-024235	T31N R02W 23CCCCr	1,120	1,200	570	550	120	690	430	170	290	--
9	372140	0910651	ML-024242	T31N R02W 24CACr	1,180	1,400	750	430	140	890	290	165	305	--
10	372027	0910924	CL-LC-503	T31N R02W 34BBB	1,000	--	758	242	--	871	129	--	--	--
11	372003	0910833	CL-02S-09	T31N R02W 34DAA	947	--	--	--	--	838	109	158	--	--
12	372946	0910330	CL-MW-417	T32N R01W 04CAA	850	824	275	575	105	380	470	155	260	56
13	372936	0910511	ML-019072	T32N R01W 06DCr	916	1,235	375	541	130	505	411	150	280	--
14	372913	0910438	ML-019008	T32N R01W 08BBD	898	955	320	578	120	440	458	155	275	--
15	372747	0910054	ML-018761	T32N R01W 14DCD	840	794	205	635	115	320	520	165	280	--
16	372801	0910512	ML-019007	T32N R01W 18ADC	1,260	1,205	680	580	100	780	480	150	250	--
17	372752	0910605	CL-61W41	T32N R01W 18CBC	1,054	--	500	554	90	590	464	146	236	--
18	372719	0910508	ML-019441	T32N R01W 19AAC	980	1,124	455	525	115	570	410	160	275	--
19	372648	0910527	CL-60W130	T32N R01W 19DCB	1,074	--	530	544	117	647	427	153	270	--
20	372628	0910223	ML-018699	T32N R01W 27BDC	900	950	400	500	135	535	365	160	295	--
21	372639	0910418	ML-018922	T32N R01W 29ABB	896	1,367	445	451	105	550	346	155	260	--
22	372552	0910447	ML-019019	T32N R01W 29CCD	1,165	1,722	715	450	120	835	330	155	275	--
23	372627	0910520	ML-018840	T32N R01W 30ABD	920	1,059	385	535	140	525	395	145	285	--
24	372616	0910530	ML-018927	T32N R01W 30ACC	957	1,030	415	542	125	540	417	155	280	--
25	372603	0910543	ML-020135	T32N R01W 30CAC	966	1,064	450	516	125	575	391	150	275	--
26	372517	0910432	CL-1-RY	T32N R01W 32CACr	1,130	1,313	721	409	100	821	309	158	258	77
27	372944	0910620	ML-018944	T32N R02W 01ADB	1,034	1,384	515	519	135	650	384	150	285	--
28	372952	0910656	ML-019432	T32N R02W 01BBD	914	1,035	430	484	135	565	349	150	285	--
29	372926	0910701	ML-018894	T32N R02W 01CBD	924	1,060	425	499	140	565	359	155	295	--
30	372931	0910632	ML-018857	T32N R02W 01DBN2	910	1,310	425	485	130	555	355	195	325	--

Table 1. Viburnum Trend core log analysis data—Continued
[DDMMSS, degrees, minutes, seconds; all units for depth and thickness are in feet; units for altitude are in feet above NGVD 29; depth and altitude refer to the formation top; --, no data; a, net shale determined by detailed core log]

Site number (fig. 4)	Latitude (DDMMSS)	Longitude (DDMMSS)	Borehole identification	Local well number	Altitude of land surface			Borehole			Bonnetere Formation			Lamotte Sandstone			Precambrian		
					Depth	Altitude	Thickness	Depth	Altitude	Thickness	Depth	Altitude	Thickness	Depth	Altitude	Thickness	Depth	Altitude	
1	372446	0910540	ML-019576	T31N R01W 06BACr	1,198	1,741	1,080	118	300	1,380	-182	360	1,740	-	-	-	-542		
2	372257	0910057	ML-019013	T31N R01W 14ACA	980	1,184	860	120	290	1,150	-170	--	--	--	--	--	--		
3	372059	0910035	CL-CO-1	T31N R01W 25CB	1,100	--	1,022	78	--	--	--	--	--	--	--	--	--		
4	372351	0910717	CL-AC-37	T31N R02W 11AAA	1,160	--	--	--	--	--	--	--	--	--	--	--	--		
5	372235	0910920	CL-AC-84	T31N R02W 15CBB	1,100	--	--	--	--	--	--	--	--	--	--	--	--		
6	372241	0911102	CL-AC-45	T31N R02W 17DBB	1,270	--	--	--	--	--	--	--	--	--	--	--	--		
7	372125	0910821	CL-LC-12	T31N R02W 23CCC	1,170	--	889	281	--	--	--	--	--	--	--	--	--		
8	372127	0910816	ML-024235	T31N R02W 23CCCCr	1,120	1,200	860	260	310	1,170	-50	--	--	--	--	--	--		
9	372140	0910651	ML-024242	T31N R02W 24CACr	1,180	1,400	1,055	125	325	1,380	-200	--	--	--	--	--	--		
10	372027	0910924	CL-LC-503	T31N R02W 34BBBB	1,000	--	--	--	--	--	--	--	--	--	--	--	--		
11	372003	0910833	CL-02S-09	T31N R02W 34DAA	947	--	996	-49	--	--	--	--	--	--	--	--	--		
12	372946	0910330	CL-MW417	T32N R01W 04CAA	850	824	535	315	250	785	65	--	--	--	--	--	--		
13	372936	0910511	ML-019072	T32N R01W 06DCr	916	1,235	655	261	325	980	-64	250	1,230	-	-314	-	-		
14	372913	0910438	ML-019008	T32N R01W 08BBBD	898	955	595	303	255	850	48	100	950	-52	-	-	-		
15	372747	0910054	ML-018761	T32N R01W 14DCD	840	794	485	355	260	745	95	--	--	--	--	--	--		
16	372801	0910512	ML-019007	T32N R01W 18ADC	1,260	1,205	930	330	--	--	--	--	--	1,192	68	-	-		
17	372752	0910605	CL-61W41	T32N R01W 18CBC	1,054	--	736	318	--	--	--	--	--	--	--	--	--		
18	372719	0910508	ML-019441	T32N R01W 19AAC	980	1,124	730	250	280	1,010	-30	100	1,110	-	-130	-	-		
19	372648	0910527	CL-60W130	T32N R01W 19DCB	1,074	--	800	274	244	1,044	30	--	--	--	--	--	--		
20	372628	0910223	ML-018699	T32N R01W 27BDC	900	950	695	205	250	945	-45	--	--	--	--	--	--		
21	372639	0910418	ML-018922	T32N R01W 29ABB	896	1,367	705	191	290	995	-99	340	1,335	-	-439	-	-		
22	372552	0910447	ML-019019	T32N R01W 29CCCD	1,165	1,722	990	175	320	1,310	-145	355	1,665	-	-500	-	-		
23	372627	0910520	ML-018840	T32N R01W 30ABD	920	1,059	670	250	280	950	-30	80	1,030	-	-110	-	-		
24	372616	0910530	ML-018927	T32N R01W 30ACC	957	1,030	695	262	280	975	-18	35	1,010	-	-53	-	-		
25	372603	0910543	ML-020135	T32N R01W 30CAC	966	1,064	725	241	315	1,040	-74	--	--	--	--	--	--		
26	372517	0910432	CL-1RY	T32N R01W 32CACr	1,130	1,313	979	151	320	1,299	-169	--	--	--	--	--	--		
27	372944	0910620	ML-018944	T32N R02W 01ADB	1,034	1,384	800	234	310	1,110	-76	270	1,380	-	-346	-	-		
28	372952	0910656	ML-019432	T32N R02W 01BBD	914	1,035	715	199	300	1,015	-101	--	--	--	--	--	--		
29	372926	0910701	ML-018894	T32N R02W 01CBD	924	1,060	720	204	305	1,025	-101	--	--	--	--	--	--		
30	372931	0910632	ML-018857	T32N R02W 01DBN2	910	1,310	750	160	253	1,003	-93	302	1,305	-	-395	-	-		

Table 1. Viburnum Trend core log analysis data—Continued

[DDMMSS, degrees, minutes, seconds; all units for depth and thickness are in feet; units for altitude are in feet above NGVD 29; depth and altitude refer to the formation top; --, no data; a, net shale determined by detailed core log]

Site number (fig. 4)	Latitude (DDMMSS)	Longitude (DDMMSS)	Borehole identification	Local well number	Davis Formation			Thickness of St. Francois confining unit						
					Altitude of land surface	Borehole depth	Depth	Derby-Doerun Dolomite	Altitude	Thickness	Depth	Altitude	Thickness	Total
31	372906	0910718	ML-019678	T32N R02W 11AAN2	995	1,108	495	500	120	615	380	160	280	--
32	372852	0910736	CL-60W166	T32N R02W 11ACA	1,192	--	736	456	74	810	382	149	223	--
33	372851	0910638	ML-018896	T32N R02W 12ACW2	962	1,025	425	537	120	545	417	140	260	--
34	372841	0910641	CL-60W189	T32N R02W 12DBC	1,023	--	547	477	84	631	393	150	234	--
35	372737	0910643	CL-73C04	T32N R02W 13DCB	1,220	--	735	485	81	816	404	150	231	86a
36	372800	0910727	CL-60W144	T32N R02W 14ADB	1,216	--	--	--	876	340	150	--	--	
37	372808	0910800	ML-019674	T32N R02W 14BAC	1,200	1,380	780	420	125	905	295	145	270	--
38	372755	0911058	CL-HA-11	T32N R02W 17	1,310	--	908	402	--	1,016	294	--	300	72
39	372637	0910728	CL-92W57	T32N R02W 23DDC	1,101	--	--	--	788	313	150	--	--	
40	372702	0910626	CL-59W63	T32N R02W 24ADC	1,051	--	595	456	85	680	371	159	244	--
41	372639	0910627	ML-019020	T32N R02W 24DCD	952	1,040	455	497	85	540	412	155	240	--
42	372615	0910627	CL-60W03	T32N R02W 25ADB	1,092	--	636	456	77	713	379	159	236	--
43	372545	0910802	CL-89W17	T32N R02W 26CDC	1,232	--	811	421	80	891	341	163	243	--
44	372606	0910807	ML-020617	T32N R02W 26W2Cr	1,082	1,229	605	477	145	750	332	160	305	--
45	372458	0911150	ML-019404	T32N R02W 31DDC	1,140	1,480	755	385	125	880	260	160	285	--
46	372503	0911013	ML-019937	T32N R02W 33CDB	1,293	1,881	920	373	125	1,045	248	155	280	--
47	372512	0910814	CL-RC-106	T32N R02W 35CBA	1,218	--	--	--	895	323	158	--	--	
48	372456	0910721	CL-98W14	T32N R02W 35DDD	1,194	--	795	399	130	925	269	106	236	--
49	372456	0910652	CL-66-593	T32N R02W 36BDB	1,213	--	822	391	111	933	280	151	262	--
50	372507	0910646	ML-018970	T32N R02W 36CAD	1,142	1,550	715	427	135	850	292	155	290	--
51	373521	0910123	CL-3-MR	T33N R01W 02CBB	1,238	990	435	803	110	545	693	165	275	20
52	373458	0910306	ML-019703	T33N R01W 04CAD	1,043	885	360	683	110	470	573	130	240	--
53	373508	0910546	CL-64-746	T33N R01W 06BB	1,192	--	491	701	90	581	611	143	233	--
54	373401	0910552	ML-018630	T33N R01W 07CBB	1,095	665	285	810	100	385	710	130	230	--
55	373355	0910549	CL-64-696	T33N R01W 07CCB	1,085	--	200	885	198	398	687	125	323	--
56	373344	0910555	ML-024592	T33N R01W 07CCC	1,200	475	457	743	--	--	--	--	--	--
57	373338	0905955	ML-024244	T33N R01W 13CAE2	997	565	180	817	110	290	707	155	265	--
58	373351	0910124	ML-020973	T33N R01W 14BBC	936	826	275	661	105	380	556	125	230	--
59	373337	0910549	CL-448	T33N R01W 18BBB	1,200	--	462	738	--	568	632	--	92	--
60	373158	0910158	CL-5-MR	T33N R01W 27AW2	1,001	--	406	595	--	490	511	--	219	43

Table 1. Viburnum Trend core log analysis data—Continued
[DDMMSS, degrees, minutes, seconds; all units for depth and thickness are in feet; units for altitude are in feet above NGVD 29; depth and altitude refer to the formation top; --, no data; a, net shale determined by detailed core log]

Site number (fig. 4)	Latitude (DDMMSS)	Longitude (DDMMSS)	Borehole identification	Local well number	Altitude of land surface			Borehole depth			Bonnetere Formation			Lamotte Sandstone			Precambrian	
					Depth	Altitude	Thickness	Depth	Altitude	Thickness	Depth	Altitude	Thickness	Depth	Altitude	Thickness	Depth	Altitude
31	372906	0910718	ML-019678	T32N R02W 11AAN2	995	1,108	775	220	325	1,100	-105	--	--	--	--	--	--	
32	372852	0910736	CL-60W166	T32N R02W 11ACA	1,192	--	959	233	322	1,281	-89	--	--	--	--	--	--	
33	372851	0910638	ML-018896	T32N R02W 12ACW2	962	1,025	685	277	315	1,000	-38	--	--	--	--	--	--	
34	372841	0910641	CL-60W189	T32N R02W 12DBC	1,023	--	781	243	306	1,087	-64	--	--	--	--	--	--	
35	372737	0910643	CL-73C04	T32N R02W 13DCB	1,220	--	966	254	301	1,267	-47	--	--	--	--	--	--	
36	372800	0910727	CL-60W144	T32N R02W 14ADB	1,216	--	1,026	190	317	1,343	-127	--	--	--	--	--	--	
37	372808	0910800	ML-019674	T32N R02W 14BAC	1,200	1,380	1,050	150	--	--	--	--	--	--	--	--	--	
38	372755	0911058	CL-HA-11	T32N R02W 17	1,310	--	1,208	102	--	--	--	--	--	--	--	--	--	
39	372637	0910728	CL-92W57	T32N R02W 23DDC	1,101	--	938	163	327	1,265	-164	--	--	--	--	--	--	
40	372702	0910626	CL-59W63	T32N R02W 24ADC	1,051	--	839	212	314	1,153	-102	--	--	--	--	--	--	
41	372639	0910627	ML-019020	T32N R02W 24DCD	952	1,040	695	257	300	995	-43	35	1,030	-78	--	--	--	
42	372615	0910627	CL-60W03	T32N R02W 25ADB	1,092	--	872	220	294	1,166	-74	--	--	--	--	--	--	
43	372545	0910802	CL-89W17	T32N R02W 26CDC	1,232	--	1,054	178	310	1,364	-132	--	--	--	--	--	--	
44	372606	0910807	ML-020617	T32N R02W 26W2Cr	1,082	1,229	910	172	310	1,220	-138	--	--	--	--	--	--	
45	372458	0911150	ML-019404	T32N R02W 31DDC	1,140	1,480	1,040	100	330	1,370	-230	--	--	--	--	--	--	
46	372503	0911013	ML-019937	T32N R02W 33CDB	1,293	1,881	1,200	93	324	1,524	-231	351	1,875	-582	--	--		
47	372512	0910814	CL-RC-106	T32N R02W 35CBA	1,218	--	1,053	165	--	--	--	--	--	--	--	--	--	
48	372456	0910721	CL-98W14	T32N R02W 35DDD	1,194	--	1,031	163	337	1,368	-174	--	--	--	--	--	--	
49	372456	0910652	CL-66-593	T32N R02W 36BDB	1,213	--	1,084	129	--	--	--	--	--	--	--	--	--	
50	372507	0910646	ML-018970	T32N R02W 36CAD	1,142	1,550	1,005	137	315	1,320	-178	--	--	--	--	--	--	
51	373521	0910123	CL-3MR	T33N R01W 02CBB	1,238	990	710	528	270	980	258	--	--	--	--	--	--	
52	373458	0910306	ML-019703	T33N R01W 04CAD	1,043	885	600	443	275	875	168	--	--	--	--	--	--	
53	373508	0910546	CL-64-746	T33N R01W 06BB	1,192	--	724	468	--	--	--	--	--	--	--	--	--	
54	373401	0910552	ML-018630	T33N R01W 07CBB	1,095	665	515	580	--	--	--	--	--	615	480	--	--	
55	373355	0910549	CL-64-696	T33N R01W 07CCB	1,085	--	523	562	--	--	--	--	--	--	--	--	--	
56	373344	0910555	ML-024592	T33N R01W 07CCC	1,200	475	--	--	--	--	--	--	--	--	--	--	--	
57	373338	0905955	ML-024244	T33N R01W 13CAE2	997	565	445	552	--	--	--	--	--	555	442	--	--	
58	373351	0910124	ML-020973	T33N R01W 14BBC	936	826	505	431	270	775	161	--	--	--	--	--	--	
59	373337	0910549	CL-448	T33N R01W 18BBB	1,200	--	--	--	--	--	--	--	--	--	--	--	--	
60	373158	0910158	CL-5-MR	T33N R01W 27AW2	1,001	--	625	376	--	--	--	--	--	--	--	--	--	

Table 1. Viburnum Trend core log analysis data—Continued

[DDMMSS, degrees, minutes, seconds; all units for depth and thickness are in feet; units for altitude are in feet above NGVD 29; depth and altitude refer to the formation top; --, no data; a, net shale determined by detailed core log]

Site number (fig. 4)	Latitude (DDMMSS)	Longitude (DDMMSS)	Borehole identification	Local well number	Altitude of land surface			Borehole depth			Derby-Doerun Dolomite			Davis Formation			Thickness of St. Francois confining unit	
					Depth	Altitude	Thickness	Depth	Altitude	Thickness	Depth	Altitude	Thickness	Depth	Altitude	Thickness	Total	Net shale
61	373110	0910554	ML-024238	T33N R01W 30CCCr	1,000	810	92	410	92	682	318	--	--	--	--	--	--	--
62	373023	0910546	ML-019430	T33N R01W 31CCCr	965	1,232	395	570	115	510	455	145	260	--	--	--	--	--
63	373503	0910629	CL-93DR01	T33N R02W 01ABC	1,291	--	646	645	69	715	576	144	213	--	--	--	--	--
64	373453	0910654	ML-024231	T33N R02W 01BCD	1,280	875	615	665	125	740	540	--	--	--	--	--	--	60
65	373400	0911147	CL-CN-280	T33N R02W 07	1,300	--	734	566	--	800	500	--	--	--	--	--	--	--
66	373334	0910829	ML-024230	T33N R02W 10DDC	1,320	1,274	635	685	75	710	610	128	203	--	--	--	--	--
67	373349	0910728	CL-96B02	T33N R02W 11DBD	1,268	--	678	590	82	760	508	148	230	--	--	--	--	--
68	373337	0910737	CL-84B09	T33N R02W 11DCC	1,217	--	--	--	--	699	518	146	--	--	--	--	64a	--
69	373412	0910649	CL-92DR03	T33N R02W 12BA	1,281	--	650	631	80	730	551	167	247	--	--	--	--	--
70	373353	0910646	CL-02B-06	T33N R02W 12CAB	1,123	--	--	--	--	519	604	128	--	--	--	--	--	--
71	373326	0910608	CL-64-743	T33N R02W 13AAA	1,202	--	368	834	144	512	690	128	272	--	--	--	--	--
72	373326	0910727	CL-84B02	T33N R02W 14ABA	1,232	--	--	--	--	699	533	151	--	--	--	--	88a	--
73	373318	0910754	CL-94B01	T33N R02W 14BDB	1,338	--	776	562	90	866	472	161	251	--	--	--	--	--
74	373238	0910836	ML-024229	T33N R02W 22ABA	1,200	945	645	555	150	795	405	--	--	--	--	--	--	--
75	373236	0910632	ML-024251	T33N R02W 24ABB	1,200	915	665	535	--	--	--	--	--	--	--	--	--	--
76	373129	0910649	CL-96B06	T33N R02W 25BDB	1,193	--	691	502	95	786	407	134	229	--	--	--	--	--
77	373118	0910736	CL-93B12	T33N R02W 26DBB	1,250	--	756	494	92	848	402	146	238	--	--	--	--	--
78	373051	0910745	ML-024587	T33N R02W 35BAA	1,150	650	610	540	--	--	--	--	--	--	--	--	--	--
79	373037	0910745	CL-79B14	T33N R02W 35BDA	1,143	--	662	481	75	737	406	149	224	82a	--	--	--	--
80	373046	0910638	CL-99B11	T33N R02W 36ABC	1,196	--	680	516	90	770	426	146	236	--	--	--	--	--
81	373025	0910644	ML-020150	T33N R02W 36C	1,012	1,070	485	527	140	625	387	145	285	--	--	--	--	--
82	373017	0910624	ML-020618	T33N R02W 36D	981	1,060	450	531	140	590	391	150	290	--	--	--	--	--
83	374132	0910101	CL-12-EE	T34N R01W 02BBBD	1,199	587	150	1,049	125	275	924	143	268	50	--	--	--	--
84	374136	0910212	ML-019697	T34N R01W 03BBCr	1,095	610	65	1,030	105	170	925	140	245	--	--	--	--	--
85	374034	0910247	ML-019494	T34N R01W 04S2AC	1,211	845	290	921	115	405	806	134	249	--	--	--	--	--
86	374136	0910429	ML-019562	T34N R01W 05N2BB	1,155	825	295	860	100	395	760	145	245	--	--	--	--	--
87	374043	0910541	ML-020970	T34N R01W 06CBN2	1,109	775	110	999	--	--	--	--	--	--	--	--	--	--
88	374123	0910528	ML-019574	T34N R01W 06N2BC	1,296	840	280	1,016	130	410	886	150	280	--	--	--	--	--
89	374031	0910519	ML-019515	T34N R01W 06S2N2Cr	1,185	600	315	870	110	425	760	140	250	--	--	--	--	--
90	374020	0910508	CL-1079	T34N R01W 06D	1,261	--	450	811	--	544	717	--	232	232	--	--	--	46

Table 1. Viburnum Trend core log analysis data—Continued
[DDMMSS, degrees, minutes, seconds; all units for depth and thickness are in feet; units for altitude are in feet above NGVD 29; depth and altitude refer to the formation top; --, no data; a, net shale determined by detailed core log]

Site number (fig. 4)	Latitude (DDMMSS)	Longitude (DDMMSS)	Borehole identification	Local well number	Altitude of land surface	Borehole			Bonnetere Formation			Lamotte Sandstone			Precambrian
						Depth	Altitude	Thickness	Depth	Altitude	Thickness	Depth	Altitude	Thickness	Depth
61	373110	0910554	ML-024238	T33N R01W 30CCCCr	1,000	810	--	--	310	960	5	--	--	--	--
62	373023	0910546	ML-019430	T33N R01W 31CCCCr	965	1,232	655	--	859	432	282	1,141	150	--	--
63	373503	0910629	CL-93DR01	T33N R02W 01ABC	1,291	--	--	--	--	--	--	--	--	--	--
64	373453	0910654	ML-024231	T33N R02W 01BCD	1,280	875	--	--	--	--	--	--	--	--	--
65	373400	0911147	CL-CN-280	T33N R02W 07	1,300	--	--	--	--	--	--	--	--	--	--
66	373334	0910829	ML-024230	T33N R02W 10DDC	1,320	1,274	838	482	417	1,255	65	--	--	--	--
67	373349	0910728	CL-96B02	T33N R02W 11DBD	1,268	--	908	360	300	1,208	60	--	--	--	--
68	373337	0910737	CL-84B09	T33N R02W 11DCC	1,217	--	845	372	251	1,096	121	--	--	--	--
69	373412	0910649	CL-92DR03	T33N R02W 12BA	1,281	--	897	384	260	1,157	124	--	--	--	--
70	373353	0910646	CL-02B-06	T33N R02W 12CAB	1,123	--	647	476	--	--	--	--	--	--	--
71	373326	0910608	CL-64-743	T33N R02W 13AAA	1,202	--	640	562	--	--	--	--	--	--	--
72	373326	0910727	CL-84B02	T33N R02W 14ABA	1,232	--	850	382	286	1,136	96	--	--	--	--
73	373318	0910754	CL-94B01	T33N R02W 14BDB	1,338	--	1,027	311	281	1,308	30	--	--	--	--
74	373238	0910836	ML-024229	T33N R02W 22ABA	1,200	945	--	--	--	--	--	--	--	--	--
75	373236	0910632	ML-024251	T33N R02W 24ABB	1,200	915	--	--	--	--	--	--	--	--	--
76	373129	0910649	CL-96B06	T33N R02W 25BDB	1,193	--	920	273	282	1,202	-9	--	--	--	--
77	373118	0910736	CL-93B12	T33N R02W 26DBB	1,250	--	994	257	304	1,298	-48	--	--	--	--
78	373051	0910745	ML-024587	T33N R02W 35BAA	1,150	650	--	--	--	--	--	--	--	--	--
79	373037	0910745	CL-79B14	T33N R02W 35BDA	1,143	--	886	257	305	1,191	-48	--	--	--	--
80	373046	0910638	CL-99B11	T33N R02W 36ABC	1,196	--	916	280	299	1,215	-19	--	--	--	--
81	373025	0910644	ML-020150	T33N R02W 36C	1,012	1,070	770	242	295	1,065	-53	--	--	--	--
82	373017	0910624	ML-020618	T33N R02W 36D	981	1,060	740	241	305	1,045	-64	--	--	--	--
83	374132	0910101	CL-12EE	T34N R01W 02BBBD	1,199	587	418	781	--	--	--	--	577	622	--
84	374136	0910212	ML-019697	T34N R01W 03BBCr	1,095	610	310	785	270	580	515	10	590	505	--
85	374034	0910247	ML-019494	T34N R01W 04S2AC	1,211	845	539	672	--	--	--	--	--	--	--
86	374136	0910429	ML-019562	T34N R01W 05N2BB	1,155	825	540	615	--	--	--	--	--	--	--
87	374043	0910541	ML-020970	T34N R01W 06CBN2	1,109	775	--	--	--	--	--	--	752	357	--
88	374123	0910528	ML-019574	T34N R01W 06N2BC	1,296	840	560	736	275	835	461	--	--	--	--
89	374031	0910519	ML-019515	T34N R01W 06S2N2C	1,185	600	565	620	--	--	--	--	--	--	--
90	374020	0910508	CL-1079	T34N R01W 06D	1,261	--	682	579	--	--	--	--	--	--	--

Table 1. Viburnum Trend core log analysis data—Continued

[DDMMSS, degrees, minutes, seconds; all units for depth and thickness are in feet; units for altitude are in feet above NGVD 29; depth and altitude refer to the formation top; --, no data; a, net shale determined by detailed core log]

Site number (fig. 4)	Latitude (DDMMSS)	Longitude (DDMMSS)	Borehole identification	Local well number	Altitude of land surface	Borehole depth	Davis Formation			Thickness of St. Francois confining unit		
							Depth	Altitude	Thickness	Depth	Altitude	Thickness
91	373933	0910435	ML-019700	T34N R01W 07ADA	1,296	1,090	540	756	110	650	646	155
92	373952	0910100	ML-023807	T34N R01W 11BCD	1,130	670	120	1,010	87	207	923	143
93	373719	0910331	ML-018837	T34N R01W 20DDD	1,282	1,132	530	752	135	665	617	160
94	373657	0910554	CL-64-740	T34N R01W 30BBB	1,336	--	654	682	67	721	615	215
95	373524	0910554	CL-64-698	T34N R01W 31CC	1,213	--	540	673	124	664	549	158
96	373531	0910359	ML-019252	T34N R01W 32DCS2	1,315	1,080	485	830	165	650	665	141
97	373555	0910136	ML-018467	T34N R01W 34DDC	960	764	240	720	85	325	635	100
98	374138	0910654	CL-92V37	T34N R02W 01BBB	1,226	--	411	816	80	491	736	159
99	374029	0910652	CL-90V51	T34N R02W 01CBB	1,260	--	--	--	--	633	627	150
100	374035	0910708	CL-95V47	T34N R02W 02DAA	1,310	--	624	686	67	691	619	143
101	374016	0910714	CL-88V15	T34N R02W 02DAD	1,299	--	--	--	--	669	630	155
102	374137	0910815	ML-018839	T34N R02W 03N2AA	1,255	1,146	530	725	125	655	600	165
103	374128	0910813	ML-018863	T34N R02W 03N2AD	1,258	1,136	530	728	125	655	603	170
104	373955	0910939	CL-MW 134	T34N R02W 04DC	1,259	--	598	661	59	657	602	159
105	373901	0911028	CL-MW 132	T34N R02W 08DAD	1,257	--	609	648	69	678	579	158
106	373854	0911033	CL-USA-14	T34N R02W 08DDC	1,221	--	581	640	--	662	559	--
107	373900	0911004	CL-MW 177	T34N R02W 09	1,190	--	420	770	62	482	708	145
108	373850	0911002	CL-MW 170	T34N R02W 09CD	1,240	--	599	641	63	662	578	157
109	373911	0910911	CL-MW 114	T34N R02W 10CB	1,283	--	548	735	81	629	654	156
110	373908	0910914	CL-MW 184	T34N R02W 10CBB	1,302	--	535	767	51	586	716	147
111	373856	0910908	CL-VLP-10-02	T34N R02W 10CC	1,298	--	--	--	--	658	640	154
112	373931	0910758	CL-88V03	T34N R02W 11BB	1,270	--	--	--	--	557	713	161
113	373855	0910623	CL-84V39	T34N R02W 12DC	1,321	--	--	--	--	722	599	149
114	373806	0910803	ML-027408	T34N R02W 14CCB	1,374	860	705	669	135	840	534	--
115	373807	0910736	CL-64-709	T34N R02W 14DBC	1,330	--	665	665	119	784	546	136
116	373828	0910903	CL-VLP-15-47	T34N R02W 15BC	1,323	--	660	663	115	775	548	157
117	373820	0910950	CL-MW 182	T34N R02W 16CAA	1,165	--	575	590	46	621	544	157
118	373801	0911010	CL-MW 143	T34N R02W 16CC	1,208	--	595	613	72	667	541	156
119	373708	0911204	ML-016824	T34N R02W 19CDD	1,170	525	440	730	--	--	228	228
120	373729	0910715	CL-64-738	T34N R02W 23BDC	1,353	--	593	760	158	751	602	223

Table 1. Viburnum Trend core log analysis data—Continued
[DDMMSS, degrees, minutes, seconds; all units for depth and thickness are in feet; units for altitude are in feet above NGVD 29; depth and altitude refer to the formation top; --, no data; a, net shale determined by detailed core log]

Site number (fig. 4)	Latitude (DDMMSS)	Longitude (DDMMSS)	Borehole identification	Local well number	Altitude of land surface	Bonne Terre Formation			Lamotte Sandstone			Precambrian		
						Depth	Altitude	Thickness	Depth	Altitude	Thickness	Depth	Altitude	Thickness
91	373933	0910435	ML-019700	T34N R01W 07ADA	1,296	1,090	805	491	--	--	--	--	--	--
92	373952	0910100	ML-023807	T34N R01W 11BCD	1,130	670	350	780	290	640	490	--	--	--
93	373719	0910331	ML-018837	T34N R01W 20DDD	1,282	1,132	825	457	250	1,075	207	--	--	--
94	373657	0910554	CL-64-740	T34N R01W 30BBB	1,336	--	936	400	--	--	--	--	--	--
95	373524	0910554	CL-64-698	T34N R01W 31CC	1,213	--	822	391	--	--	--	--	--	--
96	373531	0910359	ML-019252	T34N R01W 32DCS2	1,315	1,080	791	524	267	1,058	257	--	--	--
97	373555	0910136	ML-018467	T34N R01W 34DDC	960	764	425	535	295	720	240	--	--	--
98	374138	0910654	CL-92V37	T34N R02W 01BBBB	1,226	--	650	577	285	935	292	--	--	--
99	374029	0910652	CL-90V51	T34N R02W 01CBB	1,260	--	783	477	272	1,055	205	--	--	--
100	374035	0910708	CL-95V47	T34N R02W 02DAA	1,310	--	834	476	275	1,109	201	--	--	--
101	374016	0910714	CL-88V15	T34N R02W 02DAD	1,299	--	824	475	273	1,097	202	--	--	--
102	374137	0910815	ML-018839	T34N R02W 03N2AA	1,255	1,146	820	435	285	1,105	150	--	--	--
103	374128	0910813	ML-018863	T34N R02W 03N2AD	1,258	1,136	825	433	275	1,100	158	--	--	--
104	373955	0910939	CL-MW 134	T34N R02W 04DC	1,259	--	816	443	289	1,105	154	--	--	--
105	373901	0911028	CL-MW 132	T34N R02W 08DAD	1,257	--	836	421	311	1,147	110	--	--	--
106	373854	0911033	CL-JUSA-14	T34N R02W 08DDC	1,221	--	820	401	--	--	--	--	--	--
107	373900	0911004	CL-MW 177	T34N R02W 09	1,190	--	626	564	--	--	--	--	--	--
108	373850	0911002	CL-MW 170	T34N R02W 09CD	1,240	--	819	421	307	1,126	114	--	--	--
109	373911	0910911	CL-MW 114	T34N R02W 10CB	1,283	--	784	499	279	1,063	220	--	--	--
110	373908	0910914	CL-MW 184	T34N R02W 10CBB	1,302	--	733	569	--	--	--	--	--	--
111	373856	0910908	CL-VLP-10-02	T34N R02W 10CC	1,298	--	812	486	286	1,097	201	--	--	--
112	373931	0910758	CL-88V03	T34N R02W 11BB	1,270	--	717	553	--	--	--	--	--	--
113	373855	0910623	CL-84V39	T34N R02W 12DC	1,321	--	871	450	284	1,155	166	--	--	--
114	373806	0910803	ML-027408	T34N R02W 14CCB	1,374	860	--	--	--	--	--	--	--	--
115	373807	0910736	CL-64-709	T34N R02W 14DBC	1,330	--	920	410	--	--	--	--	--	--
116	373828	0910903	CL-VLP15-47	T34N R02W 15BC	1,323	--	932	391	--	--	--	--	--	--
117	373820	0910950	CL-MW 182	T34N R02W 16CAA	1,165	--	778	387	295	1,073	92	--	--	--
118	373801	0911010	CL-MW 143	T34N R02W 16CC	1,208	--	823	385	309	1,132	77	--	--	--
119	373708	0911204	ML-016824	T34N R02W 19CDD	1,170	525	--	--	--	--	--	--	--	--
120	373729	0910715	CL-64-738	T34N R02W 23BDC	1,353	--	974	379	--	--	--	--	--	--

Table 1. Viburnum Trend core log analysis data—Continued

[DDMMSS, degrees, minutes, seconds; all units for depth and thickness are in feet; units for altitude are in feet above NGVD 29; depth and altitude refer to the formation top; --, no data; a, net shale determined by detailed core log]

Site number (fig. 4)	Latitude (DDMMSS)	Longitude (DDMMSS)	Borehole identification	Local well number	Altitude of land surface			Borehole depth			Derby-Doerun Dolomite			Davis Formation			Thickness of St. Francois confining unit	
					Depth	Altitude	Thickness	Depth	Altitude	Thickness	Depth	Altitude	Thickness	Depth	Altitude	Thickness	Total	Net shale
121	373729	0910616	CL-64-729	T34N R02W 24ACD	1,300	--	585	715	135	720	580	153	288	--	--	--	--	
122	373721	0910620	CL-MW 436	T34N R02W 24DBC _r	1,400	1,304	720	680	120	840	560	--	--	--	--	59	--	
123	373651	0910729	CL-64-752	T34N R02W 26ABC	1,400	--	764	636	110	874	526	152	262	--	--	--	--	
124	373625	0910951	ML-016821	T34N R02W 28CAD	1,185	540	500	685	--	--	--	--	--	--	--	--	--	
125	373628	0911047	ML-016822	T34N R02W 29DBC	1,150	580	455	695	--	--	--	--	--	--	--	--	--	
126	373627	0911147	ML-016823	T34N R02W 30DBD	1,120	495	405	715	--	--	--	--	--	--	--	--	--	
127	374659	0910038	ML-012290	T35N R01W 02BAS2	1,030	645	90	940	115	205	825	115	230	--	--	--	--	
128	374654	0910126	ML-012308	T35N R01W 03ABC _r	1,054	877	225	829	110	335	719	175	285	--	--	--	--	
129	374658	0910143	ML-013011	T35N R01W 03BAC _r	1,025	730	165	860	105	270	755	145	250	--	--	--	--	
130	374631	0910429	ML-012296	T35N R01W 06DAC _r	1,015	645	55	960	120	175	840	155	275	--	--	--	--	
131	374603	0910240	ML-020388	T35N R01W 09ABN2	940	990	--	795	--	295	645	20	--	--	--	--	--	
132	374546	0910233	CL-A-201	T35N R01W 09ACD	1,100	--	305	--	--	376	724	--	219	29	--	--	--	
133	374544	0910219	ML-019495	T35N R01W 09ADD	1,000	656	60	940	110	170	830	170	280	--	--	--	--	
134	374556	0910042	ML-020353	T35N R01W 11BAS2	1,150	1,172	--	--	--	450	700	20	--	--	--	--	--	
135	374536	0910036	ML-020382	T35N R01W 11CAN2	1,023	--	--	--	--	330	693	5	--	--	--	--	--	
136	374428	0905955	ML-012297	T35N R01W 13CCCr	1,059	590	45	1,014	125	170	889	155	280	--	--	--	--	
137	374448	0905859	ML-012164	T35N R01W 13DAC _r	1,040	575	5	1,035	120	125	915	160	280	--	--	--	--	
138	374429	0905906	ML-012450	T35N R01W 13DDCr	1,157	255	170	987	--	--	--	--	--	--	--	--	--	
139	374512	0910042	CL-CT 9	T35N R01W 14BAN2	1,067	1,020	--	--	--	375	692	--	--	46	--	--	--	
140	374443	0910025	ML-020229	T35N R01W 14DBB	1,251	1,071	--	--	--	520	731	10	--	--	--	--	--	
141	374458	0910257	ML-020182	T35N R01W 16BDB	1,009	485	--	--	--	220	789	10	--	--	--	--	--	
142	374429	0910301	ML-020154	T35N R01W 16CS2Cr	1,077	495	--	--	--	270	807	5	--	--	--	--	--	
143	374457	0910411	CL-92V40	T35N R01W 17BCA	1,040	--	195	845	70	265	775	163	233	--	--	--	--	
144	374350	0910510	CL-89V30	T35N R01W 19CA	981	--	120	861	65	185	796	160	225	--	--	--	--	
145	374404	0910417	ML-013208	T35N R01W 20BCCr	1,124	795	120	1,004	210	330	794	75	285	--	--	--	--	
146	374333	0910401	ML-012293	T35N R01W 20CDCr	1,173	610	195	978	47	242	931	153	200	--	--	--	--	
147	374412	0910146	ML-012304	T35N R01W 22BAC _r	1,245	859	300	945	115	415	830	155	270	--	--	--	--	
148	374330	0910207	ML-012325	T35N R01W 22CCCCr	1,037	632	45	992	120	165	872	160	280	--	--	--	--	
149	374358	0910009	ML-012463	T35N R01W 23ADC _r	1,083	200	--	--	--	--	--	--	--	--	--	--	--	
150	374352	0910023	ML-020248	T35N R01W 23DBA	1,246	755	--	--	--	--	--	--	--	--	--	--	--	

Table 1. Viburnum Trend core log analysis data—Continued
[DDMMSS, degrees, minutes, seconds; all units for depth and thickness are in feet; units for altitude are in feet above NGVD 29; depth and altitude refer to the formation top; --, no data; a, net shale determined by detailed core log]

Site number (fig. 4)	Latitude (DDMMSS)	Longitude (DDMMSS)	Borehole identification	Local well number	Altitude of land surface			Borehole depth			Bonnetiere Formation			Lamotte Sandstone			Precambrian		
					Depth	Altitude	Thickness	Depth	Altitude	Thickness	Depth	Altitude	Thickness	Depth	Altitude	Thickness	Depth	Altitude	
121	373729	0910616	CL-64-729	T34N R02W 24ACD	1,300	--	873	427	--	--	1,286	11	--	--	--	--	--	--	
122	373721	0910620	CL-MW436	T34N R02W 24DBC _r	1,400	1,304	--	374	--	--	1,026	--	--	--	--	--	--	--	
123	373651	0910729	CL-64-752	T34N R02W 26ABC	1,400	--	1,026	--	--	--	540	--	--	--	--	--	--	--	
124	373625	0910951	ML-016821	T34N R02W 28CAD	1,185	--	580	--	--	--	1,025	--	--	--	--	--	--	--	
125	373628	0911047	ML-016822	T34N R02W 29DBC	1,150	--	580	--	--	--	580	--	--	--	--	--	--	--	
126	373627	09111147	ML-016823	T34N R02W 30DBD	1,120	495	--	--	--	--	645	320	710	305	625	405	--	--	
127	374659	0910038	ML-012290	T35N R01W 02BAS2	1,030	--	524	576	--	--	877	510	544	330	840	214	--	--	
128	374654	0910126	ML-012308	T35N R01W 03ABC _r	1,054	--	660	340	--	--	730	415	610	280	695	330	--	--	
129	374658	0910143	ML-013011	T35N R01W 03BAC _r	1,025	--	645	330	--	--	730	415	610	280	695	330	--	--	
130	374631	0910429	ML-012296	T35N R01W 06DAC _r	1,015	--	685	290	--	--	685	330	685	290	620	395	--	--	
131	374603	0910240	ML-020388	T35N R01W 09ABN2	940	990	315	625	290	605	660	576	710	305	625	405	933	7	
132	374546	0910233	CL-A-201	T35N R01W 09ACD	1,100	--	524	576	--	--	656	340	660	290	630	370	--	--	
133	374544	0910219	ML-019495	T35N R01W 09ADD	1,000	--	656	340	--	--	1,172	470	680	280	750	400	1,156	-6	
134	374556	0910042	ML-020353	T35N R01W 11BAS2	1,150	--	335	688	260	--	1,023	--	688	260	595	428	--	--	
135	374536	0910036	ML-020382	T35N R01W 11CAN2	--	--	--	--	--	--	--	--	--	--	--	--	--	--	
136	374428	0905955	ML-012297	T35N R01W 13CCCr	1,059	590	325	734	250	575	590	575	285	755	555	485	--	--	
137	374448	0905859	ML-012164	T35N R01W 13DAC _r	1,040	--	575	270	--	--	1,157	255	275	802	--	--	--	--	
138	374429	0905906	ML-012450	T35N R01W 13DDCr	--	--	--	--	--	--	1,067	1,020	380	687	265	645	422	370	1,015
139	374512	0910042	CL-CT9	T35N R01W 14BAN2	--	--	--	--	--	--	1,251	1,071	530	721	265	795	456	235	52
140	374443	0910025	ML-020229	T35N R01W 14DBB	--	--	--	--	--	--	--	--	--	--	--	--	1,030	221	
141	374458	0910257	ML-020182	T35N R01W 16BDB	1,009	485	230	779	--	--	1,077	495	275	802	--	--	--	480	529
142	374429	0910301	ML-020154	T35N R01W 16CS2Cr	--	--	--	--	--	--	1,040	--	428	612	238	666	374	--	587
143	374457	0910411	CL-92V40	T35N R01W 17BCA	--	--	--	--	--	--	981	--	345	636	248	593	388	--	--
144	374350	0910510	CL-89V30	T35N R01W 19CA	--	--	--	--	--	--	1,124	795	405	719	260	665	459	100	765
145	374404	0910417	ML-013208	T35N R01W 20BCCr	--	--	--	--	--	--	--	--	--	--	--	--	--	359	
146	374333	0910401	ML-012293	T35N R01W 20CDCr	1,173	610	395	778	--	--	859	570	675	265	835	410	580	593	
147	374412	0910146	ML-012304	T35N R01W 22BACr	1,245	--	632	325	712	265	1,037	632	200	125	590	447	--	--	
148	374330	0910207	ML-012325	T35N R01W 22CCCr	--	--	--	--	--	--	1,083	1,083	958	--	--	--	--	--	
149	374358	0910009	ML-012463	T35N R01W 23ADC _r	--	--	--	--	--	--	1,246	755	500	746	--	--	--	--	
150	374352	0910023	ML-020248	T35N R01W 23DBA	--	--	--	--	--	--	--	--	--	--	--	--	--	--	

Table 1. Viburnum Trend core log analysis data—Continued

[DDMMSS, degrees, minutes, seconds; all units for depth and thickness are in feet; units for altitude are in feet above NGVD 29; depth and altitude refer to the formation top; --, no data; a, net shale determined by detailed core log]

Site number (fig. 4)	Latitude (DDMMSS)	Longitude (DDMMSS)	Borehole identification	Local well number	Altitude of land surface	Borehole depth	Davis Formation			Thickness of St. Francois confining unit		
							Depth	Altitude	Thickness	Depth	Altitude	Thickness
151	374337	0910034	ML-020254	T35N R01W 23DCB	1,260	917	245	1,015	--	--	814	65
152	374312	0910029	ML-020272	T35N R01W 26ACN2	1,239	775	--	--	425	769	10	--
153	374257	0910028	ML-020286	T35N R01W 26DBC _r	1,284	810	--	--	515	778	--	--
154	374640	0910603	CL-CZ-286	T35N R02W 01BD	1,280	--	462	818	502	660	185	178
155	374555	0911138	ML-018966	T35N R02W 07	1,145	1,012	360	785	125	485	310	43
156	374531	0911014	ML-012462	T35N R02W 08DCCR	882	155	40	842	70	110	772	--
157	374527	0910958	ML-012448	T35N R02W 08DDCr	986	175	130	856	--	--	--	--
158	374540	0910921	ML-012313	T35N R02W 09CACr	1,000	728	140	860	105	245	755	280
159	374533	0910939	ML-012309	T35N R02W 09CCC _r	964	598	45	919	115	160	804	300
160	374525	0910852	ML-012449	T35N R02W 09DDCr	1,037	235	145	892	--	--	--	--
161	374543	0910733	ML-027537	T35N R02W 11CBB	1,100	300	290	810	--	--	--	--
162	374542	0910601	CL-94V02	T35N R02W 12CAA	1,036	--	192	844	73	265	771	205
163	374426	0910532	CL-95V22	T35N R02W 13DDD	1,049	--	197	852	78	275	774	148
164	374501	0910733	ML-026096	T35N R02W 14BCCr	1,192	891	280	912	85	365	827	226
165	374501	0910853	ML-0122285	T35N R02W 16ADCr	1,080	740	175	905	100	275	805	260
												305
166	374514	0911000	ML-012446	T35N R02W 17AACr	887	498	30	857	--	--	--	--
167	374418	0910804	CL-57VB113	T35N R02W 22AB	1,128	--	--	--	407	721	172	--
168	374342	0910711	CL-89V03	T35N R02W 23CD	1,180	--	425	755	40	465	715	201
169	374310	0910638	CL-96V04	T35N R02W 26ADD	1,107	--	308	799	77	385	722	252
170	374254	0910731	ML-025772	T35N R02W 26CCA	1,241	1,200	455	786	110	565	676	275
171	374308	0910820	ML-024337	T35N R02W 27CAA	1,260	1,104	420	840	185	605	655	--
172	374332	0910934	ML-018756	T35N R02W 28BAB	1,242	1,095	455	787	205	660	582	375
173	374215	0910908	ML-024239	T35N R02W 33DBA	1,193	810	490	703	135	625	568	--
174	374151	0910820	CL-426	T35N R02W 34CDD	1,280	--	584	696	--	674	606	47
175	374226	0910727	CL-96V26	T35N R02W 35BDB	1,190	--	447	743	91	538	652	249
												31
												31
Minimum					5	242	40	110	109	5	178	20
25th Quartile					293	522	85	413	403	145	233	48
50th Quartile					462	673	110	605	576	154	260	64
75th Quartile					635	818	125	733	714	160	282	77
Maximum					920	1,049	210	1,045	931	223	381	104
Count					151	151	122	159	159	135	123	31

Table 1. Viburnum Trend core log analysis data—Continued
[DDMMSS, degrees, minutes, seconds; all units for depth and thickness are in feet; units for altitude are in feet above NGVD 29; depth and altitude refer to the formation top; --, no data; a, net shale determined by detailed core log]

Site number (fig. 4)	Latitude (DDMMSS)	Longitude (DDMMSS)	Borehole identification	Local well number	Altitude of land surface	Borehole			Bonnetere Formation			Lamotte Sandstone			Precambrian	
						Depth	Altitude	Thickness	Depth	Altitude	Thickness	Depth	Altitude	Thickness	Depth	Altitude
151	374337	0910034	ML-020254	T35N R01W 23DCB	1,260	917	520	740	260	780	480	116	896	364		
152	374312	0910029	ML-020272	T35N R01W 26ACN2	1,239	775	490	749	280	770	469	--	--	--		
153	374257	0910028	ML-020286	T35N R01W 26DBC	1,284	810	525	759	--	--	--	--	--	--		
154	374640	0910603	CL-CZ-286	T35N R02W 01BD	1,280	--	640	640	--	--	--	--	--	--		
155	374555	0911138	ML-018966	T35N R02W 07	1,145	1,012	670	475	305	975	170	--	--	--		
156	374531	0911014	ML-012462	T35N R02W 08DCC	882	155	--	--	--	--	--	--	--	--		
157	374527	0910958	ML-012448	T35N R02W 08DDCr	986	175	--	--	--	--	--	--	--	--		
158	374540	0910921	ML-012313	T35N R02W 09CACr	1,000	728	420	580	280	700	300	15	715	285		
159	374533	0910939	ML-012309	T35N R02W 09CCCR	964	598	345	619	--	--	--	--	570	394		
160	374525	0910852	ML-012449	T35N R02W 09DDCr	1,037	235	--	--	--	--	--	--	--	--		
161	374543	0910733	ML-027537	T35N R02W 11CBB	1,100	300	--	--	--	--	--	--	--	--		
162	374542	0910601	CL-94V02	T35N R02W 12CAA	1,036	--	397	639	285	682	354	--	--	--		
163	374426	0910532	CL-95V22	T35N R02W 13DDD	1,049	--	423	626	249	672	377	--	--			
164	374501	0910733	ML-026096	T35N R02W 14BCCr	1,192	891	540	652	295	835	357	20	855	337		
165	374501	0910853	ML-012285	T35N R02W 16ADC	1,080	740	480	600	--	--	--	--	--	--		
166	374514	0911000	ML-012446	T35N R02W 17AACr	887	498	--	--	--	--	--	--	--	--		
167	374418	0910804	CL-57VB113	T35N R02W 22AB	1,128	--	579	549	--	--	--	--	--	--		
168	374342	0910711	CL-89V03	T35N R02W 23CD	1,180	--	626	554	293	919	261	--	--	--		
169	374310	0910638	CL-96V04	T35N R02W 26ADD	1,107	--	560	547	270	830	277	--	--	--		
170	374254	0910731	ML-025772	T35N R02W 26CCA	1,241	1,200	730	511	295	1,025	216	--	--	--		
171	374308	0910820	ML-024337	T35N R02W 27CAA	1,260	1,104	--	--	--	1,070	19	--	--	--		
172	374332	0910934	ML-018756	T35N R02W 28BAB	1,242	1,095	830	412	245	1,075	167	--	--	--		
173	374215	0910908	ML-024239	T35N R02W 33DBA	1,193	810	--	--	--	--	--	--	--	--		
174	374151	0910820	CL-426	T35N R02W 34CDD	1,280	--	--	--	--	--	--	--	--	--		
175	374226	0910727	CL-96V26	T35N R02W 35BDB	1,190	--	696	494	293	989	201	--	--	--		
					Minimum	125	-49	238	555	-231	10	480	-582			
					25th Quartile	525	257	270	830	-53	80	640	-125			
					50th Quartile	725	432	290	1,044	114	235	980	60			
					75th Quartile	865	590	305	1,153	277	340	1,183	387			
					Maximum	1,208	958	417	1,524	515	406	1,875	622			
					Count	147	147	103	105	105	21	30	30			

Table 2. Adjacent property core log analysis data
[DDMMSS, degrees, minutes, seconds; all units for depth and thickness are in feet; units for altitude are in feet above NGVD 29; depth and altitude refer to the formation top; --, no data]

Site number (fig. 4)	Latitude (DDMMSS)	Longitude (DDMMSS)	Borehole identification	Local well number	Altitude of land surface	Borehole depth	Davis Formation		Thickness of St. Francois confining unit		
							Depth	Thickness	Depth	Altitude	Thickness
201	371813	0904901	ML-021057	T30N R02E 03DBD	856	1,470	545	311	150	695	161
202	371802	0904855	ML-021324	T30N R02E 03DDC	769	1,080	445	324	130	575	194
203	371725	0905205	ML-018562	T30N R02E 07DAD	630	650	165	465	180	345	285
204	371625	0905117	ML-021596	T30N R02E 17DCA	622	670	195	427	115	310	312
205	371912	0905640	ML-021245	T30N R01E 04ABE2	832	1,466	465	367	140	605	227
206	371927	0905852	ML-021326	T30N R01E 06ABA	1,030	1,315	720	310	110	830	200
207	371653	0905832	ML-021327	T30N R01E 17CCC	769	1,000	515	254	145	660	109
208	371706	0910239	CL-5-EX	T30N R01W 15CDB	980	1,146	755	225	110	865	115
209	371502	0910437	CL-11-FX	T30N R01W 32ABC	978	1,565	840	138	115	955	23
210	371505	0910221	ML-018207	T30N R01W 34ABC _r	747	1,274	405	342	220	625	122
211	371452	0910030	CL-EX-16	T30N R01W 36CD	840	--	777	63	--	862	-22
212	371757	0910846	CL-LC-810	T30N R02W 10DCD	1,100	--	965	135	--	1,065	35
213	371821	0910722	CL-GO-1	T30N R02W 11ADD	900	1,330	680	220	130	810	90
214	371857	0905129	ML-021246	T31N R02E 32CDD	952	1,470	515	437	120	635	317
215	372027	0905430	ML-021248	T31N R01E 26AS2Cr	915	1,175	470	445	150	620	295
216	372021	0905557	ML-021230	T31N R01E 27CDC _r	800	984	230	570	125	355	445
217	372045	0905748	ML-014158	T31N R01E 29DBA	850	405	385	465	--	--	--
218	371921	0905325	ML-018312	T31N R01E 36ADC	730	994	320	410	175	495	235
219	372115	0911300	CL-HA-15	T31N R03W 25AAC	1,235	--	--	--	--	1,132	103
220	372918	0905033	ML-011886	T32N R02E 04BBB	704	158	--	--	--	--	--
221	372709	0904758	ML-024737	T32N R02E 14BDD	742	220	--	--	--	--	--
222	372658	0904932	ML-023928	T32N R02E 15CBC	680	205	30	650	95	125	555
223	372645	0904915	ML-025419	T32N R02E 15CDC	683	125	--	--	--	--	--
224	372713	0905002	ML-018803	T32N R02E 16ACC	697	100	25	672	--	--	--
225	372716	0905104	ML-011451	T32N R02E 17ACS2	723	130	70	653	--	--	--
226	372712	0905057	ML-023643	T32N R02E 17ACD	717	605	--	--	--	--	--
227	372648	0905148	ML-020423	T32N R02E 18DDD	685	749	--	--	--	280	405
228	372641	0904901	ML-018753	T32N R02E 22ABB	660	560	--	--	--	25	635
229	372612	0904906	ML-013326	T32N R02E 22CAA	650	210	--	--	--	--	--
230	372455	0904619	ML-021598	T32N R02E 25DDD	775	815	--	--	--	400	375

Table 2. Adjacent property core log analysis data—Continued

[DDMMSS, degrees, minutes, seconds; all units for depth and thickness are in feet; units for altitude are in feet above NGVD 29; depth and altitude refer to the formation top; --, no data]

Site number (fig. 4)	Latitude (DDMMSS)	Longitude (DDMMSS)	Borehole identification	Local well number	Altitude of land surface		Borehole		Bonnetiere Formation			Lamotte Sandstone			Precambrian	
					Depth	Altitude	Depth	Thickness	Depth	Altitude	Thickness	Depth	Altitude	Thickness	Depth	Altitude
201	371813	0904901	ML-021057	T30N R02E 03DBD	856	1,470	870	-14	295	1,165	-309	260	1,425	--	-569	
202	371802	0904855	ML-021324	T30N R02E 03DDC	769	1,080	750	19	315	1,065	-296	--	--	--	--	
203	371725	0905205	ML-018562	T30N R02E 07DAD	630	650	480	150	--	--	--	--	625	5	--	
204	371625	0905117	ML-021596	T30N R02E 17DCA	622	670	480	142	--	--	--	--	--	--	--	
205	371912	0905640	ML-021245	T30N R01E 04ABE2	832	1,466	770	62	325	1,095	-263	--	--	--	--	
206	371927	0905852	ML-021326	T30N R01E 06ABA	1,030	1,315	1,000	30	305	1,305	-275	--	--	--	--	
207	371653	0905832	ML-021327	T30N R01E 17CCC	769	1,000	830	-61	--	--	--	--	--	--	--	
208	371706	0910239	CL-5-EX	T30N R01W 15CDB	980	1,146	1,035	-55	--	--	--	--	--	--	--	
209	371502	0910437	CL-11-EX	T30N R01W 32ABC	978	1,565	1,190	-212	350	1,540	-562	--	--	--	--	
210	371505	0910221	ML-018207	T30N R01W 34ABCr	747	1,274	845	-98	365	1,210	-463	--	--	--	--	
211	371452	0910030	CL-EX-16	T30N R01W 36CD	840	--	1,060	-220	--	--	--	--	--	--	--	
212	371757	0910846	CL-LG-810	T30N R02W 10DCD	1,100	--	--	--	--	--	--	--	--	--	--	
213	371821	0910722	CL-GO-1	T30N R02W 11ADD	900	1,330	980	-80	340	1,320	-420	--	--	--	--	
214	371857	0905129	ML-021246	T31N R02E 32CDD	952	1,470	795	157	320	1,115	-163	355	1,470	-518	--	
215	372027	0905430	ML-021248	T31N R01E 26AS2Cr	915	1,175	785	130	305	1,090	-175	--	--	--	--	
216	372021	0905557	ML-021230	T31N R01E 27CDCr	800	984	530	270	440	970	-170	--	--	--	--	
217	372045	0905748	ML-014158	T31N R01E 29DBA	850	405	--	--	--	--	--	--	--	--	--	
218	371921	0905325	ML-018312	T31N R01E 36ADC	730	994	705	25	220	925	-195	--	--	--	--	
219	372115	0911300	CL-HA-15	T31N R03W 25AAC	1,235	--	1,311	-76	--	--	--	--	--	--	--	
220	372918	0905033	ML-011886	T32N R02E 04BBB	704	158	10	694	--	--	--	--	150	554	--	
221	372709	0904758	ML-024737	T32N R02E 14BDD	742	220	50	692	--	--	--	--	105	637	--	
222	372658	0904932	ML-023928	T32N R02E 15CBC	680	205	--	--	--	--	--	--	--	--	--	
223	372645	0904915	ML-025419	T32N R02E 15CDC	683	125	45	638	--	--	--	--	--	--	--	
224	372713	0905002	ML-018803	T32N R02E 16ACC	697	100	--	--	--	--	--	--	--	--	--	
225	372716	0905104	ML-011451	T32N R02E 17ACs2	723	130	--	--	--	--	--	--	--	--	--	
226	372712	0905057	ML-023643	T32N R02E 17ACD	717	605	315	402	--	--	--	--	575	142	--	
227	372648	0905148	ML-020423	T32N R02E 18DDD	685	749	310	375	315	625	60	--	--	--	--	
228	372641	0904901	ML-018753	T32N R02E 22ABB	660	560	255	405	230	485	175	70	555	105	--	
229	372612	0904906	ML-013326	T32N R02E 22CAA	650	210	20	630	--	--	--	--	--	--	--	
230	372455	0904619	ML-021598	T32N R02E 25DDD	775	815	425	350	305	730	45	--	--	--	--	

Table 2. Adjacent property core log analysis data—Continued

[DDMMSS, degrees, minutes, seconds; all units for depth and thickness are in feet, units for altitude are in feet above NGVD 29; depth and altitude refer to the formation top. --, no data]

Site number (fig. 4)	Latitude (DDMMSS)	Longitude (DDMMSS)	Borehole identification	Local well number	Altitude of land surface			Borehole depth			Derby-Doerun Dolomite			Davis Formation			Thickness of St. Francois confining unit	
					Depth	Altitude	Thickness	Depth	Altitude	Thickness	Depth	Altitude	Thickness	Depth	Altitude	Thickness	Total	Net shale
231	372527	0904947	ML-020457	T32N R02E 28ADB	664	225	70	594	90	160	504	--	--	--	--	--	--	
232	372541	0905118	ML-013324	T32N R02E 29BAD	800	245	185	615	--	--	--	--	--	--	--	--	--	
233	372511	0905105	ML-013330	T32N R02E 29DCA	710	895	205	505	140	345	365	110	250	--	--	--	--	
234	372821	0905647	ML-003421	T32N R01E 09CDD	1,162	1,084	500	662	140	640	522	115	255	--	--	--	--	
235	372813	0905533	ML-018434	T32N R01E 10DCB	855	140	25	830	--	--	--	--	--	--	--	--	--	
236	372809	0905508	ML-018432	T32N R01E 10DDA	790	450	35	755	120	155	635	75	195	--	--	--	--	
237	372836	0905447	ML-017494	T32N R01E 11BDB	792	165	70	722	--	--	--	--	--	--	--	--	--	
238	372657	0905358	ML-021599	T32N R01E 13CCCCr	697	700	70	627	115	185	512	175	290	--	--	--	--	
239	372713	0905721	ML-005983	T32N R01E 20ADD	831	804	250	581	70	320	511	110	180	--	--	--	--	
240	372616	0905809	ML-018666	T32N R01E 29CBA	790	834	250	540	125	375	415	155	280	--	--	--	--	
241	372606	0905731	ML-025634	T32N R01E 29DAB	747	800	250	497	130	380	367	120	250	--	--	--	--	
242	372730	0911241	ML-021677	T32N R03W 24AAA	1,384	850	835	549	--	--	--	--	--	--	--	--	--	
243	373446	0904828	ML-025356	T33N R02E 0352AA	950	140	--	--	--	--	20	930	30	--	--	--	--	
244	373127	0905208	ML-023200	T33N R02E 19DBB	871	75	--	--	--	--	15	856	--	--	--	--	--	
245	373106	0904838	ML-013719	T33N R02E 22DDC	817	175	--	--	--	--	--	--	--	--	--	--	--	
246	373017	0904906	ML-011808	T33N R02E 27CDD	755	115	--	--	--	--	--	--	--	--	--	--	--	
247	373352	0905733	ML-002199	T33N R01E 08DS2Cr	890	677	85	805	195	280	610	130	325	--	--	--	--	
248	373346	0905548	ML-002196	T33N R01E 10CBCr	830	363	--	--	--	--	--	--	--	--	--	--	--	
249	373253	0905452	ML-002195	T33N R01E 14BCCr	830	379	--	--	--	--	--	--	--	--	--	--	--	
250	373252	0905435	ML-019670	T33N R01E 14N2S2Cr	840	447	--	--	--	--	5	835	110	--	--	--	--	
251	373250	0905512	ML-002194	T33N R01E 15DCr	795	341	--	--	--	--	--	--	--	--	--	--	--	
252	373309	0905614	ML-002197	T33N R01E 16ADC	875	398	--	--	--	--	--	--	--	--	--	--	--	
253	373329	0905645	ML-002198	T33N R01E 16BACr	900	320	--	--	--	--	--	--	--	--	--	--	--	
254	373228	0905530	ML-002193	T33N R01E 22ABCr	790	498	--	--	--	--	--	--	--	--	--	--	--	
255	373111	0905440	ML-002190	T33N R01E 26BCr	810	694	30	780	120	150	660	100	220	--	--	--	--	
256	373013	0905542	ML-019807	T33N R01E 34CE2Cr	735	654	--	--	--	--	220	515	145	--	--	--	--	
257	373138	0911410	ML-019190	T33N R03W 26ACB	1,050	1,430	550	500	90	640	410	170	260	--	--	--	--	
258	374109	0904914	ML-009442	T34N R02E 03BCB	1,087	80	--	--	--	--	9	1,078	36	--	--	--	--	
259	374059	0904912	ML-009550	T34N R02E 03CAA	1,077	175	--	--	--	--	10	1,067	30	--	--	--	--	
260	374056	0904836	ML-009444	T34N R02E 03DBC	1,148	100	--	--	--	--	15	1,133	--	--	--	--	--	

Table 2. Adjacent property core log analysis data—Continued

[DDMMSS, degrees, minutes, seconds; all units for depth and thickness are in feet; units for altitude are in feet above NGVD 29; depth and altitude refer to the formation top; --, no data]

Site number (fig. 4)	Latitude (DDMMSS)	Longitude (DDMMSS)	Borehole identification	Local well number	Altitude of land surface			Borehole			Bonnetiere Formation			Lamotte Sandstone			Precambrian		
					Depth	Altitude	Thickness	Depth	Altitude	Thickness	Depth	Altitude	Thickness	Depth	Altitude	Thickness	Depth	Altitude	
231	372527	0904947	ML-020457	T32N R02E 28ADB	664	225	--	--	--	--	--	--	--	--	--	--	--	--	
232	372541	0905118	ML-013324	T32N R02E 29BAD	800	245	--	--	--	--	--	--	--	--	--	--	--	--	
233	372511	0905105	ML-013330	T32N R02E 29DCDA	710	895	455	255	395	850	-140	--	--	--	--	--	--	--	
234	372821	0905647	ML-003421	T32N R01E 09CDD	1,162	1,084	755	407	275	1,030	132	--	--	--	--	--	--	--	
235	372813	0905533	ML-018434	T32N R01E 10DCB	855	140	--	--	--	--	--	--	--	--	--	--	--	--	
236	372809	0905508	ML-018432	T32N R01E 10DDA	790	450	230	560	--	--	--	--	--	--	--	435	355		
237	372836	0905447	ML-017494	T32N R01E 11BDB	792	165	--	--	--	--	--	--	--	--	--	--	--	--	
238	372657	0905538	ML-021599	T32N R01E 13CCCCr	697	700	360	337	290	650	47	--	--	--	--	--	--	--	
239	372713	0905721	ML-005983	T32N R01E 20ADD	831	804	430	401	345	775	56	--	--	--	--	--	--	--	
240	372616	0905809	ML-018666	T32N R01E 29CBA	790	834	530	260	265	795	-5	--	--	--	--	--	--	--	
241	372606	0905731	ML-025634	T32N R01E 29DAB	747	800	500	247	290	790	-43	--	--	--	--	--	--	--	
242	372730	0911241	ML-021677	T32N R03W 24AAA	1,384	850	--	--	--	--	--	--	--	--	--	--	--	--	
243	373446	0904828	ML-025356	T33N R02E 03S2AA	950	140	50	900	--	--	--	--	--	--	--	--	--	--	
244	373127	0905208	ML-023200	T33N R02E 19DBB	871	75	--	--	--	--	--	--	--	--	--	--	--	--	
245	373106	0904838	ML-013719	T33N R02E 22DDC	817	175	170	647	--	--	--	--	--	--	--	--	--	--	
246	373017	0904906	ML-011808	T33N R02E 27CDD	755	115	10	745	--	--	--	--	--	--	85	670			
247	373352	0905733	ML-002199	T33N R01E 08DS2Cr	890	677	410	480	--	--	--	--	--	--	--	--	--	--	
248	373346	0905548	ML-002196	T33N R01E 10CBCr	830	363	10	820	305	315	51.5	--	--	--	--	--	--	--	
249	373253	0905452	ML-002195	T33N R01E 14BCCR	830	379	30	800	340	370	460	--	--	--	--	--	--	--	
250	373252	0905435	ML-019670	T33N R01E 14N2S2Cr	840	447	115	725	310	425	415	--	--	--	--	--	--	--	
251	373250	0905512	ML-002194	T33N R01E 15DCr	795	341	15	780	305	320	47.5	--	--	--	--	--	--	--	
252	373309	0905614	ML-002197	T33N R01E 16ADC	875	398	50	825	345	395	480	--	--	--	--	--	--	--	
253	373329	0905645	ML-002198	T33N R01E 16BACr	900	320	10	890	--	--	--	--	--	--	--	--	--	--	
254	373228	0905530	ML-002193	T33N R01E 22ABCr	790	498	5	785	265	270	520	--	--	--	--	--	--	--	
255	373111	0905440	ML-002190	T33N R01E 26BCr	810	694	250	560	355	605	205	85	690	690	120				
256	373013	0905542	ML-019807	T33N R01E 34CE2Cr	735	654	370	285	650	85	--	--	--	--	--	--	--	--	
257	373138	0911410	ML-019190	T33N R03W 26ACB	1,050	1,430	810	240	317	1,127	-77	298	1,425	-375					
258	374109	0904914	ML-009442	T34N R02E 03BCB	1,087	80	45	1,042	--	--	--	--	--	--	--	--	--	--	
259	374059	0904912	ML-009550	T34N R02E 03CAA	1,077	175	40	1,037	--	--	--	--	--	--	--	--	--	--	
260	374056	0904836	ML-009444	T34N R02E 03DBC	1,148	100	--	--	--	--	--	--	--	--	--	--	--	--	

Table 2. Adjacent property core log analysis data—Continued

[DDMMSS, degrees, minutes, seconds; all units for depth and thickness are in feet, units for altitude are in feet above NGVD 29; depth and altitude refer to the formation top. --, no data]

Site number (fig. 4)	Latitude (DDMMSS)	Longitude (DDMMSS)	Borehole identification	Local well number	Altitude of land surface			Borehole depth			Derby-Doerun Dolomite			Davis Formation			Thickness of St. Francois confining unit	
					Depth	Altitude	Thickness	Depth	Altitude	Thickness	Depth	Altitude	Thickness	Depth	Altitude	Thickness	Total	Net shale
261	374049	0904841	ML-018002	T34N R02E 03DCB	1,068	514	--	--	--	--	--	--	--	--	--	--	--	--
262	374027	0904926	ML-024336	T34N R02E 09AACr	1,150	705	--	--	--	--	5	1,145	135	--	--	--	--	--
263	374001	0904814	ML-024277	T34N R02E 10DACr	1,130	580	--	--	--	--	10	1,120	54	--	--	--	--	--
264	373956	0904727	ML-024247	T34N R02E 11IDCr	1,180	690	--	--	--	--	20	1,160	93	--	--	--	--	--
265	373924	0904614	ML-024278	T34N R02E 13ACA	1,370	684	--	--	--	--	20	1,350	135	--	--	--	--	--
266	373827	0904752	ML-023213	T34N R02E 23BCA	1,156	100	30	1,126	--	--	--	--	--	--	--	--	--	--
267	374023	0905329	ML-007007	T34N R01E 12BAD	1,095	60	20	1,075	--	--	--	--	--	--	--	--	--	--
268	373639	0911423	ML-023793	T34N R03W 26CAB	1,224	1,205	560	664	135	695	529	185	320	--	--	--	--	--
269	374615	0904623	ML-023804	T35N R02E 01CACr	956	240	--	--	--	--	--	--	--	--	--	--	--	--
270	374643	0904721	ML-025146	T35N R02E 02ABN2	995	200	--	--	--	--	--	--	--	--	--	--	--	--
271	374643	0905001	ML-007419	T35N R02E 04BAB	904	40	--	--	--	--	--	--	--	--	--	--	--	--
272	374547	0904626	ML-003674	T35N R02E 12BCr	923	150	--	--	--	--	--	--	--	--	--	--	--	--
273	374230	0904642	ML-007439	T35N R02E 25CCD	1,060	60	--	--	--	--	--	--	--	--	--	--	--	--
274	374206	0904928	ML-007433	T35N R02E 33ADB	1,010	55	--	--	--	--	--	--	--	--	--	--	--	--
275	374701	0905842	ML-012142	T35N R01E 06BBCr	1,068	615	35	1,033	120	155	913	160	280	--	--	--	--	--
276	374529	0905648	ML-020385	T35N R01E 08DAN2	1,318	--	--	--	--	--	430	888	10	--	--	--	--	--
277	374537	0905539	ML-012447	T35N R01E 09ADD	1,234	600	95	1,139	85	180	1,054	140	225	--	--	--	--	--
278	374533	0905257	ML-022142	T35N R01E 12BDA	940	125	--	--	--	--	--	--	--	--	--	--	--	--
279	374458	0905437	ML-007423	T35N R01E 15AAA	1,018	60	--	--	--	--	--	--	--	--	--	--	--	--
280	374455	0905547	ML-012451	T35N R01E 16AACr	1,246	714	215	1,031	--	--	--	--	--	--	--	--	--	--
281	374448	0905647	ML-020386	T35N R01E 16BW2Cr	1,158	--	--	--	--	--	285	873	5	--	--	--	--	--
282	374452	0905733	ML-012314	T35N R01E 17BDCr	1,083	601	60	1,023	115	175	908	135	250	--	--	--	--	--
283	374404	0905637	ML-020380	T35N R01E 21BBBD	1,297	590	--	--	--	--	390	907	10	--	--	--	--	--
284	374230	0905651	ML-020384	T35N R01E 28CCCC	1,342	845	--	--	--	--	550	792	25	--	--	--	--	--
285	374306	0905851	ML-020207	T35N R01E 30BCS2	1,292	541	--	--	--	--	375	917	5	--	--	--	--	--
286	374240	0905851	ML-020363	T35N R01E 30CCS2	1,183	862	--	--	--	--	400	783	10	--	--	--	--	--
287	374136	0905307	ML-003144	T35N R01E 36DCB	1,180	800	200	980	--	--	90	1,090	165	55	--	--	--	--
288	374502	0911314	ML-003367	T35N R03W 14ADD	1,150	1,027	405	745	120	525	625	160	280	--	--	--	--	--
289	374216	0911820	ML-018177	T35N R03W 31CBD	1,325	1,344	500	825	220	720	605	255	475	--	--	--	--	--
290	374258	0911911	ML-019225	T35N R04W 25CDD	1,340	1,316	655	685	120	775	565	180	300	--	--	--	--	--

Table 2. Adjacent property core log analysis data—Continued

[DDMMSS, degrees, minutes, seconds; all units for depth and thickness are in feet; units for altitude are in feet above NGVD 29; depth and altitude refer to the formation top; --, no data]

Site number (fig. 4)	Latitude (DDMMSS)	Longitude (DDMMSS)	Borehole identification	Local well number	Altitude of land surface		Borehole depth		Bonnetiere Formation			Lamotte Sandstone			Precambrian	
					Depth	Altitude	Thickness	Depth	Altitude	Thickness	Depth	Altitude	Thickness	Depth	Altitude	
261	374049	0904841	ML-018002	T34N R02E 03DCB	1,068	514	5	1,063	330	335	733	--	--	--	--	
262	374027	0904926	ML-024336	T34N R02E 09AACr	1,150	705	140	1,010	--	--	--	644	506	506	506	
263	374001	0904814	ML-024277	T34N R02E 10DACr	1,130	580	64	1,066	471	535	595	37	572	558	558	
264	373956	0904727	ML-024247	T34N R02E 11IDCr	1,180	690	113	1,067	--	--	--	647	533	533	533	
265	373924	0904614	ML-024278	T34N R02E 13ACA	1,370	684	155	1,215	468	623	747	--	--	--	--	
266	373827	0904752	ML-023213	T34N R02E 23BCA	1,156	100	--	--	--	--	--	--	--	--	--	
267	374023	0905329	ML-007007	T34N R01E 12BAD	1,095	60	--	--	--	--	--	--	--	--	--	
268	373639	0911423	ML-023793	T34N R03W 26CAB	1,224	1,205	880	344	305	1,185	39	--	--	--	--	
269	374615	0904623	ML-023804	T35N R02E 01CACr	956	240	--	--	20	936	75	95	861	861	861	
270	374643	0904721	ML-025146	T35N R02E 02ABBN2	995	200	5	990	--	--	--	--	--	--	--	
271	374643	0905001	ML-007419	T35N R02E 04BAB	904	40	4	900	--	--	--	--	--	--	--	
272	374547	0904626	ML-003674	T35N R02E 12BCr	923	150	--	--	30	893	--	--	--	--	--	
273	374230	0904642	ML-007439	T35N R02E 25CCD	1,060	60	0	1,060	--	--	--	--	--	--	--	
274	374206	0904928	ML-007433	T35N R02E 33ADB	1,010	55	5	1,005	--	--	--	--	--	--	--	
275	374701	0905842	ML-012142	T35N R01E 06BBCr	1,068	615	315	753	275	590	478	--	--	--	--	
276	374529	0903648	ML-020385	T35N R01E 08DAN2	1,318	--	440	878	250	690	628	66	756	562	562	
277	374537	0905539	ML-012447	T35N R01E 09ADD	1,234	600	320	914	250	570	664	--	--	--	--	
278	374533	0905257	ML-022142	T35N R01E 12BDA	940	125	15	925	--	--	--	--	--	--	--	
279	374458	0905437	ML-007423	T35N R01E 15AAA	1,018	60	5	1,013	--	--	--	--	--	--	--	
280	374455	0905547	ML-012451	T35N R01E 16AACr	1,246	714	--	--	--	--	--	--	712	534	534	
281	374448	0905647	ML-020386	T35N R01E 16BW2Cr	1,158	--	290	868	260	550	608	--	--	--	--	
282	374452	0905733	ML-012314	T35N R01E 17BDCr	1,083	601	310	773	270	580	503	--	--	--	--	
283	374404	0905637	ML-020380	T35N R01E 21BBD	1,297	590	400	897	--	--	--	580	717	717	717	
284	374230	0905651	ML-020384	T35N R01E 28CCC	1,342	845	575	767	265	840	502	--	--	--	--	
285	374306	0905851	ML-020207	T35N R01E 30BCS2	1,292	541	380	912	--	--	--	--	525	767	767	
286	374240	0903851	ML-020363	T35N R01E 30CCS2	1,183	862	410	773	260	670	513	186	856	327	327	
287	374136	0905307	ML-003144	T35N R01E 36DCB	1,180	800	255	925	380	635	545	130	765	415	415	
288	374502	0911314	ML-003367	T35N R03W 14ADD	1,150	1,027	685	465	270	955	195	--	--	--	--	
289	374216	0911820	ML-018177	T35N R03W 31CBD	1,325	1,344	975	350	265	1,240	85	--	--	--	--	
290	374258	0911911	ML-019225	T35N R04W 25CDD	1,340	1,316	955	385	285	1,240	100	55	1,295	45	45	

Table 2. Adjacent property core log analysis data—Continued

[DDMMSS, degrees, minutes, seconds; all units for depth and thickness are in feet, units for altitude are in feet above NGVD 29; depth and altitude refer to the formation top; --, no data]

Site number (fig. 4)	Latitude (DDMMSS)	Longitude (DDMMSS)	Borehole identification	Local well number	Altitude of land surface			Borehole depth			Derby-Doerun Dolomite			Davis Formation			Thickness of St. Francois confining unit	
					Depth	Altitude	Thickness	Depth	Altitude	Thickness	Depth	Altitude	Thickness	Depth	Altitude	Thickness	Total	Net shale
291	375109	0904907	ML-008892	T36N R02E 09ADCr	1,190	630	590	--	--	--	--	--	--	--	--	--	--	--
292	375058	0904920	ML-008896	T36N R02E 09DBCt	1,108	535	593	--	--	--	--	--	--	--	--	--	--	--
293	375125	0904827	ML-008895	T36N R02E 10BACr	1,088	550	553	--	--	--	--	--	--	--	--	--	--	--
294	375123	0904845	ML-008894	T36N R02E 10BBCr	1,141	555	591	--	--	--	--	--	--	--	--	--	--	--
295	375048	0904619	ML-008899	T36N R02E 12CDCr	1,028	586	475	553	95	570	458	--	--	--	--	--	--	--
296	375046	0904554	ML-008898	T36N R02E 12DCCr	1,059	606	475	584	65	540	519	--	--	--	--	--	--	--
297	375034	0904633	ML-008897	T36N R02E 13BBCr	1,050	599	470	580	105	575	475	--	--	--	--	--	--	--
298	374837	0904735	ML-012193	T36N R02E 26BBBD	907	215	--	--	--	--	--	--	--	--	--	--	--	--
299	374820	0904726	ML-007428	T36N R02E 26CAB	829	50	--	--	--	--	--	--	--	--	--	--	--	--
300	374745	0905053	ML-017882	T36N R02E 32BAC	951	150	--	--	--	--	--	--	--	--	--	--	--	--
301	374730	0904630	ML-008286	T36N R02E 36CAA	914	39	--	--	--	--	--	--	--	--	--	--	--	--
302	375140	0905710	ML-011333	T36N R01E 05CDCr	1,133	1,335	830	303	80	910	223	180	260	--	--	--	--	--
303	375159	0905745	ML-009380	T36N R01E 06DAB	1,109	1,446	--	--	--	1,013	96	117	--	--	--	--	--	--
304	375139	0905806	ML-009526	T36N R01E 06DCC	1,089	445	420	669	--	--	--	--	--	--	--	--	--	--
305	375144	0905748	ML-009378	T36N R01E 06DDDB	1,138	1,111	470	668	110	580	558	175	285	--	--	--	--	--
306	375130	0905746	ML-009374	T36N R01E 07AACr	1,174	1,099	495	679	90	585	589	175	265	--	--	--	--	--
307	375111	0905740	ML-009376	T36N R01E 07ADD	1,068	1,023	410	658	110	520	548	180	290	--	--	--	--	--
308	375130	0905825	ML-009522	T36N R01E 07BN2Cr	1,057	445	335	722	95	430	627	--	--	--	--	--	--	--
309	375106	0905825	ML-009497	T36N R01E 07CAC	1,002	450	340	662	--	--	--	--	--	--	--	--	--	--
310	375053	0905841	ML-023492	T36N R01E 07CCB	1,042	475	400	642	--	--	--	--	--	--	--	--	--	--
311	375114	0905653	ML-009513	T36N R01E 08ACE2	1,176	420	360	816	--	--	--	--	--	--	--	--	--	--
312	375109	0905706	ML-009493	T36N R01E 08BDD	1,185	976	--	--	--	--	--	--	--	--	--	--	--	--
313	375051	0905728	ML-009492	T36N R01E 08CCCN2	1,087	864	310	777	--	--	--	--	--	--	--	--	--	--
314	375035	0905643	ML-009496	T36N R01E 17AACr	1,078	425	275	803	110	385	693	--	--	--	--	--	--	--
315	375019	0905713	ML-009498	T36N R01E 17BDD	1,127	450	330	797	100	430	697	--	--	--	--	--	--	--
316	374914	0905748	ML-013626	T36N R01E 19DACK	939	830	275	664	105	380	559	165	270	--	--	--	--	--
317	374944	0905642	ML-013628	T36N R01E 20AACr	1,096	990	375	721	135	510	586	165	300	--	--	--	--	--
318	374914	0905527	ML-015656	T36N R01E 22W2W2Cr	1,118	475	440	678	--	--	--	--	--	--	--	--	--	--
319	374848	0905651	ML-013204	T36N R01E 29AACr	1,158	500	475	683	--	--	--	--	--	--	--	--	--	--
320	374734	0905822	ML-012455	T36N R01E 31CACr	1,194	375	300	894	--	--	--	--	--	--	--	--	--	--

Table 2. Adjacent property core log analysis data—Continued

[DDMMSS, degrees, minutes, seconds; all units for depth and thickness are in feet; units for altitude are in feet above NGVD 29; depth and altitude refer to the formation top; --, no data]

Site number (fig. 4)	Latitude (DDMMSS)	Longitude (DDMMSS)	Borehole identification	Local well number	Altitude of land surface			Borehole			Bonnetiere Formation			Lamotte Sandstone			Precambrian		
					Depth	Altitude	Thickness	Depth	Altitude	Thickness	Depth	Altitude	Thickness	Depth	Altitude	Thickness	Depth	Altitude	
291	375109	0904907	ML-008892	T36N R02E 09ADCr	1,190	630	--	--	--	--	--	--	--	--	--	--	--	--	
292	375058	0904920	ML-008896	T36N R02E 09DBCr	1,108	535	--	--	--	--	--	--	--	--	--	--	--	--	
293	375125	0904827	ML-008895	T36N R02E 10BACr	1,088	550	--	--	--	--	--	--	--	--	--	--	--	--	
294	375123	0904845	ML-008894	T36N R02E 10BBCr	1,141	555	--	--	--	--	--	--	--	--	--	--	--	--	
295	375048	0904619	ML-008899	T36N R02E 12CDCr	1,028	586	--	--	--	--	--	--	--	--	--	--	--	--	
296	375046	0904554	ML-008898	T36N R02E 12DCCr	1,059	606	--	--	--	--	--	--	--	--	--	--	--	--	
297	375034	0904633	ML-008897	T36N R02E 13BBCr	1,050	599	--	--	--	--	--	--	--	--	--	--	--	--	
298	374837	0904735	ML-012193	T36N R02E 26BBBD	907	215	195	712	--	--	--	--	--	--	--	--	--	--	
299	374820	0904726	ML-007428	T36N R02E 26CAB	829	50	15	814	--	--	--	--	--	--	--	--	--	--	
300	374745	0905053	ML-017882	T36N R02E 32BAC	951	150	15	936	--	--	--	--	--	--	--	--	--	--	
301	374730	0904630	ML-008286	T36N R02E 36CAA	914	39	--	--	--	--	0	914	25	25	25	889	889	889	
302	375140	0905710	ML-011333	T36N R01E 05CDCr	1,133	1,335	1,090	43	--	--	--	--	--	--	--	--	--	--	
303	375159	0905745	ML-009380	T36N R01E 06DAB	1,109	1,446	1,130	-21	--	--	--	--	--	--	--	--	--	--	
304	375139	0905806	ML-009526	T36N R01E 06DCC	1,089	445	--	--	--	--	--	--	--	--	--	--	--	--	
305	375144	0905748	ML-009378	T36N R01E 06DDB	1,138	1,111	755	383	307	1,062	76	--	--	--	--	--	--	--	
306	375130	0905746	ML-009374	T36N R01E 07AACr	1,174	1,099	760	414	285	1,045	129	--	35	1,080	94	94	94	94	
307	375111	0905740	ML-009376	T36N R01E 07ADD	1,068	1,023	700	368	296	996	72	--	--	--	--	--	--	--	
308	375130	0905825	ML-009522	T36N R01E 07BN2Cr	1,057	445	--	--	--	--	--	--	--	--	--	--	--	--	
309	375106	0905825	ML-009497	T36N R01E 07CAC	1,002	450	--	--	--	--	--	--	--	--	--	--	--	--	
310	375053	0905841	ML-023492	T36N R01E 07CCB	1,042	475	--	--	--	--	--	--	--	--	--	--	--	--	
311	375114	0905653	ML-009513	T36N R01E 08ACE2	1,176	420	--	--	--	--	--	--	--	--	--	--	--	--	
312	375109	0905706	ML-009493	T36N R01E 08BDD	1,185	976	--	--	--	--	--	--	--	--	951	234	234	234	
313	375051	0905728	ML-009492	T36N R01E 08CCN2	1,087	864	--	--	--	--	--	--	--	--	847	240	240	240	
314	375035	0905643	ML-009496	T36N R01E 17AACr	1,078	425	--	--	--	--	--	--	--	--	--	--	--	--	
315	375019	0905713	ML-009498	T36N R01E 17BDD	1,127	450	--	--	--	--	--	--	--	--	--	--	--	--	
316	374914	0905748	ML-013626	T36N R01E 19DACr	939	830	545	394	--	--	--	--	--	--	--	--	--	--	
317	374944	0905642	ML-013628	T36N R01E 20AACr	1,096	990	675	421	270	945	151	--	--	--	--	--	--	--	
318	374914	0905527	ML-015656	T36N R01E 22W2W2C	1,118	475	--	--	--	--	--	--	--	--	--	--	--	--	
319	374848	0905651	ML-013204	T36N R01E 29AACr	1,158	500	--	--	--	--	--	--	--	--	--	--	--	--	
320	374734	0905822	ML-012455	T36N R01E 31CACr	1,194	375	--	--	--	--	--	--	--	--	--	--	--	--	

Table 2. Adjacent property core log analysis data—Continued

[DDMMSS, degrees, minutes, seconds; all units for depth and thickness are in feet, units for altitude are in feet above NGVD 29; depth and altitude refer to the formation top. --, no data]

Site number (fig. 4)	Latitude (DDMMSS)	Longitude (DDMMSS)	Borehole identification	Local well number	Altitude of land surface			Borehole depth			Derby-Doerun Dolomite			Davis Formation			Thickness of St. Francois confining unit		
					Depth	Altitude	Thickness	Depth	Altitude	Thickness	Depth	Altitude	Thickness	Depth	Altitude	Thickness	Total	Net shale	
321	374747	0905660	ML-012303	T36N R01E 32AACr	1,010	803	255	755	90	345	665	165	255	--	--	--	--		
322	375147	0905847	ML-009375	T36N R01W 01DDE2	1,092	858	375	717	100	475	617	175	275	--	--	--	--		
323	375132	0905906	ML-009487	T36N R01W 12ABA	1,110	600	450	660	120	570	540	--	--	--	--	--	--		
324	375114	0905920	ML-009514	T36N R01W 12BDD	999	365	335	664	--	--	--	--	--	--	--	--	--		
325	375109	0905943	ML-009489	T36N R01W 12CBN2	1,055	425	405	650	--	--	--	--	--	--	--	--	--		
326	375040	0905920	ML-009529	T36N R01W 13BAB	1,050	415	375	675	--	--	--	--	--	--	--	--	--		
327	375035	0910129	ML-009532	T36N R01W 15BAA	854	460	385	469	--	--	--	--	--	--	--	--	--		
328	374948	0910327	ML-009533	T36N R01W 17DCA	827	350	250	577	--	--	--	--	--	--	--	--	--		
329	374855	0910144	ML-009531	T36N R01W 22CDC	923	818	220	703	100	320	603	190	290	--	--	--	--		
330	374938	0910006	ML-009535	T36N R01W 23AAB	914	330	315	599	--	--	--	--	--	--	--	--	--		
331	374934	0905939	ML-009538	T36N R01W 24BCA	901	270	200	701	--	--	--	--	--	--	--	--	--		
332	374714	0910133	ML-012307	T36N R01W 34DCCr	970	763	130	840	120	250	720	170	290	--	--	--	--		
333	374724	0910036	ML-012322	T36N R01W 35CACr	1,030	837	235	795	105	340	690	165	270	--	--	--	--		
334	374722	0905854	ML-013116	T36N R01W 36Dacr	1,172	835	--	--	--	520	652	115	--	--	--	--	--	--	
335	374733	0905920	ML-013163	T36N R01W 36DBCcr	1,215	450	420	795	--	--	--	--	--	--	--	--	--		
336	374840	0910831	ML-019640	T36N R02W 27BBCr	930	799	145	785	135	280	650	181	316	--	--	--	--		
337	374841	0911044	ML-018318	T36N R02W 29BDA	818	191	70	748	110	180	638	--	--	--	--	--	--		
338	374956	0911601	ML-002168	T36N R03W 16CCr	905	915	300	605	100	400	505	165	265	--	--	--	--		
339	374919	0911559	ML-002170	T36N R03W 21CAB	999	950	370	629	70	440	559	210	280	--	--	--	--		
340	374939	0911956	ML-019720	T36N R04W 23AW2Cr	1,140	1,185	565	575	115	680	460	155	270	--	--	--	--		
				Minimum	20	63	65	5	-22	5	55	57							
				25th Quartile	201	542	100	203	371	110	265	77							
				50th Quartile	365	656	115	400	559	165	280	79							
				75th Quartile	475	747	130	595	709	175	305	83							
				Maximum	965	1,139	220	1,132	1,350	255	475	87							
				Count	90	90	57	83	83	69	49	5							

Table 2. Adjacent property core log analysis data—Continued

[DDMMSS, degrees, minutes, seconds; all units for depth and thickness are in feet; units for altitude are in feet above NGVD 29; depth and altitude refer to the formation top; --, no data]

Site number (fig. 4)	Latitude (DDMMSS)	Longitude (DDMMSS)	Borehole identification	Local well number	Altitude of land surface		Borehole depth		Bonnetiere Formation			Lamotte Sandstone			Precambrian	
					Depth	Altitude	Depth	Thickness	Depth	Altitude	Thickness	Depth	Altitude	Thickness	Depth	Altitude
321	374747	0905660	ML-012303	T36N R01W 32AACr	1,010	803	510	500	290	800	210	--	--	--	--	
322	375147	0905847	ML-009375	T36N R01W 01DDE2	1,092	858	650	442	--	--	--	--	--	--	--	
323	375132	0905906	ML-009487	T36N R01W 12ABA	1,110	600	--	--	--	--	--	--	--	--	--	
324	375114	0905920	ML-009514	T36N R01W 12BDD	999	365	--	--	--	--	--	--	--	--	--	
325	375109	0905943	ML-009489	T36N R01W 12CBN2	1,055	425	--	--	--	--	--	--	--	--	--	
326	375040	0905920	ML-009529	T36N R01W 13BAB	1,050	415	--	--	--	--	--	--	--	--	--	
327	375035	0910129	ML-009532	T36N R01W 15BAA	854	460	--	--	--	--	--	--	--	--	--	
328	374948	0910327	ML-009533	T36N R01W 17DCA	827	350	--	--	--	--	--	--	--	--	--	
329	374855	0910144	ML-009531	T36N R01W 22CDC	923	818	510	413	290	800	123	--	--	--	--	
330	374938	0910006	ML-009535	T36N R01W 23AAB	914	330	--	--	--	--	--	--	--	--	--	
331	374934	0905939	ML-009538	T36N R01W 24BCA	901	270	--	--	--	--	--	--	--	--	--	
332	374714	0910133	ML-012307	T36N R01W 34DCCr	970	763	420	550	320	740	230	--	--	--	--	
333	374724	0910036	ML-012322	T36N R01W 35CACr	1,030	837	505	525	310	815	215	--	--	--	--	
334	374722	0905854	ML-013116	T36N R01W 36DACr	1,172	835	635	537	155	790	382	--	--	--	--	
335	374733	0905920	ML-013163	T36N R01W 36DBCr	1,215	450	--	--	--	--	--	--	--	--	--	
336	374840	0910831	ML-019640	T36N R02W 27BBCr	930	799	461	469	301	762	168	--	--	--	--	
337	374841	0911044	ML-018318	T36N R02W 29BDA	818	191	--	--	--	--	--	--	--	--	--	
338	374956	0911601	ML-002168	T36N R03W 16CCr	905	915	565	340	280	845	60	--	--	--	--	
339	374919	0911559	ML-002170	T36N R03W 21CAB	999	950	650	349	--	--	--	--	--	--	--	
340	374939	0911956	ML-019720	T36N R04W 23AW2Cr	1,140	1,185	835	305	300	1,135	5	--	--	--	--	
				Minimum	0	-220	155	0	-562	25	25	-569				
				25th Quartile	64	305	274	585	0	55	533	109				
				50th Quartile	420	480	303	790	132	75	646	385				
				75th Quartile	705	820	321	1,054	491	186	854	561				
				Maximum	1,311	1,215	471	1,540	936	355	1,470	889				
				Count	93	93	56	59	59	13	26	26				

Table 3. Porosity, vertical permeability, and vertical hydraulic conductivity data

[Data for West and East Exploration areas from Kleeschulte and Seeger (2000, 2001); ft, feet; psi, pounds per square inch; g/cc, grams per cubic centimeter; mD, millidarcies; ft/s, foot per second; POT, Potosi Dolomite; DDR, Derby-Doerun Dolomite; DVS, Davis Formation; BNT, Bonneterre Formation; LMT, Lamotte Sandstone; C, carbonate rock; S, shale; B; both carbonate and shale; Q, sandstone; --, no data; NA, not applicable]

Sample number	Borehole identification	Formation	Sample depth, in ft	Confining pressure, in psi (gauged)	Porosity, in percent	Density, in g/cc	Vertical permeability, in mD	Vertical hydraulic conductivity, in ft/s	Rock type
West Exploration Area (fig. 1) ^a									
101	801-002	DDR	1,479	1,120	3.54	2.84	4.000E-06	1.27E-13	C
102	801-002	DVS	1,508	1,140	1.73	2.76	1.000E-06	3.17E-14	C
103	801-002	DVS	1,521	1,150	.73	2.71	1.000E-05	3.17E-13	C
104	801-002	DVS	1,544	1,170	4.02	2.68	2.200E-05	6.97E-13	B
105	801-002	DVS	1,578	1,200	.88	2.75	1.000E-06	3.17E-14	C
106	801-009	DDR	1,409	1,070	4.57	2.85	1.181E-02	3.74E-10	C
107	801-009	DVS	1,435	1,090	2.31	2.84	2.500E-05	7.83E-13	C
108	801-009	DVS	1,457	1,100	2.59	2.64	2.100E-05	6.56E-13	S
109	801-009	DVS	1,485	1,125	2.61	2.70	4.300E-05	1.37E-12	C
110	801-009	DVS	1,512	1,150	4.49	2.66	1.000E-06	3.17E-14	S
111	801-009	DVS	1,535	1,160	2.15	2.70	1.900E-05	5.86E-13	B
112	801-010	DDR	1,492	1,130	2.69	2.84	1.500E-05	4.82E-13	C
113	801-010	DVS	1,512	1,150	5.14	2.85	2.307E-03	7.31E-11	C
114	801-010	DVS	1,536	1,160	7.38	2.70	8.000E-05	2.52E-12	C
115	801-010	DVS	1,564	1,190	2.65	2.70	1.600E-05	5.10E-13	B
116	801-010	DVS	1,585	1,200	4.52	2.67	1.000E-06	3.17E-14	S
117	801-010	DVS	1,608	1,220	.82	2.72	1.600E-05	5.17E-13	B
118	801-016	DDR	1,528	1,160	1.23	2.84	1.600E-05	4.91E-13	C
119	801-016	DDR	1,560	1,180	.71	2.80	5.000E-06	1.65E-13	S
120	801-016	DVS	1,602	1,210	3.13	2.72	1.000E-06	3.17E-14	B
121	801-016	DVS	1,630	1,240	2.39	2.66	1.000E-06	3.17E-14	S
122	801-016	DVS	1,649	1,250	2.51	2.69	1.000E-06	3.17E-14	B
123	801-016	DVS	1,689	1,280	2.98	2.69	5.000E-06	1.65E-13	B
124	801-031	DDR	1,478	1,120	1.40	2.84	1.000E-06	3.17E-14	C
125	801-031	DDR	1,523	1,150	2.19	2.87	1.000E-06	3.17E-14	C
126	801-031	DVS	1,554	1,180	.66	2.85	1.000E-06	3.17E-14	C
127	801-031	DVS	1,579	1,200	2.12	2.68	1.000E-06	3.17E-14	S
128	801-031	DVS	1,606	1,220	2.04	2.66	1.400E-05	4.44E-13	S
129	801-031	DVS	1,640	1,240	.96	2.69	1.000E-06	3.17E-14	C
130	82W03	DDR	1,564	1,190	.61	2.83	1.000E-06	3.17E-14	C
131	82W03	DDR	1,581	1,200	.80	2.82	1.000E-06	3.17E-14	C
132	82W03	DVS	1,624	1,230	2.37	2.82	3.500E-05	1.11E-12	C
133	82W03	DVS	1,692	1,280	3.49	2.68	1.000E-06	3.17E-14	S
134	82W03	DVS	1,841	1,400	4.93	2.75	9.800E-05	3.11E-12	S
135	82W27	DDR	1,445	1,100	1.08	2.83	1.000E-06	3.17E-14	C
136	82W27	DDR	1,479	1,120	1.16	2.81	1.000E-06	3.17E-14	C
137	82W27	DVS	1,522	1,150	5.00	2.68	1.900E-05	6.15E-13	S
138	82W27	DVS	1,597	1,210	3.23	2.72	1.000E-06	3.17E-14	B
139	82W27	DVS	1,679	1,280	6.70	2.78	3.600E-05	1.14E-12	S
140	83W17	DDR	1,493	1,120	2.95	2.84	2.066E-01	6.55E-09	C

Table 3. Porosity, vertical permeability, and vertical hydraulic conductivity data—Continued

[Data for West and East Exploration areas from Kleeschulte and Seeger (2000, 2001); ft, feet; psi, pounds per square inch; g/cc, grams per cubic centimeter; mD, millidarcies; ft/s, foot per second; POT, Potosi Dolomite; DDR, Derby-Doerun Dolomite; DVS, Davis Formation; BNT, Bonneterre Formation; LMT, Lamotte Sandstone; C, carbonate rock; S, shale; B; both carbonate and shale; Q, sandstone; --, no data; NA, not applicable]

Sample number	Borehole identification	Formation	Sample depth, in ft	Confining pressure, in psi (gauged)	Porosity, in percent	Density, in g/cc	Vertical permeability, in mD	Vertical hydraulic conductivity, in ft/s	Rock type
West Exploration Area (fig. 1)^a—Continued									
141	83W17	DDR	1,542	1,170	4.06	2.85	1.000E-06	6.14E-12	C
142	83W17	DVS	1,615	1,220	5.64	2.73	1.000E-06	3.17E-14	S
143	83W17	DVS	1,692	1,280	1.40	2.70	1.000E-06	3.17E-14	C
144	83W17	DVS	1,762	1,340	3.12	2.73	1.000E-06	3.17E-14	B
^b 145	83W30	DDR	1,445	1,095	17.47	2.83	2.743E+00	8.70E-08	B
^b 145	83W30	DDR	1,445	1,095	17.60	2.83	3.988E+00	1.18E-08	B
^b 145	83W30	DDR	1,445	1,095	17.84	2.83	2.974E+00	9.43E-08	B
146	83W30	DDR	1,494	1,130	1.99	2.83	1.200E-05	3.90E-13	C
147	83W30	DVS	1,591	1,210	4.47	2.72	2.600E-05	8.24E-13	B
148	83W30	DVS	1,727	1,310	.46	2.70	1.000E-06	3.17E-14	C
149	83W30	DVS	1,796	1,360	5.74	2.78	2.100E-05	6.66E-13	S
^b 150	83W34	DDR	1,511	1,145	11.76	2.84	5.846E-01	1.85E-08	B
^b 150	83W34	DDR	1,511	1,145	11.60	2.85	4.724E-01	1.40E-09	B
^b 150	83W34	DDR	1,511	1,145	10.53	2.84	9.573E-02	3.03E-09	B
151	83W34	DVS	1,573	1,190	1.93	2.75	1.000E-06	3.17E-14	C
152	83W34	DVS	1,685	1,280	5.32	2.69	5.400E-05	1.71E-12	S
153	83W34	DVS	1,725	1,310	5.61	2.72	5.100E-05	1.62E-12	S
154	83W34	DVS	1,785	1,350	3.28	2.80	1.000E-06	3.17E-14	C
155	83W34	DVS	1,791	1,360	5.99	2.75	1.000E-06	3.17E-14	B
156	83W35	DDR	1,333	1,010	2.37	2.80	1.000E-06	3.17E-14	C
157	83W35	DDR	1,350	1,020	4.49	2.84	7.290E-04	2.31E-11	C
158	83W35	DVS	1,475	1,120	4.27	2.72	7.000E-06	2.22E-13	B
159	83W35	DVS	1,495	1,130	5.18	2.72	5.000E-06	1.59E-13	S
160	83W35	DVS	1,516	1,150	2.46	2.71	8.150E-03	2.58E-10	B
161	83W35	DVS	1,597	1,210	3.88	2.75	1.000E-06	3.17E-14	B
East Exploration Area (fig. 1)^a									
201	12-01A	DDR	941	715	6.40	2.84	7.43E-03	2.20E-11	C
202	12-01A	DVS	1,054	801	3.20	2.71	2.58E-06	7.65E-15	C
203	122-A	DDR	1,523	1,157	2.50	2.84	4.59E-04	1.36E-12	C
204	122-A	DVS	1,666	1,266	.50	2.72	3.43E-05	1.01E-13	C
205	76W10	DVS	1,287	975	2.77	2.79	3.53E-05	1.05E-13	B
206	76W10	DVS	1,333	1,010	5.13	2.76	5.52E-05	1.64E-13	S
207	76W15	DDR	1,728	1,310	1.56	2.85	1.23E-05	3.66E-14	C
208	76W15	DDR	1,762	1,340	1.35	2.83	9.27E-05	2.75E-13	C
209	76W15	DVS	1,832	1,390	1.82	2.83	3.59E-06	1.06E-14	C
210	76W15	DVS	1,855	1,390	1.30	2.84	1.25E-04	3.72E-13	C
211	76W17	DDR	1,301	990	1.71	2.84	5.47E-05	1.62E-13	C
212	76W17	DVS	1,377	1,040	1.96	2.74	1.20E-04	3.57E-13	B
213	76W19	DVS	1,104	840	3.60	2.83	7.78E-05	2.31E-13	C
214	76W19	DVS	1,198	910	6.23	2.74	2.62E-04	7.78E-13	S
215	76W19	DVS	1,237	940	3.84	2.79	1.27E-05	3.76E-14	B

Table 3. Porosity, vertical permeability, and vertical hydraulic conductivity data—Continued

[Data for West and East Exploration areas from Kleeschulte and Seeger (2000, 2001); ft, feet; psi, pounds per square inch; g/cc, grams per cubic centimeter; mD, millidarcies; ft/s, foot per second; POT, Potosi Dolomite; DDR, Derby-Doerun Dolomite; DVS, Davis Formation; BNT, Bonneterre Formation; LMT, Lamotte Sandstone; C, carbonate rock; S, shale; B; both carbonate and shale; Q, sandstone; --, no data; NA, not applicable]

Sample number	Borehole identification	Formation	Sample depth, in ft	Confining pressure, in psi (gauged)	Porosity, in percent	Density, in g/cc	Vertical permeability, in mD	Vertical hydraulic conductivity, in ft/s	Rock type
East Exploration Area (fig. 1)^a—Continued									
216	801-018	DDR	1,362	1,035	2.40	2.81	1.86E-04	5.51E-13	C
217	801-018	DVS	1,427	1,084	2.20	2.84	4.28E-04	1.27E-12	C
218	801-026	DDR	1,442	1,095	1.20	2.84	3.23E-04	9.59E-13	C
219	801-026	DVS	1,549	1,177	.90	2.75	1.04E-03	3.09E-12	C
220	BCN-01	DDR	1,525	1,159	2.60	2.83	7.19E-04	2.13E-12	C
221	CF-01	DVS	1,701	1,290	3.37	2.83	2.29E-04	6.79E-13	C
222	SF-01	DDR	1,620	1,231	3.10	2.83	2.49E-03	7.37E-12	C
223	SF-01	DVS	1,725	1,311	2.90	2.82	2.97E-03	8.80E-12	B
224	SF-20	DDR	1,283	975	1.70	2.83	2.26E-04	6.71E-13	B
225	SF-20	DVS	1,430	1,086	.50	2.84	2.03E-04	6.03E-13	C
226	SF-21	DVS	1,375	1,040	2.19	2.81	1.35E-04	4.02E-13	B
227	STH-02	DDR	1,839	1,397	1.50	2.82	7.00E-02	2.08E-10	C
228	STH-02	DVS	1,978	1,503	4.20	2.82	9.65E-04	2.86E-12	C
229	VB-06	DDR	1,592	1,209	3.00	2.83	4.23E-04	1.25E-12	C
230	VB-06	DVS	1,682	1,278	2.80	2.82	1.43E-03	4.24E-12	C
231	VB-16	DVS	1,441	1,095	5.00	2.84	5.09E-04	1.51E-12	C
232	VB-24	DDR	1,255	953	1.90	2.83	7.52E-04	2.23E-12	C
233	VB-24	DVS	1,360	1,033	4.80	2.83	1.67E-04	4.96E-13	C
Viburnum Trend Area									
301	417	DDR	296	224	4.22	2.82	3.456E-04	1.10E-11	C
302	417	DVS	478	362	.75	2.69	1.446E-04	4.58E-12	B
303	1079	DDR	494	374	3.68	2.81	1.281E-04	4.06E-12	C
304	1079	DVS	620	470	5.18	2.72	1.581E-04	5.01E-12	B
305	02B06	DDR	485	368	2.81	2.82	3.995E-06	1.27E-13	C
306	02B06	DVS	595	451	1.56	2.77	3.971E-06	1.26E-13	S
307	02B06	DVS	636	482	.80	2.71	6.456E-06	2.05E-13	B
308	02S09	DVS	881	668	.57	2.78	3.990E-06	1.26E-13	B
309	02S09	DVS	925	701	5.56	2.73	--	--	S
310	02S09	DVS	977	740	1.35	2.75	1.618E-06	5.13E-14	B
311	12-EE	DDR	263	199	3.19	2.81	2.612E-04	8.28E-12	C
312	12-EE	DVS	365	277	3.05	2.77	3.627E-04	1.15E-11	B
313	1-RY	DDR	761	577	2.60	2.87	7.834E-05	2.48E-12	C
314	1-RY	DVS	928	703	.58	2.73	1.439E-04	4.56E-12	B
315	1-RY	BNT	1,006	763	1.69	2.83	5.146E-04	1.63E-11	B
316	3-MR	DDR	594	450	2.67	2.83	5.733E-04	1.82E-11	C
317	3-MR	DVS	681	516	2.32	2.79	4.293E-04	1.36E-11	C
318	3-MR	BNT	812	615	.79	2.82	1.712E-03	5.43E-11	C
319	5-EX	DDR	834	632	.25	2.80	2.498E-04	7.92E-12	B
320	5-EX	DVS	874	662	1.01	2.73	1.733E-04	5.49E-12	B

Table 3. Porosity, vertical permeability, and vertical hydraulic conductivity data—Continued

[Data for West and East Exploration areas from Kleeschulte and Seeger (2000, 2001); ft, feet; psi, pounds per square inch; g/cc, grams per cubic centimeter; mD, millidarcies; ft/s, foot per second; POT, Potosi Dolomite; DDR, Derby-Doerun Dolomite; DVS, Davis Formation; BNT, Bonneterre Formation; LMT, Lamotte Sandstone; C, carbonate rock; S, shale; B; both carbonate and shale; Q, sandstone; --, no data; NA, not applicable]

Sample number	Borehole identification	Formation	Sample depth, in ft	Confining pressure, in psi (gauged)	Porosity, in percent	Density, in g/cc	Vertical permeability, in mD	Vertical hydraulic conductivity, in ft/s	Rock type
Viburnum Trend Area—Continued									
321	5-MR	DDR	453	343	6.35	2.83	6.361E-02	2.02E-09	C
322	5-MR	DVS	589	446	2.84	2.76	2.188E-04	6.93E-12	B
323	A-201	DDR	362	374	4.03	2.81	1.773E-02	5.62E-10	C
324	A-201	DVS	470	356	10.98	2.71	2.732E-01	8.66E-09	C
325	CN-280	DDR	759	545	5.54	2.79	1.370E-05	4.34E-13	C
326	CN-280	DVS	927	703	.44	2.70	6.236E-06	1.98E-13	B
327	CO-1	DDR	836	634	6.22	2.82	3.739E-02	1.19E-09	C
328	CO-1	DVS	951	721	1.52	2.65	3.224E-04	1.02E-11	B
329	CO-1	BNT	1,062	805	4.82	2.84	2.498E-05	7.92E-13	B
330	HA-11	DDR	978	741	3.27	2.81	6.749E-04	2.14E-11	C
331	HA-11	DVS	1,121	850	.26	2.72	1.715E-04	5.44E-12	B
332	LC 810	DDR	1,023	780	3.24	2.79	6.200E-05	1.96E-12	B
333	LC 810	DDR	1,060	810	3.99	2.81	9.000E-06	2.86E-13	B
334	LC 810	DVS	1,096	830	7.25	2.71	1.000E-06	3.17E-14	S
335	LC 810	DVS	1,159	880	2.19	2.71	1.000E-06	3.17E-14	C
336	LC 810	DVS	1,204	920	1.59	2.70	1.000E-06	3.17E-14	B
337	RC105	DDR	839	636	2.70	2.83	4.592E-05	1.46E-12	C
338	RC105	DDR	877	665	4.74	2.82	4.718E-05	1.50E-12	C
339	RC105	DVS	935	709	7.00	2.77	2.347E-06	7.44E-14	S
340	RC105	DVS	1,054	799	4.12	2.83	5.759E-06	1.83E-13	B
341	USA-14	DDR	641	486	2.26	2.81	2.863E-05	9.08E-13	C
342	USA-14	DVS	796	603	4.20	2.76	4.197E-04	1.33E-11	B
^d 343	Generic F	DDR	NA	NA	NA	NA	NA	7.73E-13	NA
344	Generic F	DVS	NA	NA	NA	NA	NA	3.17E-14	NA
345	Generic L	NA	NA	NA	NA	NA	NA	4.73E-13	C
346	Generic L	NA	NA	NA	NA	NA	NA	7.26E-13	S
^d 347	Generic L	NA	NA	NA	NA	NA	NA	1.57E-12	B

^aSee Kleeschulte and Seeger (2000, 2001) for location information.

^bDuplicate sample, data previously reported in Kleeschulte and Seeger (2000, 2001).

^cSample deteriorated during the vertical permeability measurement; no value available.

^dDuplicate sample from AC-84 was included in determination of these median values for vertical hydraulic conductivity.

Kleeschulte and Seeger—STRATIGRAPHY AND VERTICAL HYDRAULIC CONDUCTIVITY OF THE ST. FRANCOIS CONFINING UNIT IN THE VIBURNUM TREND AND —USGS/WRIR 03-4329
EVALUATION OF THE UNIT IN THE VIBURNUM TREND AND EXPLORATION AREAS, SOUTHEASTERN MISSOURI